

**UCLA**

**UCLA Electronic Theses and Dissertations**

**Title**

An Investigation into the Benefits of Tactile Feedback for Laparoscopic, Robotic, and Remote Surgery

**Permalink**

<https://escholarship.org/uc/item/7w74q3wh>

**Author**

Wottawa, Christopher Robert

**Publication Date**

2013

Peer reviewed|Thesis/dissertation

UNIVERSITY OF CALIFORNIA

Los Angeles

An Investigation into the Benefits of Tactile Feedback  
for Laparoscopic, Robotic, and Remote Surgery

A dissertation submitted in partial satisfaction of  
the requirements for the degree Doctor of Philosophy  
in Biomedical Engineering

by

Christopher Robert Wottawa

2013

© Copyright by  
Christopher Robert Wottawa  
2013

## **ABSTRACT OF THE DISSERTATION**

# **An Investigation into the Benefits of Tactile Feedback for Laparoscopic, Robotic, and Remote Surgery**

**by**

**Christopher Robert Wottawa**

Doctor of Philosophy in Biomedical Engineering

University of California, Los Angeles, 2013

Professor Warren Grundfest, Chair

Minimally invasive surgery (MIS) provides profound and well-known benefits to patients at the cost of increased technical difficulty for surgeons. In all types of minimally invasive surgery, including robotic, laparoscopic, and remote surgery, tactile information is altered, or in the case of robotic procedures, completely absent.

The first version of a tactile feedback system for robotic surgery was completed in 2008. During the course of this research, the feedback system was iteratively redesigned in order to address some of its shortcomings, improve its performance, and to allow the necessary expansion to other applications and *in-vivo* use.

When the improved tactile feedback system was integrated with a non-robotic laparoscopic grasper, it was found that tactile feedback significantly decreased the grip force of novice subjects during laparoscopic training, but had little impact on experts.

After designing a new water insulation methodology, the system was integrated with the da Vinci surgical robot and used for the first time in a live tissue experiment. This experiment showed that there was a high variability between subjects, and that there was a correlation between the amount of force used and amount of damage observed. Most expert and novice subjects used significantly decreased grasping forces, and had significantly fewer sites of damage when evaluated by a blinded pathologist, but some of this may have been caused by familiarization with the task.

The first prototype remote surgery system with tactile feedback was developed by combining three existing systems: The University of Washington RAVEN-II, the UCLA LapaRobot, and the improved tactile feedback system. In a preliminary investigation of remote surgery over a simulated network with delays of 100 ms and then 1 ms, there were decreases in grasping force for most subjects, and more significant retention when the time delay was minimized.

Together these findings suggest that tactile feedback may be a beneficial addition to minimally invasive surgical systems – especially for cases with heavy cognitive demand, such as training of novice users, challenging control schemes, and when handling delicate tissue – and that efforts should continue to advance the feedback system towards clinical viability.

The dissertation of Christopher Robert Wottawa is approved.

Erik P. Dutson

James Warwick Bisley

Martin O. Culjat

Victor R. Edgerton

E. Carmack Holmes

Warren Grundfest, Committee Chair

University of California, Los Angeles

2013

Dedicated to my parents: Kathy and Robert,  
my sisters: Allison, Kaitlin, and Lorraine,  
and to Betty, my partner in crime.

# Table of Contents

<b>1</b>	<b>Introduction.....</b>	<b>1</b>
<b>2</b>	<b>Background .....</b>	<b>4</b>
2.1	Minimally Invasive Surgery (MIS).....	4
2.1.1	Laparoscopic Surgery .....	4
2.1.2	Robotic Surgery .....	6
2.1.3	Remote Surgery and Mentoring.....	8
2.2	Feedback Modalities .....	9
2.3	Tactile Sensing Physiology.....	11
2.4	Tactile Feedback .....	12
2.4.1	Tactile Actuation.....	13
2.4.2	Tactile Actuation Technologies .....	14
2.4.3	Force Sensing.....	15
2.4.4	Force Sensing Technologies .....	16
2.4.5	Complete Tactile Feedback Systems .....	20
2.4.6	Initial Version of the CASIT Tactile Feedback System .....	23
<b>3</b>	<b>Research Objectives.....</b>	<b>27</b>
<b>4</b>	<b>Improvements to Tactile Feedback System Design .....</b>	<b>29</b>
4.1	Force Sensors .....	30
4.1.1	Initial Version .....	31
4.1.2	Sensor Improvements.....	32
4.1.3	Insulating Sensors From Moisture .....	33
4.1.4	Validation of Waterproof Sensors .....	36
4.2	Balloon Actuators .....	39
4.2.1	Initial Version: Six Tube Actuator for Robotic Surgery.....	39
4.2.2	Single Tube Actuator for Laparoscopic Grasper .....	40
4.3	Pneumatic System.....	42
4.3.1	Initial Version (Electro-Pneumatic Regulator) .....	42
4.3.2	Three-Level Digital Valve System .....	43
4.3.3	Five-Level Digital Valve System.....	44
4.4	Electronic System .....	46
4.4.1	Initial Version (Texas Instruments Evaluation Board) .....	46
4.4.2	Two-Part Wireless System (dsPIC / Bluetooth) .....	47
4.5	User Interface.....	50
4.6	Control Software.....	52
4.6.1	Functional Overview.....	53
4.6.2	Data Collection .....	53
4.6.3	Communication.....	54
4.6.4	Data Processing: Jitter Reduction Algorithm .....	56
4.6.5	Actuator Control .....	58
4.6.6	Complete System .....	58
4.7	Summary of System Improvements.....	59
<b>5</b>	<b>Evaluation of Tactile Feedback in Laparoscopic Surgical Training .....</b>	<b>61</b>
5.1	Laparoscopic Grasper Tactile Feedback System Integration.....	61
5.2	Laparoscopic Grasper Grip Force Study.....	63



5.2.1	Methods.....	63
5.2.2	Results.....	65
5.2.3	Discussion.....	67
<b>6</b>	<b>Evaluation of Tactile Feedback in Robotic Surgery for Potential Clinical Application using an Animal Model.....</b>	<b>68</b>
6.1	System Preparation and Integration with da Vinci Surgical System.....	68
6.2	Robotic Surgery Grip Force Study in an Animal Model.....	72
6.2.1	Methods.....	72
6.2.2	Statistical Analysis and Results.....	78
6.2.3	Discussion.....	99
6.2.4	Conclusion.....	101
<b>7</b>	<b>Expansion of Tactile Feedback to Remote Surgical Systems.....</b>	<b>103</b>
7.1	Remote Tactile Feedback System.....	103
7.1.1	System Development.....	103
7.1.2	Estimating Transcontinental Latency.....	104
7.2	Initial Integration with Remote Surgery Systems.....	107
7.2.1	University of Washington RAVEN II.....	107
7.2.2	UCLA LapaRobot Tele-Mentoring System.....	110
7.3	The LapaRaven: A Combination Remote Surgery System with Integrated Tactile Feedback.....	113
7.3.1	LapaRaven Hardware.....	114
7.3.2	LapaRaven Software.....	115
7.3.3	Tactile Feedback Integration.....	122
7.4	Remote Surgery Grip Force Study.....	124
7.4.1	Methods.....	124
7.4.2	Statistical Analysis and Results.....	126
7.4.3	Discussion.....	128
<b>8</b>	<b>Conclusion.....</b>	<b>130</b>
<b>9</b>	<b>Future Work.....</b>	<b>132</b>
9.1	Robotic Surgery Training Study.....	132
9.2	Evaluating Tactile Feedback on Additional Performance Metrics.....	133
9.3	Custom Micro-scale Force Sensing Array.....	133
9.4	Improvements to the Tactile Feedback System.....	135
9.4.1	Scalable Continuous Pneumatic System.....	135
9.4.2	On-board Wireless Integration.....	136
9.5	Continued RAVEN-II Collaborations.....	136
9.6	Trans-continental Remote Surgery Tactile Feedback Studies.....	138
	<b>References.....</b>	<b>138</b>

## LIST OF FIGURES

Figure 1. Laparoscopic surgery involves several small "keyhole" incisions around a patient's abdomen. Open surgery provides access to internal structures through a single large incision. ....	4
Figure 2. Laparoscopic Graspers .....	5
Figure 3. The da Vinci Surgical System .....	7
Figure 4. (Left) The da Vinci control console. (Right) The EndoWrist robotic end-effector.....	7
Figure 5. Mechanoreceptors [].....	12
Figure 6. Tactile feedback system concept. ....	13
Figure 7. Da Vinci Surgical Grasper.....	15
Figure 8. (Left) Flexiforce commercial piezoresistive sensor from Tekscan. (Right) The layers of a Flexiforce sensor. The Pressure sensitive ink is the piezoresistive material.....	17
Figure 9. Pressure Profile Systems Digitacts Technology.....	18
Figure 10. Cross section of capacitive sensor by Schostek et. al. [138].....	19
Figure 11. The grasper mounted sensor and motor driven tactile display by Ottermo et. al.....	21
Figure 12. Ottermo et. al. tactile feedback system laparoscopic training simulator.....	21
Figure 13. One degree of freedom tactile feedback grasper from Hasha et. al.....	22
Figure 14. Tactile Feedback System Block Diagram. ....	23
Figure 15. Optimized actuator configuration in the.....	24
Figure 16. (Right) Grasping of the tissue phantom with the da Vinci robotic system. Marks appeared on the film at grasping locations; color intensity of the marks was proportional to the grasping force. (Left) Pressure-indicating film resulting from a grasping trial without tactile feedback (top) and with tactile feedback (bottom). ....	25
Figure 17. Mean grip force results for one expert subject .....	25
Figure 18. Results from perceptual study, (D-C-P: Dorsal, Central, Proximal / L-R: Left-Right). .....	26
Figure 19. System Block Diagram for Improved Tactile Feedback System .....	30
Figure 20. Example initial version of trimmed sensor.....	31
Figure 21. Initial version of force sensor. (Left) Single Element and (Right) Six element array. ....	32
Figure 22. Improved trimming process replaces two.....	33
Figure 23. Improved sensor mounting process, (Left) on a laparoscopic instrument (Right) On a da Vinci Grasper .....	33
Figure 24. Parylene Coater from Specialty Coating Systems.....	34
Figure 25. Flow chart for sensor insulation process. (1) Start with full sensor. (2) Cut bottom and crimp wires (3) Trim top of sensor to size. (4) Wrap trimmed sensor completely using parafilm. (5) Coat in parylene. (6) Perform submersion tests. (7) Trim box out of center. (8) Coat box using Silithane 803. Allow it to dry overnight. (9) Add a second coat of parylene. (10) Perform a second submersion test. ....	35
Figure 26. (Left) Sensors wrapped in a wet paper towel. (Right) Sensors submerged in a water bath.....	36
Figure 27. Waterproof sensors were validated by performing an underwater peg transfer.....	37
Figure 28. (Left) Sensor-equipped graspers on tissue in a leporine cadaver. (Right) Grip force recordings.....	37
Figure 29. Moisture insulated sensors used for live tissue experiments.....	38
Figure 30. Characterization of coated and uncoated sensors. Dashed lines are a linear fit. ....	38
Figure 31. Initial version of actuators .....	40

Figure 32. (Left) CAD Drawing of mold for single tube actuator. (Right) Single tube actuator during fabrication.....	41
Figure 33. The single tube is cut so that it joins easily and supports the actuator substrate.....	41
Figure 34. (Left) Single-Tube actuator mold for laparoscopic surgery .....	42
Figure 35. (Left) SMC ITV-0010 pressure regulators mounted in the da Vinci Surgical System (Right) Functional Block diagram of initial pneumatic system.....	43
Figure 36. Three-Level Valve Pneumatic System .....	43
Figure 37. Block Diagram of Three-Level Valve Pneumatic Systems.....	44
Figure 38. Version 3 of pneumatic system (five-level) with high precision regulators and solenoid valves.....	45
Figure 39. Block diagram for Five-Level Valve Pneumatic System .....	45
Figure 40. (Left) Two part control system with using DSP Evaluation Board (TI ezDSP2808) and a custom signal conditioning board. (Right) Block diagram for Version 1 Control Hardware .....	46
Figure 41. Block diagram for second version of electrical control system. ....	47
Figure 42. Transmitter mounted on the da Vinci robot .....	48
Figure 43. Transmitter Circuit Board, System Block Diagram .....	48
Figure 44. Receiver circuit placed near the da Vinci console.....	49
Figure 45. Receiver Circuit Board, System Block Diagram.....	49
Figure 46. Haptic Controller Interface – Data Collection Window .....	51
Figure 47. Haptic Controller Interface – Parameter Adjustment Window .....	52
Figure 48. Control Software, top level functional block diagram. ....	53
Figure 49. Data Collection Block Diagram .....	54
Figure 50. Communication block. Arrows represent different message types. ....	54
Figure 51. Layered code Infrastructure.....	55
Figure 52. Data Processing Block.....	57
Figure 53. Simple threshold algorithm suffers from sporadic balloon inflation/deflation when the sensor signal hovers around the level transition threshold. ....	57
Figure 54. Anti-jitter algorithm separates the rising and falling thresholds, resulting in smoother balloon behavior.....	58
Figure 55. Actuator Control Block .....	58
Figure 56. Full Block Diagram of Control Software .....	59
Figure 57. (Top) Completed Laparoscopic grasper. (Bottom left) Piezoresistive force sensors mounted onto the grasper tip. (Bottom Right) Single-tube actuators mounted flush in the handles. ....	61
Figure 58. Tactile feedback system mounted in a plastic project enclosure.....	62
Figure 59. Tactile Feedback system integrated into a non-robotic laparoscopic grasper.....	63
Figure 60. Novice subjects: peak and average grip force results.....	65
Figure 61. Expert subjects: peak and average grip force results.....	66
Figure 62. Waterproof sensor mounted on robotic grasper .....	69
Figure 63. The transmitter circuit mounted on the da Vinci robotic system. ....	69
Figure 64. Actuators mounted on the da Vinci master controls. ....	70
Figure 65. The receiver circuit and pneumatic system housed in a plastic enclosure and positioned near the da Vinci console, along with a back-up air canister.....	70
Figure 66. The da Vinci with tactile feedback being used to run porcine bowel .....	73
Figure 67. Observing surgeon during the dry run of the live tissue study.....	73

Figure 69. Questionnaire for Robotic Surgery Tactile Feedback Study.....	76
Figure 70. Linear relationship between ADC values and force for coated.....	77
Figure 71. Example of damaged bowel. (Left) Gross exam indicated hemorrhagic tissue (Right) Corresponding histology image shows focal hemorrhage in muscularis propria.....	78
Figure 72. Force data for all subjects.....	80
Figure 73. Force data, expert subjects .....	80
Figure 74. Force data, novice subjects.....	80
Figure 75. Force data, attending surgeons only. ....	81
Figure 76. Force data, surgical residents .....	81
Figure 77. (Left) An example of light (L1) damage. (Right) An example of heavy (L3) damage where pathologist noted a possible disrupted serosion .....	84
Figure 78. Number of damage sites, all subjects .....	85
Figure 79. Number of damage sites, only experts .....	85
Figure 80. Number of damage sites, only novice subjects .....	86
Figure 81. Number of damage sites, only attending subjects .....	86
Figure 82. Number of damage sites, only residents.....	86
Figure 83. Correlation analysis of damage and mean grasping force.....	88
Figure 84. An example of a subject with no effect due to tactile feedback. ....	90
Figure 85. An expert subject with already low forces .....	90
Figure 86. One subject showed higher forces with tactile feedback.....	91
Figure 87. A subject with lower and completely retained forces .....	91
Figure 88. An example of subject with force results that were Lower and Not Retained. ....	92
Figure 89. An example of subject with force results that were Lower and Partially Retained. ...	93
Figure 90. Subject-by-Subject Analysis: Classification of all subjects, both hands.....	93
Figure 91. Subject-by-Subject Analysis: Classification of all subjects, (Left) only dominant hand (Right) Non-dominant hand.....	94
Figure 92. Subject-by-Subject Analysis: (Left) Classification of the five expert subjects (six or more robotic surgery cases). (Right) and the Novice subjects.....	95
Figure 93. Subject-by-Subject Analysis: Classification of (Left) attending surgeons and (Right) surgical residents.....	95
Figure 94. Live Tissue Study Survey Results, Questions 1 to 3.....	97
Figure 95. Live Tissue Study Survey Results, Questions 4 to 6.....	98
Figure 96. Live Tissue Study Survey Results, Questions 7 to 9.....	98
Figure 97. Remote Surgery Tactile Feedback System Architecture.....	103
Figure 98. Total latency of the remote tactile feedback system .....	104
Figure 99. (Left) Neither sensor nor pneumatic system is activated at 17.890 s. (Center) Sensor contact at 17.894 s. A voltage divider circuit causes an LED to turn on. (Right) Pneumatic system LED turns on at 17.947 s. Processing latency for this trial was 53 ms.....	105
Figure 100. Histogram of the one-way transcontinental internet latency. ....	106
Figure 101. (Left) Pneumatic system LED off, and no balloon inflation at 50.142 s (Center) Pneumatic system activated (LED on) at 50.146 s. (Right) Balloon inflation at 50.182 s. Filling time for this trial was 36 ms.....	106
Figure 102. The RAVEN-II Surgical Robot.....	108
Figure 103. Commercially available force feedback controllers (Phantom Omni) used for RAVEN-II control. ....	109

Figure 104. (Left) The LapaRobot Control Station allows the surgeon to tele-operate using standard laparoscopic instruments in a conventional arrangement. (Right) The surgical robot is operated to perform the training task. ....	111
Figure 105. Initial version of Remote Tactile feedback system with .....	111
Figure 106. Second Version of LapaRobot Telementoring System .....	112
Figure 107. Overview of LapaRaven Concept .....	113
Figure 108. LapaRaven Hardware .....	114
Figure 109. Software Block Diagram for LapaRaven Controller (LapaRobot) .....	116
Figure 110. LapaRaven Software Block Diagram.....	117
Figure 111. LapaRaven Console Output.....	118
Figure 112. Robot Device Data Structure.....	120
Figure 113. Param_pass data structure .....	121
Figure 114. LapaRaven with Tactile Feedback, System Overview .....	122
Figure 115. (Left) Raven grasper tip (Right) Flexiforce sensor mounted .....	123
Figure 116. Pneumatic actuator mounted on LapaRobot instrument handle.....	123
Figure 117. (Left) Subjects used the LapaRaven to retrieve six vertically mounted dimes. (Right) Perspective from the LapaRobot Master.....	125
Figure 118. Mean grip forces for remote surgery grip force study, all five subjects.....	126
Figure 119. Mean forces for all subjects when using the LapaRaven with (Left) 100 ms delay (Right) 1 ms delay.....	128
Figure 120. Process flow of the capacitive sensor design. ....	134
Figure 121. Capacitive sensor fabricated at UCLA Nanoelectronics facility.....	134
Figure 122. Design concept for motorized pneumatic regulator .....	136
Figure 123. The Mimic dV Trainer.....	137

## LIST OF TABLES

Table 1. Summary of mechanoreceptor classifications .....	11
Table 2. Communication Protocol Message Types .....	55
Table 3. Non-Robotic Training Study: Hypothesis Testing for Novices.....	65
Table 4. Non-Robotic Training Study: Hypothesis Testing for Expert Subjects .....	66
Table 5. Pressure Outputs for Live Tissue Experiments.....	71
Table 6. Live Tissue Experiment Software Thresholds.....	72
Table 7. P-Values for force data hypothesis testing using Friedman's test.....	82
Table 8. P-Values for tissue damage hypothesis testing.....	86
Table 9. Summary of latency estimates for remote tactile feedback system .....	106
Table 10. LapaRaven Run Levels.....	119
Table 11. LapaRaven Control Modes .....	119
Table 12. Hypothesis Testing for LapaRaven Grip Force Study.....	127

## ACKNOWLEDGEMENTS

I would like to acknowledge the continued support and guidance of my primary advisors, Dr. Warren Grundfest, Dr. Martin Culjat, and Dr. Erik Dutson, and committee members, Dr. James Bisley, Dr. E. Carmack Holmes, and Dr. V. Reggie Edgerton.

I would also like to thank everyone at the Center for Advanced Surgical and Interventional Technology (CASIT), specifically Cheryl Hein and Holly Chung.

I would like to thank CASIT alumni Adrienne Higa, Chih-Hung Aaron King, and Miguel Franco for starting this project, alumni Richard Fan for his electronics expertise in developing the new control system, Alan Priester for his tireless work with the RAVEN II, fellow tactile feedback researcher Zach McKinney, Jim Garritano for his advice on Matlab, statistical methods, and trunk automation, and Dr. Bryan Nowroozi for his expertise in animal research, technical writing, and staying organized.

This research continues to depend on the collaborative spirit of other research groups. I would like to especially thank the Computer Graphics and Vision Laboratory in Computer Science including Dr. Petros Faloustos, Dr. Demetri Terzopoulos, Brian Allen, Gabriel Nataneli, Konstantinos Sideris, and Matthew Wang; The Mechantronics and Controls Laboratory in Aerospace and Mechanical Engineering, including Dr. Tsu-Chin Tsao, Christopher Lim, Stephen Prince, Kevin Chu, Christopher Kang, and James Simonelli; Dr. Robert Candler's MEMS research group including Omeed Paydar, Jere Harrison, and Xiaoxu Wu, and RAVEN II collaborators Professor Blake Hannaford, Professor Jacob Rosen, and H. Hawkeye King.

Animal experiments proceeded only with support from UCLA facilities and collaborators, especially co-investigator Dr. Steven Hart in the Department of Pathology, Dr.

Joanne Sohn, Dr. Charles Gates, Guillermo Moreno and the rest of staff at the Division of Laboratory Animal Medicine (DLAM), and Dr. Clara Magyar and the staff of the Translational Pathology Core Laboratory (TPCL).

I would also like to thank Dr. Jim Sayre for his consultations on statistical methods; medical student Jeremiah Cohen for his expertise in mechanical engineering, medicine, and study design; Brett Jordan and Will Pannell for designing and machining custom laparoscopic handles; Sophie Suhna Jang for her work on the single tube actuator design; exchange students Florian Kasper and Laura Coltuc; undergraduates Adina Wolkenfield and Phillip Qian for actuator fabrication, undergraduate Jacob Sharf for software support; Dr. Shane White and Dalene Sederstrom for use of their Instron System; Professor Timothy Deming's lab including Ilya Yakovlev, Jessica Kramer, and April Rodriguez for letting me borrow large quantities liquid nitrogen for the parylene coater, and Matt Weisbart for his invaluable machining expertise.

I would like to acknowledge generous funding provided by the Telemedicine and Advanced Technology Research Center (TATRC) / Department of Defense under award numbers W81XWH-07-1-0672 (Project 2) and W81XWH-09-1-0709 (Project 10), the National Institutes of Health (NIH)/ National Institute of Biomedical Imaging and Bioengineering (NIBIB) under award 1-R21-EB-013832-01A1, the National Science Foundation (NSF) under award number CBET-0730213, the NSF Major Research Instrumentation (MRI) Group for providing funding for a RAVEN II Telesurgery System, and the John Bent Foundation.



## VITA

- 2005                    B.S. Engineering, Harvey Mudd College,  
*Tau Beta Pi Engineering Honor Society*
- 2005                    Embedded Systems Engineer, Meshtel, Inc.
- 2005 – 2007           Programmer Analyst, Evolution Robotics Retail
- 2008 – 2013           Graduate Student Researcher, Center for Advanced Surgical and  
Interventional Technology (CASIT), UCLA, Warren Grundfest
- 2009                    M.S. Biomedical Engineering, University of California, Los Angeles
- 2012                    Certified Professional Engineer, Electrical Engineering, California Board  
for Professional Engineers, Land Surveyors, and Geologists

## PUBLICATIONS AND PRESENTATIONS

- Wottawa C**, Fan RE, Lewis CE, Jordan B, Culjat MO, Grundfest WS, Dutson EP (2009). Laparoscopic grasper with an integrated tactile feedback system. *Complex Medical Engineering*, 2009 ICME/IEEE International Conference on, 9-11 April 2009, Tempe, AZ, 2009.
- Fan RE, **Wottawa C**, Boryk RJ, Sander TC, Wyatt MP, Grundfest WS, Culjat MO (2009). Pilot testing of a tactile feedback rehabilitation system on a lower-limb amputee. *Complex Medical Engineering*, 2009 ICME/IEEE International Conference on, 9-11 April 2009, Tempe, AZ, 2009.
- Natarajan S, **Wottawa CR**, Dutson, EP (2009). Minimization of patient misidentification through proximity-based medical record retrieval. *Complex Medical Engineering*, 2009 ICME/IEEE International Conference on, 9-11 April 2009, Tempe, AZ, 2009.
- Fan RE, **Wottawa CR**, Wyatt MP, Sander TD, Culjat MO, Grundfest WS. A wireless telemetry system to measure gait in patients with lower limb amputation. *International Telemetry Conference 2009*, Las Vegas, NV 26-29 October 2009

Culjat MO, Bisley JW, **Wottawa C**, Fan RE, Dutson EP, Grundfest WS. “Tactile Feedback in Surgical Robotics”, Surgical Robotics - System Applications and Visions, ed. Jacob Rosen, Blake Hannaford, Richard Satava. Springer, 2010

**Wottawa C**, Fan FE, Bisley JW, Dutson EP, Culjat MO, Grundfest WS. Applications of tactile feedback in medicine. Studies in Health Technology and Informatics. (2011) 163:703-709

Paydar OH, **Wottawa CR**, Fan RE, Dutson EP, Grundfest WS, Culjat MO, Candler RN. Fabrication of a Thin-film Capacitive Force Sensor Array for Tactile Feedback in Robotic Surgery. Engineering in Medicine and Biology Society (EMBC), 2012 pp: 2355-2358

**Wottawa CR**, Cohen JR, Fan RE, Bisley JW, Culjat MO, Grundfest WS, Dutson EP. The Role of Tactile Feedback on Grip Force during Laparoscopic Training Tasks. Proceedings Society of American Gastrointestinal and Endoscopic Surgeons (SAGES) Conference, 7-10 March 2012

**Wottawa CR**, Lim C, Fan RE, Culjat MO, Dutson EP, Tsao TC, Grundfest WS. A Remote Tactile Feedback System for Telesurgery and Telementoring. 2012 Biomedical Engineering Society (BMES) Annual Meeting: Atlanta, 24-27 October 2012

**Wottawa CR**, Cohen JR, Fan RE, Bisley JW, Culjat MO, Grundfest WS, Dutson EP. The Role of Tactile Feedback in Grip Force during Laparoscopic Training Tasks. Surgical Endoscopy (2013) 27:1111–1118

**Wottawa CR**, Priester A, Kang C, Simonelli J, Tsao TC, Dutson EP, Grundfest WS. Integration of the University of Washington RAVEN II Surgical Robot, UCLA LapaRobot Tele-mentoring System, and the UCLA Remote Tactile Feedback System. 14th UC System-wide Bioengineering Symposium. 19-21 June 2013.

# 1 Introduction

Minimally invasive surgery (MIS) has revolutionized surgical care by reducing cost, pain, and trauma to the patient, decreasing the need for medication, and shortening recovery times [1-3]. In all types of minimally invasive surgery, including robotic, laparoscopic, and remote surgery, the surgeon is no longer directly interfacing with the patient. As a result, tactile information is altered, or in the case of robotic procedures, completely absent.

A tactile feedback system was previously designed at CASIT [4] and integrated with the da Vinci Surgical System. It measured forces at the tips of a robotic grasper and provided proportional forces to the fingertips of the operating surgeon. Preliminary investigation showed that adding supplemental tactile feedback significantly reduced grip force during robotic surgery training and with tissue phantoms [5].

The purpose of this research was to extend the tactile feedback technology to three new minimally invasive surgery (MIS) applications – non-robotic laparoscopic surgery, remote surgery, and *in-vivo* robotic surgery – and to perform studies to evaluate the benefit of tactile feedback in each of these applications.

In 2008, this research inherited a functioning tactile feedback system. An analysis was performed on this system that determined improvements necessary for expansion of the system to live tissue studies and remote surgical applications. Some aspects of the system were retained, such as the optimized actuator configuration, while others, such as the pneumatic system, electronics, and software, were completely redesigned. Additional subsystems were designed and integrated, such as a new data acquisition interface and methods to protect the sensors from *in-vivo* moisture. The improvements were essential for bridging the gap between *in-vitro* testing and

*in-vivo* feasibility and resulted in a system that showed faster, more reliable performance, increased robustness, and better ergonomics.

This new tactile feedback system was integrated into a non-robotic laparoscopic grasper, which required the design of a new single-tube actuator. After a subsequent grip force study, it was found that tactile feedback significantly decreased the grip force of novice subjects during laparoscopic training, but had little impact on experts.

A new water insulation methodology was designed and implemented to protect the force sensors and allow preclinical evaluation of the system in an animal model. The improved tactile feedback system was integrated into the da Vinci surgical system and used for the first time in live tissue experiments. When attending surgeons and surgical residents used this system to run porcine bowel, it was found that tactile feedback resulted in significantly decreased grasping forces and significantly fewer sites of damage when evaluated by a blinded pathologist. These low force and damage levels were retained for the third block of trials, indicating that the improvements may have also been caused by increased familiarity with the task. A significant correlation was found between high average forces and incidence of damage, which suggested that decreasing grasping force may have clinical benefit.

The tactile feedback technology was expanded for use in remote surgery. Two remote surgical systems were considered for integration: The University of Washington's RAVEN-II, and the UCLA LapaRobot. Because of limitations in each of the systems, a new combination system, *The LapaRaven*, was developed. The tactile feedback system was expanded to remote surgery through leveraging the communication protocol and adding Ethernet-connected computers to the loop. When integrated into the LapaRaven, this demonstrated the first prototype remote surgery system with integrated tactile feedback. A preliminary investigation (five

subjects) was performed over a simulated network with a 100 ms time delay. This investigation showed that tactile feedback resulted in significant decreases in grasping force for three of the five subjects, and that this low force was not retained when the system was deactivated for the third block of trials. When the study was repeated with a minimal time delay (1 ms), results were similar to the live tissue study: decreased grip force that was retained when the system was deactivated in the third condition.

It is widely cited that one of the most significant technical disadvantages associated with robotic surgery is the complete lack of haptic feedback [6-8]. This research has shown that reductions in grasping force are correlated with reductions in damage to tissue, and that tactile feedback tends to be most beneficial when there is a large cognitive demand, such as novices learning to perform laparoscopic or robotic surgery, or subjects struggling to use the LapaRobot controller.

Together these results lend support for continued improvement of the tactile feedback technology towards clinical viability, either for training of novice surgeons or long-term use with surgical robotic and minimally invasive training systems.

## 2 Background

### 2.1 Minimally Invasive Surgery (MIS)

Traditional approaches to surgical intervention underwent a paradigm shift in the mid 1980's with the introduction of video-based laparoscopic surgery. In open surgery, a surgeon views the field directly through a single large incision and manipulates tissue directly with his or her hands or hand-held tools. In minimally invasive surgery (MIS) procedures use smaller incisions (typically < 2 cm) to accomplish similar tasks. In MIS, a surgeon views the surgical field indirectly through the use of an endoscope and external monitors and accesses internal anatomy with the help of specialized instruments.

#### 2.1.1 Laparoscopic Surgery

Minimally invasive surgery that occurs around a patient's abdomen is called *laparoscopic surgery*. A comparison between laparoscopic and open cholecystectomy is shown in Figure 1.

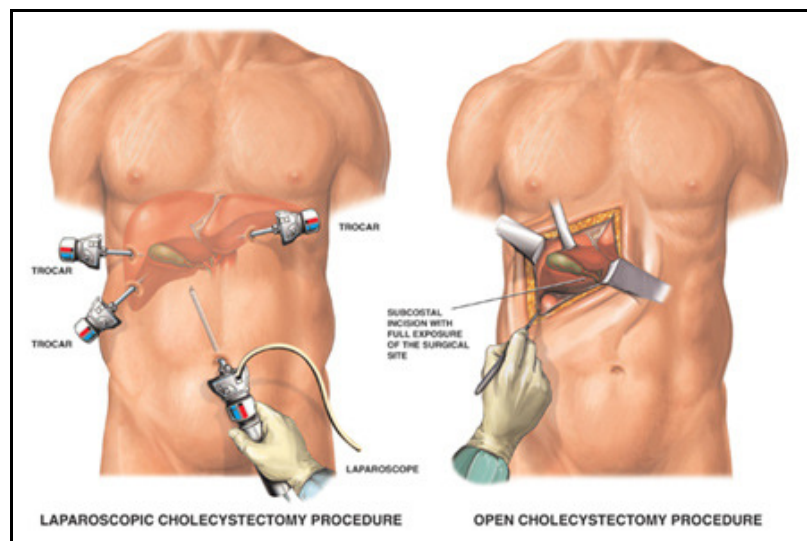


Figure 1. Laparoscopic surgery involves several small "keyhole" incisions around a patient's abdomen. Open surgery provides access to internal structures through a single large incision.

In laparoscopic surgery, the abdomen is insufflated with carbon dioxide to create a larger working area. Incisions are made and ports created into the body using trocars. The endoscope and laparoscopic instruments are inserted through the trocars and into the working space.

Various laparoscopic instruments have been made for different applications (Figure 2), including needle drivers, staplers, retractors, scissors, electrocautery hooks, and bowel graspers.



Figure 2. Laparoscopic Graspers

Currently, over 96% of cholecystectomies are performed laparoscopically, with a 5% estimated rate of conversion to open [9]. Laparoscopic techniques have also found use in adrenalectomy [1], gastric bypass [10], Nissen fundoplication [11], hysterectomy [12], colorectal resection [13], gastrectomy [14], nephrectomy [15], and splenectomy [16].

Despite the advantages of laparoscopic surgery, there are still technical difficulties. Laparoscopic instruments have only four degrees of freedom, compared to the six available in natural wrist motion (yaw and pitch are missing). This decrease has an adverse affect on range of motion and surgeon dexterity. There is a reduction in depth perception due to monoscopic endoscopes [17]. During open procedures, surgeons can directly interface with tissue, but during laparoscopic surgery, there is no direct contact between surgeon and patient, and therefore haptic

information altered, dampened, or lost. This loss of haptic information can lead to excessive grip force which has resulted in reported events of tissue damage [18-23].

Due to these drawbacks and the difficulty in performing these procedures, laparoscopic surgeries can sometimes have increased operating times and higher equipment costs. Moreover, these technical difficulties require surgeons re-learn how to perform operations with significant handicaps due to limited access to the patients' body cavities.

### **2.1.2 Robotic Surgery**

Robotic surgical systems were developed in the late 1990's to overcome some of the inherent limitations of laparoscopic surgery [6,24-28]. While still offering video-based, minimally-invasive approaches to surgical intervention, the evolving robotic systems provided surgeons with modifications such as increased degrees of freedom to better mimic natural hand and wrist gestures, stereoscopic video displays to mimic more natural visual interpretation of the surgical field, and scaling of surgical gestures to enable precision movements and eliminate natural tremor [29-30]. As of 2013, commercial robotic systems offer no mechanism for restoring lost haptic information.

Commercial robots for minimally invasive laparoscopic surgery started with the introduction of the Automated Endoscopic System for Optimal Positioning (AESOP) by Computer Motion Inc, and continued with the da Vinci Surgical system (Figure 3) by Intuitive Surgical in 1999 [31-32], and the Zeus Surgical System in 2001 by Computer Motion, Inc [6]. In 2003, there was a merger between Intuitive Surgical and Computer Motion and the Zeus and AESOP robots were discontinued. As of 2013, the da Vinci has seen three generations of improvements, including the addition of a fourth arm in 2003, the *da Vinci S* in 2006 and the *da*



*Vinci Si* in 2009 [33]. More recently, Intuitive Surgical has developed a dual console system and a *Skills Simulator* in collaboration with Mimic Technologies [34].



Figure 3. The da Vinci Surgical System

Surgeons operate with the da Vinci system by using a control console to remotely manipulate robotic arms with mounted instruments (Figure 4).

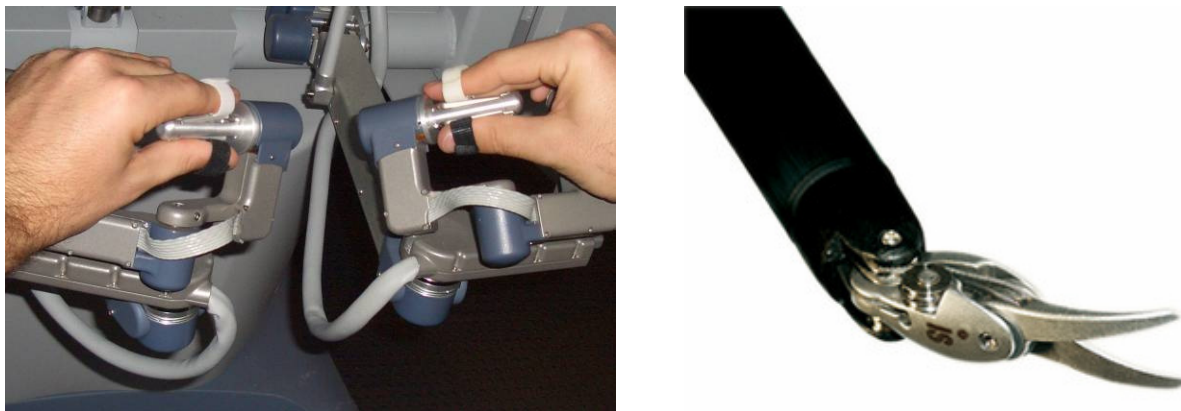


Figure 4. (Left) The da Vinci control console. (Right) The EndoWrist robotic end-effector

Robotic surgery has found most acceptance in radical prostatectomy where estimates of cases performed robotically range from 67% to 85% [35]. The tight working spaces in urological procedures benefit greatly from the improved dexterity and precision afforded by the EndoWrist instruments.

Robotic surgery has also been used for hysterectomy [36], gastric bypass [37-38], cholecystectomy [39], adrenalectomy [40], mitral valve repair [41-42], and coronary bypass [43],

among others. Despite the advantages of robotic surgery, traditional open or laparoscopic surgical techniques continue to be preferred for these types of procedures. Part of this is due to high equipment costs, the need for large equipment in a constrained operating room, the need for additional training, and the lack of evidence proving a realizable cost-benefit. A significant technical disadvantage associated with robotic surgery is the continued absence of haptic feedback [6, 7, 44].

### **2.1.3 Remote Surgery and Mentoring**

The development of surgical robotics has enabled the exploration of tele-surgery and tele-mentoring. Tele-surgery refers to procedures where a surgeon operates on a patient in a remote location, whereas tele-mentoring refers to the ability of an expert to consult on procedures from a distance.

A remote or tele-surgical cholecystectomy was successfully performed on a human in a transatlantic operation in 2001 [45-46]. Several porcine pyeloplasties were successfully performed remotely from Ontario to Nova Scotia in 2008 [47]. The NEEMO 7 underwater mission evaluated the feasibility of tele-surgery in a simulated space environment [48].

Many other research platforms have been developed for tele-surgery applications [49-55] with characterized time delays for control and video signals ranging from 155 ms to 800 ms. Much effort has been directed towards predictive algorithms and codecs to reduce critical latency [56-60], and the effect of latency on performance has been analyzed [61-64]. Interoperability of many robotic systems was also previously evaluated through a collaboration between fourteen institutions with distinct robotic platforms [65].

While it is thought that expansions in tele-surgery may improve surgical care in rural clinics, on the battlefield, and in space exploration, the prohibitive cost of dedicated

communication lines and the high availability of hospitals and surgeons in urban areas has limited its use to research [66].

In contrast to tele-surgery, the benefits of tele-mentoring are more apparent, especially for more unique cases where surgical expertise is limited [67]. Currently, tele-mentoring is achieved through a teleconferencing or tele-presence system, where the remote expert observes a video feed and provides auditory consultations to operating surgeons. Studies have shown significant performance improvements due to tele-mentoring [68], and the Society of Gastrointestinal and Endoscopic Surgeons (SAGES) has published guidelines for its continued use [69].

In robotic surgery systems, there is no tactile contact between surgeon and patient. In tele-surgical systems and hands-on tele-mentoring systems, this separation is even more pronounced. In these cases, there is a complete absence of tactile feedback, which forces mentoring or remote surgeons to rely solely on the potentially delayed video feed.

In laparoscopic, robotic, and remote surgery, the absence or altering of tactile information continues to be a significant technical drawback. Adding tactile feedback may allow surgeons to manipulate tissue with reduced grip force, significantly reducing the chances of causing tissue damage and the fatigue that may occur in longer procedures. This may accelerate the expansion of minimally invasive techniques, and its inherent benefits to the patient, into other specialties.

The purpose of this research is to evaluate the benefits of tactile feedback in laparoscopic, robotic, and remote surgery, specifically with regards to reduced grip force and tissue damage.

## ***2.2 Feedback Modalities***

Feedback systems utilize sensory substitution or sensory augmentation to provide tactile information that is previously attenuated or unavailable to the user.

Restoring this tactile information can be accomplished through a number of different feedback modalities, including visual, auditory, electrical, temperature, and tactile stimulation [70-73]. Of these modalities, electrical, visual, and tactile stimuli have been the most widely explored [74].

Electrical stimulation uses either non-invasive surface electrodes (electrocutaneous or transcutaneous) or more invasive subcutaneous and intraneural implantation methods. Practical complications can arise due to noise from skin moisture or mechanical deformations, and issues of biocompatibility and immune responses to implanted objects [75]. These difficulties as well as the surgical requirements of implanted devices have limited widespread adoption of the technology [76].

While visual information may appear to be sufficient for many procedures, the neurological processing delay can add significant challenges for tasks that requiring precise finger movements. Van der Putten et. al. (2010) performed a study comparing visual and tactile feedback and found that tactile feedback offered slightly improved performance [77].

Translating forces from surgical tools directly to the skin of the finger avoids issues related to sensory substitution. Whenever a feedback modality utilizes a mode-change (i.e. tactile to visual), there is a large temporal deficit, leading to slower response times, and a loss of efficiency. This added step may even require active processing by the surgeon, potentially attenuating the benefits of real-time sensory feedback with time delays and added stress. Using tactile feedback to display tactile information to surgeons is natural, and requires no neurological training.

## 2.3 Tactile Sensing Physiology

*Haptics* refers to the ability to perceive the environment through the sense of touch, and consists of the acquisition of both *tactile* and *kinesthetic* information [78]. Tactile perception is felt through pressure against or motion across the skin. Tactile sensations are generated by receptors on the skin in response to a mechanical deformation often caused by a local force. This differs from kinesthetic perception (i.e. proprioception), which relates to the movement of muscles and joints and is useful in determining a limb's position in space [79].

Sensory nerve afferents are classified based on the physiological response (slow-adapting or fast-adapting) and size of the receptive field (small or large). Fast adapting (FA) afferents respond only when the skin initially contacts a stimulus, whereas slowly adapting (SA) afferents respond both to the initial contact and then continue to be active throughout the period of contact. Type I afferents respond to indentation over small regions of skin. Type II afferents respond to stimuli presented over larger areas, with SA-II afferents preferring skin stretch and FA-II afferents responding best to high frequency vibration. Together, these afferents describe the interaction between the skin and the physical world (Table 1, Figure 5) [80].

Table 1. Summary of mechanoreceptor classifications

Type	Receptive Field	Adaptation	Frequency Response	Receptor
SA-I	Small	Slow	0.4 – 10 Hz	Merkel Disks
SA-II	Large	Slow	0.4 – 100 Hz	Ruffini Organs
FA-I	Small	Fast	2 – 40 Hz	Meissner Corpuscle
FA-II	Large	Fast	100 – 1000 Hz	Pacinian Corpuscle

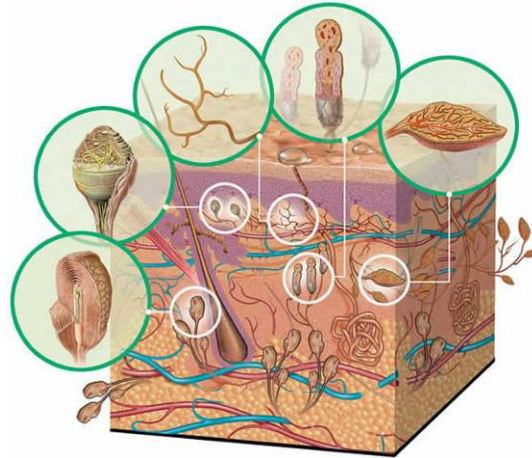


Figure 5. Mechanoreceptors [81]

When an object is held between the thumb and forefinger, it is held with just enough force to keep the object in place. Too little force drops the object, but too much force may damage it. This gripping force is usually determined by sensory-motor memory, but is fine tuned by reflexes that monitor slippage of the object. Although proprioception plays an integral role in motor control, the fine control of grip force is driven by a reflex mediated by tactile afferents innervating the fingertip [82-83].

## **2.4 Tactile Feedback**

Tactile feedback is commonly accomplished by applying mechanical deformations to the user's skin, thereby activating sensory mechanoreceptors. These systems have found applications in surgical and industrial robotics, virtual reality, and video games [84-91]. Tactile feedback systems may also have application to rehabilitation systems for tasks such as restoration of fine motor control in the hands, balance correction, and lower-limb sensory restoration [92-94].

It has been suggested that the addition of tactile feedback to robotic surgical systems may improve the precision and control of existing robotic surgery procedures, reduce the occurrence of tissue damage, and reduce the fatigue associated with longer procedures. The improved

control may also reduce the learning curve associated with robotic surgery, and facilitate its expansion to a wider range of procedures.

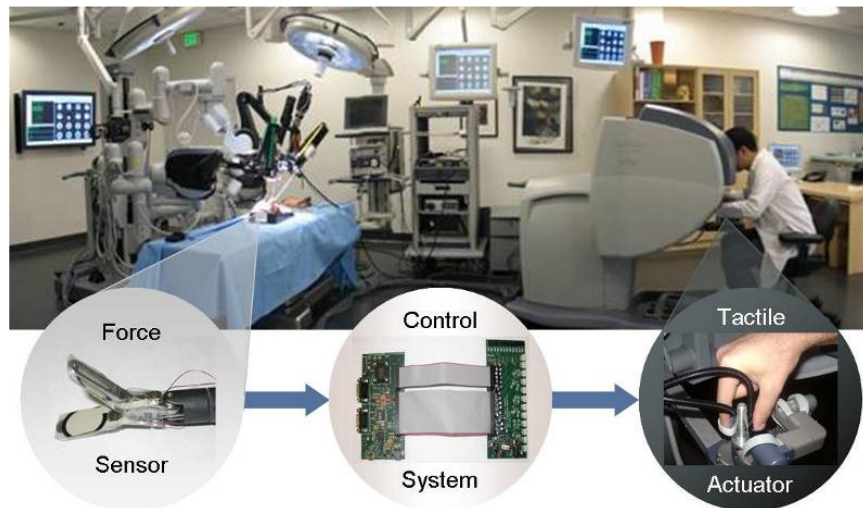


Figure 6. Tactile feedback system concept.

Tactile feedback systems require three components: sensors for measuring touch or force at the robotic instrument, actuators for conveying this information to the operator, and a control system that translates between the two (Figure 6).

### 2.4.1 Tactile Actuation

Tactile actuation designs are driven by size, perceptibility, and response time objectives. The temporal and spatial resolutions of the fingertip in response to pin stimuli are approximately 5.5 ms and 2 mm, respectively [95]. For circular or hemispherical stimuli to the fingers, Braille dots serve as a better model than pins. In Standard American Braille, Braille dots are 1.45 mm in diameter, 0.48 mm in height, spaced 0.89 mm apart, and grouped in 3.79 x 6.13 mm cells [96]. The slowly adapting (SA) mechanoreceptors of the finger are sensitive to spherical stimuli and encode Standard American Braille with high efficiency [97].

The da Vinci is a finger-controlled system with limited mounting space, and the master controls are subject to various rotational and translational movements. In order to provide

sufficient information to the operator while occupying a small footprint, the individual actuator array elements must be small (0.5 – 5.0 mm) and allow for narrow element-to-element spacing.

## **2.4.2 Tactile Actuation Technologies**

Several tactile feedback actuation schemes have been developed by others as non-invasive means to provide sensory feedback [98], including motor driven actuation [99-100], vibrotactile displays [74], piezoelectric actuators [101], shape memory alloys [102-103], rheological fluids [104, 105], vacuum systems [106], and pneumatically driven actuators [107-111]. Caldwell et. al. (1999) designed an integrative tactile feedback array which included pneumatic actuators, piezoelectric elements, and a Peltier effect system for thermoreceptor stimulation [112]. Many of these tactile systems are effective for a variety of applications. Limitations with these designs to medical applications can include adaptation effects, low force output, slow response time, or large and bulky mechanical configurations.

Vibrotactile actuators, which are among the most popular tactile actuation schemes, have been shown to function with the greatest spatial resolution at 250 Hz [113], innervating the fast adapting Pacinian corpuscle sensory receptors (FA II) [114]. While vibrotactile actuators can operate with high spatial resolution, stimulation of the fast adapting sensory receptors has a desensitizing effect, decreasing perception in the long term [74]. Therefore, this technology may not be clinically viable for extended use in surgical robotics [71].

Pneumatic balloon actuators are well suited for surgical robotics, since they address many of the design constraints described above. They have the advantage of large force output, large deflection, rapid response time, and low mass [115]. Actuation frequency and intensity can be electronically specified to respond to adaptation limitations. This concept has been explored



previously for different applications, including aerodynamic control and tactile feedback to the fingertip [110, 116-117].

### 2.4.3 Force Sensing

The limited application of tactile feedback to minimally invasive surgical systems has been primarily due to the challenge of integrating sensors into surgical graspers. A variety of force and pressure sensors have been developed, but few current technologies meet the size constraints of current laparoscopic equipment, sterilization and biocompatibility criteria, and appropriate force resolution for use in surgical operation [118].

Pressure sensing systems are primarily constrained by small mounting surfaces. The da Vinci's Cadiere graspers (Figure 7), which are among the largest instruments, have a contact area of 5 mm x 14 mm, and an end-effector thickness of 3 mm. Force sensors any wider or thicker than this results in a complete loss of functionality, as the tool no longer fits through the trocar.

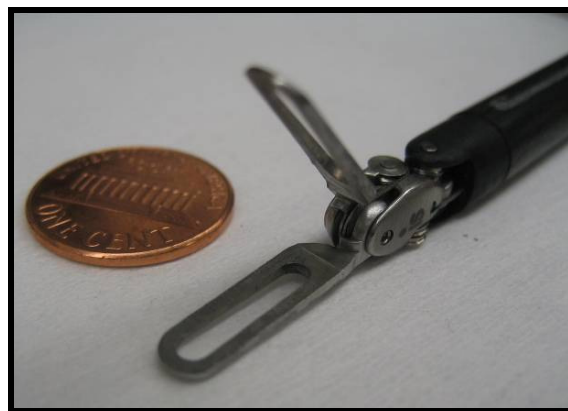


Figure 7. Da Vinci Surgical Grasper

Sensor systems must survive wet, in-vivo environments, be biocompatible, survive high temperature or chemical sterilization procedures, and not interfere with nearby electrocautery devices. The sensor must have negligible obtrusiveness and negligible latency. Forces felt by

surgical tools are typically in the 0–5 N range, but can go as high as 20 N and last an average duration of 2-3 seconds [119].

#### **2.4.4 Force Sensing Technologies**

Tactile sensing has becoming a mature field, with two commercially available thin-film sensors (Tekscan and Pressure Profile Systems) and many prototype designs across various research institutions, employing a vast array of sensing modalities and configurations. Many technologies, including capacitive, piezoresistive, and piezoelectric sensing modalities, have been used for thin film force sensing in research prototypes [120-121].

##### ***Piezoresistive Sensing***

Piezoresistive sensors make use of semiconductive materials' property of changing electrical resistance when under mechanical strain. When combined with a voltage driving circuit, changes in applied force can be converted to changes in output voltage. There are many different types of piezoresistive sensor designs. Geometries include membrane designs (strain gauge) and sandwich designs where a piezoresistive substrate sits between two metal electrodes. High stiffness semiconductor materials (polysilicon), doped elastomers, and commercial piezoresistive pastes have all been used as piezoresistive substrates. Many research groups have developed piezoresistive sensors, but none of these yet meet the size and precision constraints of surgical graspers [122-126].

Tekscan commercially sells Flexiforce sensors, which are single element piezoresistive sensors with a circular 1 cm diameter contact area, and dynamic ranges of 1, 25, and 100 lbs force [127]. The Flexiforce sensors utilize a piezoresistive paste from Electro Science Laboratories (ESL RS15114) and vary the thickness to vary the sensor's dynamic range.

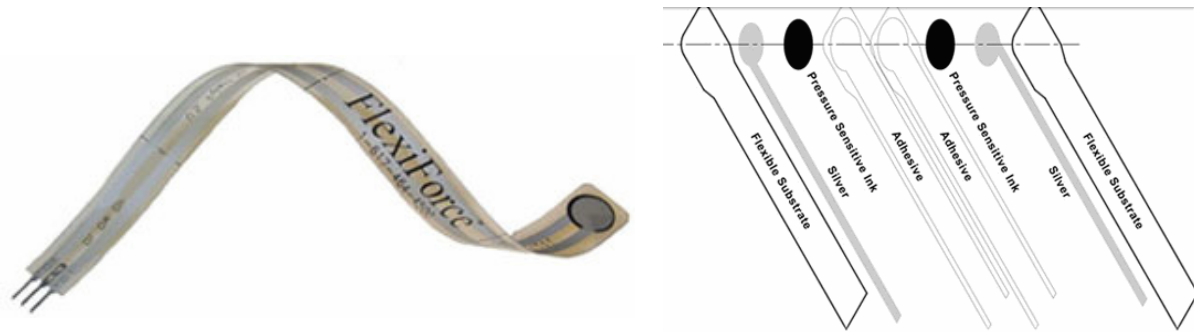


Figure 8. (Left) Flexiforce commercial piezoresistive sensor from Tekscan. (Right) The layers of a Flexiforce sensor. The Pressure sensitive ink is the piezoresistive material.

The CASIT feedback system uses modified Tekscan Flexiforce sensors (Figure 8). Benefits of using this sensor include low cost, low manufacture overhead, thin film profile, quick response time, and appropriate force resolution. It is too large for a grasper, but can be trimmed to fit. When trimmed, it is not resistant to wet environments and possibly not biocompatible (ESL RS15114 is proprietary). These constraints require additional processing to prepare sensors for in-vivo environments.

Piezoresistive sensors are cited as having disadvantages of nonlinear responses, hysteresis, the need to optimize the mechanical and electrical configurations of the piezoresistive elastomer, and a high dependence on temperature. Advantages include wide dynamic range, and durability.

### ***Piezoelectric Sensing***

Piezoelectric sensors differ from piezoresistive sensors in that certain ferromagnetic materials, such as polyvinylidene fluoride (PVDF) or lead zirconate titanate (PZT), will generate a voltage when under an applied load, rather than a change in resistance. Dargahi et. al. (2000) developed a  $1 \times 4$  piezoelectric sensor array using thin film PVDF on a custom made laparoscopic grasper [128-130]. They cited a good response for a constantly changing 120 Hz

sinusoidal force input. However, with the application of a constant load, the piezoelectric sensor output quickly decays; therefore these types of sensors are most suited towards measuring dynamic force, rather than static force.

### ***Capacitive Sensing***

Most capacitive force sensors utilize a spring-like dielectric positioned between two conducting plates. The applied force compresses the dielectric, altering the distance between the plates and thus changing the capacitance. Circuitry measures this capacitance and translates it into a force differential. In 1996, Gray and Fearing introduced a capacitive pressure sensor array using rows of orthogonal copper strips (Figure 9) [131].

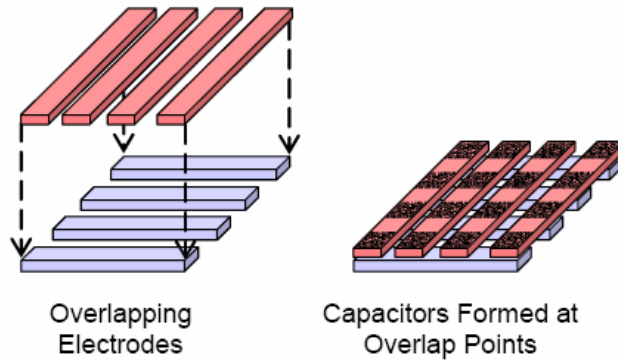


Figure 9. Pressure Profile Systems Digitacts Technology

Pressure Profile Systems (Los Angeles, CA) uses this method in their commercially available DigiTacts and TactArray systems [132]. These commercial sensors may not be suited for minimally invasive surgical applications due to size, the use of proprietary signal conditioning electronics, susceptibility to wet environments, and the use of potentially non-biocompatible materials in their design.

Other research groups have also developed sandwich geometry capacitive sensors [133-134], but these designs are generally too large for surgical instruments or only measure small force ranges.

In another capacitive sensing method, the applied force compresses two semi-conducting plates over a spherical electrode (Figure 10). In addition to changing the dielectric distance, this force increases the size of the contact area, thus increasing the capacitance. In 2006, Schostek et. al. used this method to develop a sensor array with 32 hexagonal elements into a customized 10 mm grasper tip [135]. Drawbacks cited with their array included element-to-element crosstalk and the need to individually calibrate each element. In 2010 Zhenan Bao et. al. used a similar technique with a PDMS dielectric layer and a geometry of tiny square pyramids to achieve force detection over a range of 0.003 – 0.03 N [125].

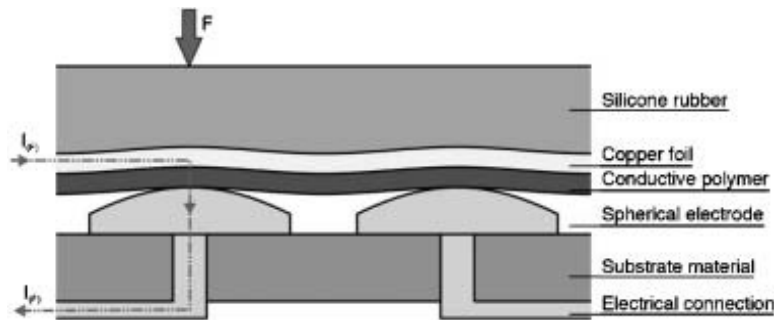


Figure 10. Cross section of capacitive sensor by Schostek et. al. [135]

Generally, advantages associated with capacitive sensors are wide dynamic range, high sensitivity, and precision. Limitations with these sensors include susceptibility to noise and limits in spatial resolution due to the physical area dependence of capacitance [120]. Due to the area constraints on capacitive sensors, fitting a high resolution sensing array onto a small mounting surface, such as the tip of a grasper, can be challenging. Potential element-to-element crosstalk increases the required spacing between elements that is required to achieve a particular signal to

noise ratio. Because of parasitic capacitance present in cabling, any signal processing electronics would need to be on the same chip.

### ***Other Methods***

Additional methods of measuring force include fluid filled elastometric skin [136], optical sensors [137-138], a membrane-enclosed vacuum chamber [139], and inductive sensor technologies [130]. These methods are not suitable for minimally invasive surgery due to thick size requirements, high complexity (moving parts), and interference to and from electrocautery systems that are commonly used during surgery. Many commercial load cells and strain gauges are also available, but are not practical for surgical robotics.

### **2.4.5 Complete Tactile Feedback Systems**

In addition to sensors and actuators, some research groups have published designs for complete tactile feedback systems for minimally invasive surgery.

Howe et. al. (1999) used a capacitive sensor array similar to that proposed by Gray and Fearing [131]. Tactile information is relayed back to the operator using shape memory alloys. Using this system, they demonstrated successful detection of sensor contact and feature localization. Drawbacks with the system include limitations in amplitude detection and encoding [8].

Moy et. al. (2002) used a similar capacitive sensor array mounted on a 1-DOF grasping jaw, and a 5 x 5 pneumatic actuator array. This system was used to detect fluid flow in artificial blood vessel. This system experienced jitter artifacts from the electronic and pneumatic components [140].

More recently, Ottermo et. al. (2009) used Pressure Profile Systems Digi-Tacts [132] commercially available capacitive sensor paired with an array of motor driven pins for providing feedback (Figure 11) [141]. This system was incorporated into a laparoscopic training simulator. (Figure 12)



Figure 11. The grasper mounted sensor and motor driven tactile display by Ottermo et. al.

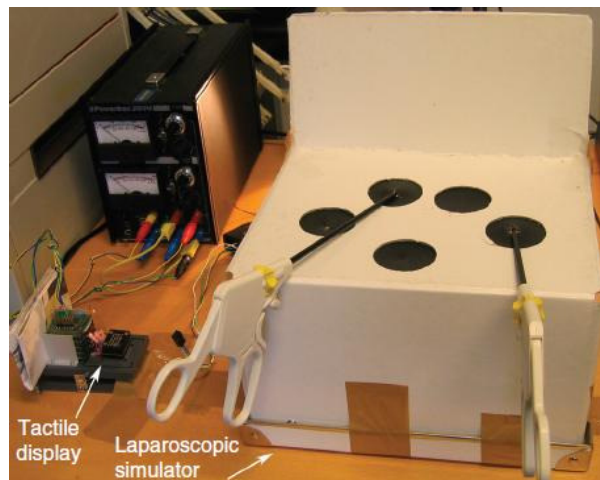


Figure 12. Ottermo et. al. tactile feedback system laparoscopic training simulator.

Kianzad et. al. (2011) paired commercial load cells with shape memory alloy wires to automatically control closure of minimally invasive graspers. In their system, force information was extracted from cable tension rather than directly from the tip of the grasper [142].

Harsha et. al. (2008) used linear motors to adjust handle resistance on a bilaterally controlled tactile feedback laparoscopic grasper master-slave robot (Figure 13) [143].

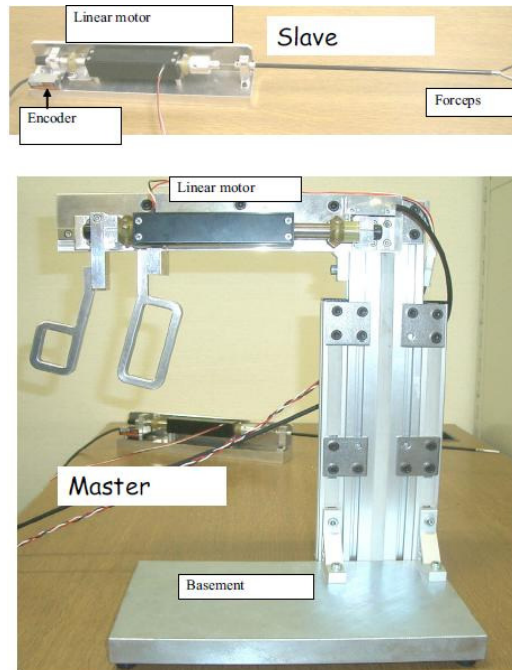


Figure 13. One degree of freedom tactile feedback grasper from Hasha et. al.

Schoonmaker et. al. (2006) designed a vibrotactile feedback system, with a magnetic vibration actuators mounted near the surgeon's foot. Force was measured by a commercial force/torque sensor mounted near the shaft of the tool [144].

Van der Putton et. al. (2010) also designed a feedback system where forces were measured using commercial load cells. In this system feedback alerts were displayed during times of excessive force through both visual and vibrotactile modalities. Using this system they found that augmented feedback improved grasping performance [77].

Rizun et. al. (2005) applied tactile feedback to a surgical laser system, where a the built-in force feedback of a PHANToM Omni haptic controller indicated contact between the laser's focal point and a surface [145].

Sarmah et. al. (2010) integrated a tactile-force feedback system onto a laparoscopic grasper. Piezoresistive sensors were used to measure force as was done with the CASIT tactile feedback system. This information is fed back to the surgeon through a visual display [146].



Custom tactile feedback devices have also been built for remote palpation applications. Zbyszewski et. al. (2008) used a fiber optic distance sensor paired with an air cushion to detect changes in soft tissue properties [147-149]. This method was successfully used in a tissue phantom [150].

## 2.4.6 Initial Version of the CASIT Tactile Feedback System

A tactile feedback system was previously designed at CASIT to measure forces at the tips of a robotic grasper and provide proportional forces to the fingertips of an operating surgeon. [4]. This system used piezoresistive force sensors mounted on a surgical grasper, silicone-based pneumatic balloon actuators mounted near the surgeon's fingertips, and electrical and pneumatic control systems that measure sensor values and control balloon inflation. A block diagram of this system architecture is shown in Figure 14.

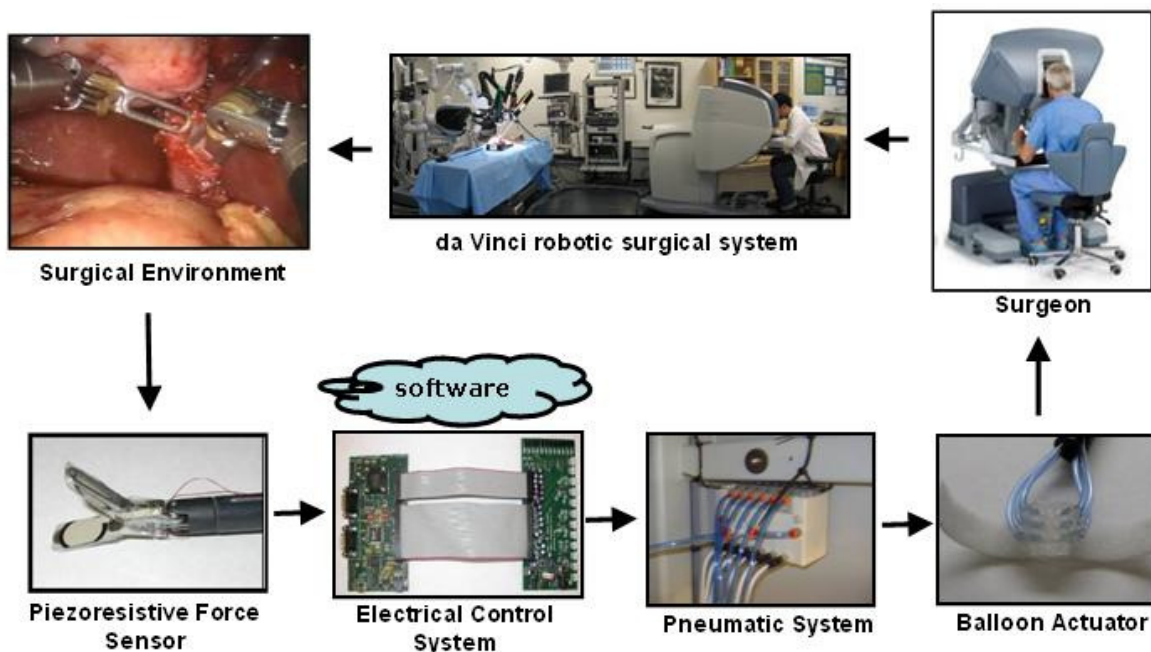


Figure 14. Tactile Feedback System Block Diagram.

Primary effort on this system included an optimization, characterization, and perceptual analysis of assorted balloon actuator configurations [5, 115, 151]. As a result of these experiments, it was determined that 3 mm diameter balloons, with 1.5 mm element spacing and 300  $\mu\text{m}$  membrane thickness provided the highest level of performance both mechanically and perceptually (Figure 15). Fatigue tests were performed and found the balloon actuators to have negligible hysteresis over at least 150,000 inflation-deflation cycles.

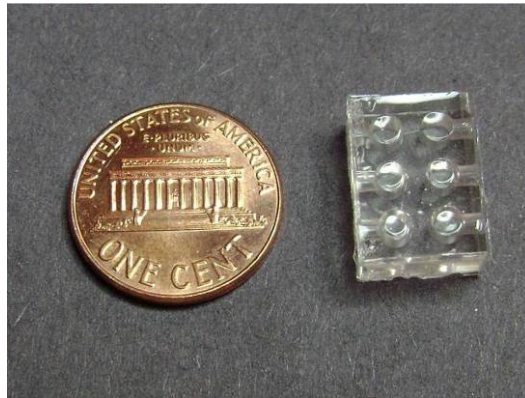


Figure 15. Optimized actuator configuration in the CASIT tactile feedback system

The system was integrated with the da Vinci Surgical System and used to perform four system evaluations and investigations into the benefits of tactile feedback during robotic surgery [152-153].

The first study explored the effect of tactile feedback on grasping. Subjects were asked to run a tissue phantom with an attached pressure-indicating film (Fuji Prescale Film LLLW). (Figure 16). All four films had fewer and lower intensity red spots when tactile feedback was used, indicating a lower grip force.

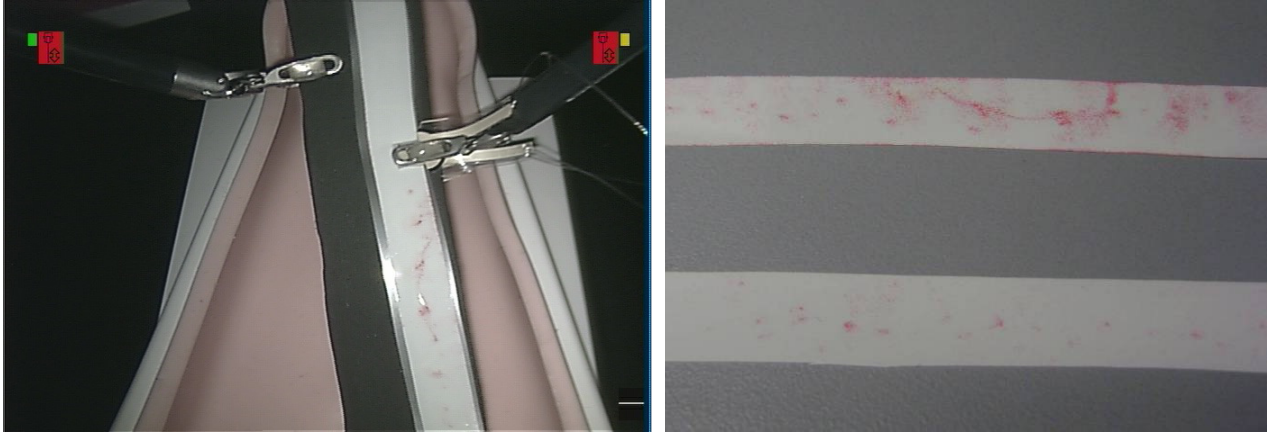


Figure 16. (Right) Grasping of the tissue phantom with the da Vinci robotic system. Marks appeared on the film at grasping locations; color intensity of the marks was proportional to the grasping force. (Left) Pressure-indicating film resulting from a grasping trial without tactile feedback (top) and with tactile feedback (bottom).

A second study quantified the effects of tactile feedback on grip force [152]. Twenty subjects (16 novices, 4 experts) used the da Vinci to perform a single-hand peg transfer task adapted from the Fundamentals of Laparoscopic Surgery (FLS) education module developed by the Society of American Gastrointestinal Endoscopic Surgeons (SAGES). Trials with tactile feedback resulted in significantly reduced grip force (Figure 17).

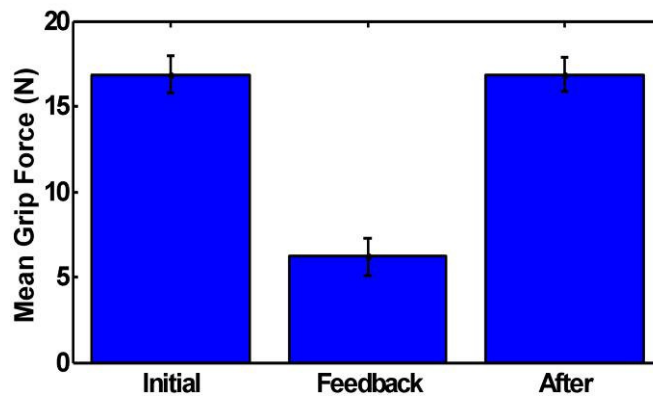


Figure 17. Mean grip force results for one expert subject

A third study, which examined system operability, found no significant difference in task performance ( $p = 0.078$ , Wilcoxon Sign Rank test) with and without the inactivated actuators, during peg transfer tests, indicating that the mounted, inactive actuators and pneumatics did not hinder task performance, ergonomics, or finger or arm movements [154].

The fourth study asked subjects to identify the location and/or sequence of the actuated stimuli on a  $3 \times 2$  element sensor array. The spatial perception tests found that there was a high accuracy in detection of single elements ( $> 96\%$ ) (Figure 18) [152].

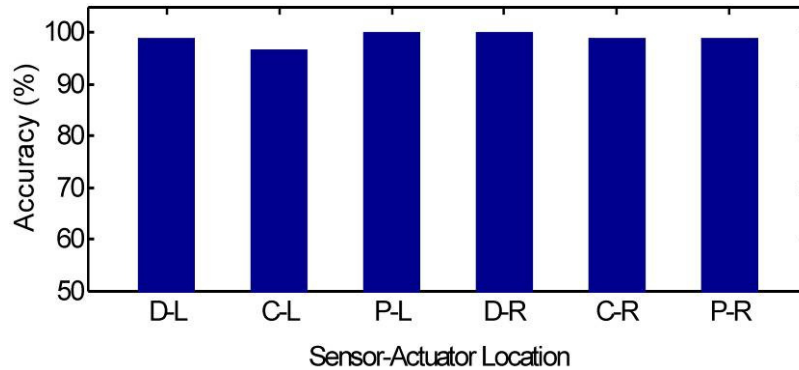


Figure 18. Results from perceptual study, (D-C-P: Dorsal, Central, Proximal / L-R: Left-Right). All elements successfully identified with 96% accuracy.

Together these studies demonstrated and quantified the benefit of tactile feedback, specifically in regards to reduced grip force for robotic surgery. However, further development of the system was needed to complete additional studies and to extend tactile feedback to other minimally invasive surgical applications, such as remote surgery and *in-vivo* use where more stringent design criteria are required.

### 3 Research Objectives

This research sought to accomplish three objectives:

- (1) Improve the tactile feedback technology, including sensors, actuators, electronics, software, and pneumatics.
- (2) Expand the tactile feedback technology to other minimally invasive surgical applications, specifically non-robotic laparoscopic surgery, remote surgery, and robotic surgery in an *in-vivo* environment for clinical evaluation.
- (3) Perform studies to evaluate the benefits of tactile feedback in minimally invasive surgery

These objectives were achieved through the completion of four tasks:

***Task I – Improve Tactile Feedback System Design:*** The previously designed system had sufficient functionality for initial evaluations of tactile feedback, but could not be used for future studies without modification. The purpose of the first task was to analyze the existing system, determine improvements necessary for future evaluations, and then perform an iterative redesign to implement these improvements.

***Task II – Evaluate Tactile Feedback in Laparoscopic Surgical Training:*** In laparoscopic surgery, the surgeon is not directly interfacing with tissue, and therefore tactile information is lost or altered. The purpose of this task was to determine if the addition of tactile feedback to non-robotic laparoscopic surgery helped novice and expert subjects perform training tasks with reduced grip force.

***Task III – Evaluate Tactile Feedback in Robotic Surgery for Potential Clinical Application using an Animal Model:*** The previous robotic surgery study suggested that tactile feedback reduced grip force during training tasks. The purpose of this task was to determine if this result extended to grip force when handling tissue, and if these differences in grip force resulted in a

reduction of tissue damage. For this purpose, a study was performed in a porcine model that evaluated grip force and tissue damage through pathological inspection of the grasped tissue.

***Task IV – Evaluate Tactile Feedback in Remote Surgery.*** In remote surgery, like robotic surgery, there is a complete absence of tactile information. Additionally, latencies in the visual feed potentially compound this loss. The purpose of this task was to integrate tactile feedback with a remote surgery system, and to perform a preliminary investigation on the impact of tactile feedback on training tasks when performed over-a-distance. A suitable, fully functioning remote surgery system was not available, and so a new one was designed by combining two available systems: The University of Washington RAVEN II and UCLA LapaRobot.

The rest of the dissertation will explore the methods and results of each of these four tasks in more detail.

## 4 Improvements to Tactile Feedback System Design

While the previously developed tactile feedback system was a suitable starting point for evaluating tactile feedback, an analysis of this system pinpointed ergonomic and functional deficiencies that prevented integration with other minimally invasive surgical systems as well as investigations using animal models.

When live tissue experiments were attempted with the original tactile feedback system, sensors quickly stopped functioning due to damage caused by the wet environment.

Surgeons and other expert users commented on the distracting nature of unintentional vibrations present in the actuator output, which was a result of the particular pneumatic system design.

The previous electrical system and control software only contained components for interfacing with the previous pneumatic system and needed to be redesigned. Additional practical concerns limited this system's use in the surgical setting, including excessive wiring that stretched from the da Vinci robot system to the da Vinci master control and the need for three separate power supplies.

The redesigned system operated with the same overall feedback architecture as before, but improvements were made to force sensors, pneumatics, electronics, and software (Figure 19). A new user interface was developed for data collection, troubleshooting, and adjusting threshold parameters during runtime, and a new single-tube actuator designed for non-robotic laparoscopic instruments.

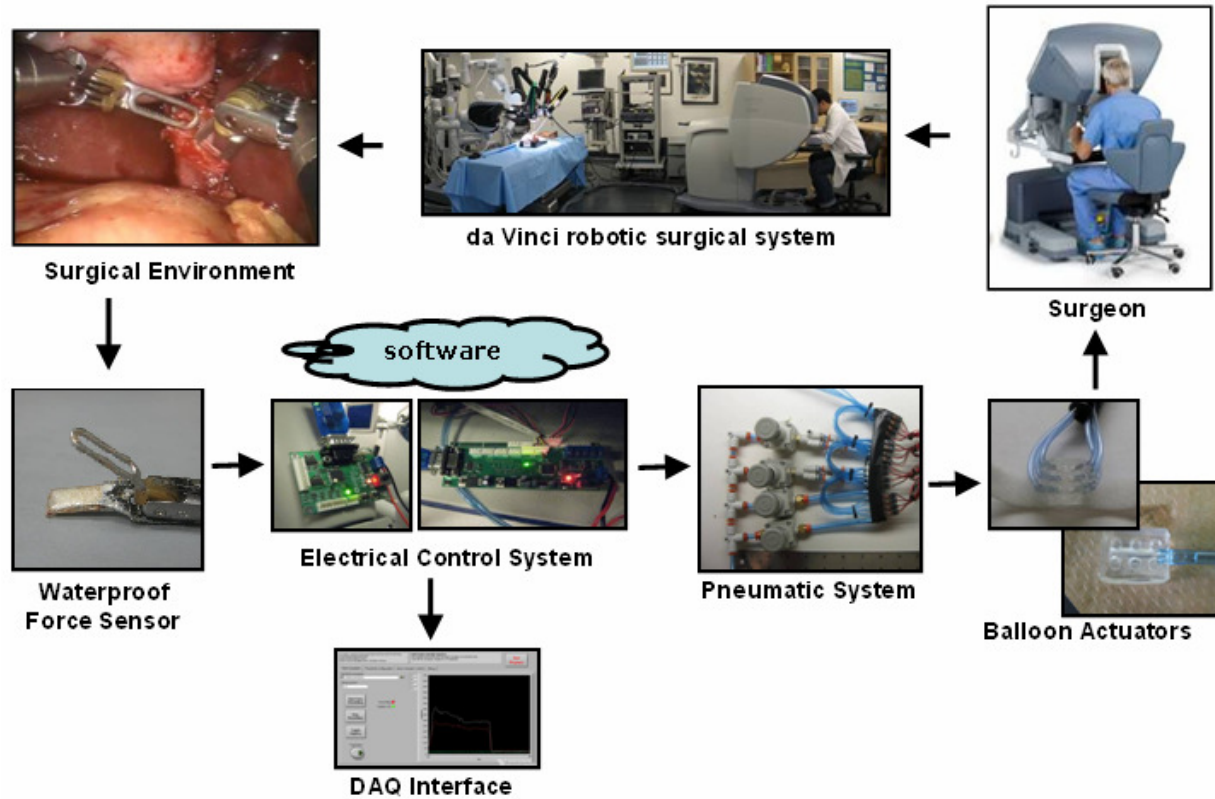


Figure 19. System Block Diagram for Improved Tactile Feedback System

The remainder of this section describes each of the subsystems in more detail, including descriptions of initial versions as well as the iterative redesign that resulted in the system used for later tactile feedback studies.

#### 4.1 Force Sensors

All versions used commercially available piezoresistive force sensors (Tekscan, Flexiforce®) mounted directly onto the end effectors of the minimally invasive surgical graspers, interfacing with the surgical environment by converting mechanical forces to changes in resistance. Improvements to the force sensor included increases in sensitivity, robustness of the mounting procedure, and a new methodology for insulating sensors from moisture.



### 4.1.1 Initial Version

In the initial system, the 25 lb model Flexiforce sensor was chosen due to its thin-film profile (208  $\mu\text{m}$ ) and small diameter (10 mm) as a low cost way of validating other components of the tactile feedback system.

The sensors were trimmed to match the size of the grasper tools (4.75 mm  $\times$  12.5 mm) (Figure 20) and mounted onto a grasper (Figure 21) [4]. Silver paste joined thin magnetic wire to the sensor leads.

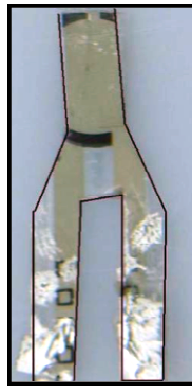


Figure 20. Example initial version of trimmed sensor.

A single element sensor had been converted into an array by incorporating a  $3 \times 2$  element array of gold electrode pads into the sensing pad. The gold sensing electrodes, traces, and interconnect electrodes were deposited on 127  $\mu\text{m}$  thick polyimide film (Dupont Kapton HN type) using a microfabrication process [154]. While the sensor array showed high perceptibility, in the end it was too large to fit comfortably on the tip of the laparoscopic grasper.

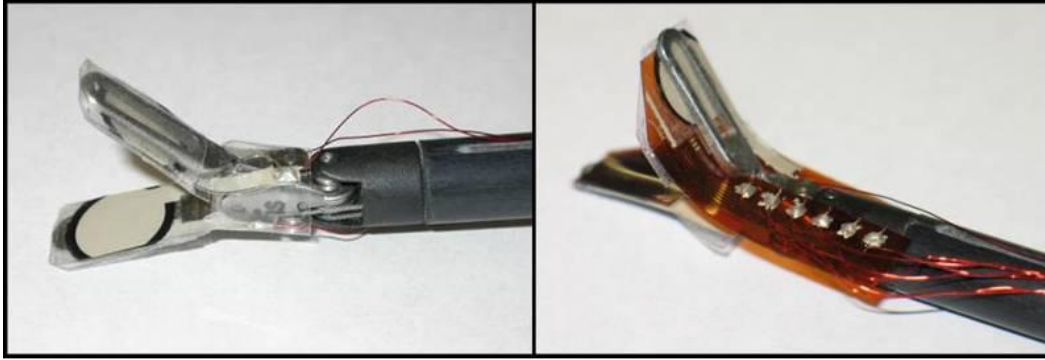


Figure 21. Initial version of force sensor. (Left) Single Element and (Right) Six element array.

The sensors were characterized using an Instron mechanical loading system (Instron 5544) over a force range of 0 to 25 N [154]. Both the single-element sensors and sensor array elements demonstrated a linear ( $R^2 > 0.99$ ) decrease in resistance with increases in force.

Despite its advantages, this sensor design suffered from drawbacks that limited both its clinical viability and short term use. Trimmed sensors often caught on objects in training field and tore. Silver paste didn't sufficiently hold the wires to the sensor pads. The thin magnetic wire became easily tangled, especially when stretched across the operating room. When this system was tested in an animal model, sensors quickly stopped functioning due to moisture damage.

#### **4.1.2 Sensor Improvements**

To improve sensitivity, the 1 lb Flexiforce sensor was used instead of the original 25 lb sensors. This allowed for detection of lighter forces, but also resulted in more frequent saturation.

To improve durability, the sensor modification and mounting procedure was completely redesigned. The sensor trimming process was changed so that the two tails were replaced with a box to provide access for the grasper (Figure 22).

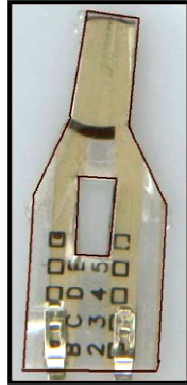


Figure 22. Improved trimming process replaces two tails with box slit for mounting on grasper.

Magnetic wire was replaced with 30 gauge wire wrap wire, which was better insulated, slightly sturdier, and also still flexible. The silver paste connection was replaced with sturdier crimps. Finally, heat shrink tubing was used as an added measure to secure the wires to the shaft of the non-robotic grasper.



Figure 23. Improved sensor mounting process, (Left) on a laparoscopic instrument (Right) On a da Vinci Grasper

These modifications resulted in a more robust grasper-mounted force sensor (Figure 23).

### 4.1.3 Insulating Sensors From Moisture

When live tissue experiments were attempted with the original tactile feedback system, sensors quickly stopped functioning due to damage caused by the wet environment.

Several moisture insulation methods were tested, including thin-film lamination, sealing with adhesives, heat shrink tubing, melting sensor edges, and parylene coating, but none of these

methods worked individually. Thin lamination (250  $\mu\text{m}$ ) and heat shrink tubing materials were too stiff, resulting in a significant damping effect. Sealing with tape did not offer sufficient protection from water. Other adhesives, such as RTV, added too much thickness to the sensor pad.

Parylene coating is a common method of coating materials. Some of the benefits of parylene coating include thin deposition ( $< 1 \mu\text{m}$ ), uniformity, high resistance to moisture, biocompatibility, electrical insulation, and high resistance to acids, bases, solvents, and bacterial agents. Parylene is coated through a process of chemical vapor deposition (CVD) using specialized equipment (PDS 2010, Specialty Coating Systems®) (Figure 24).



Figure 24. Parylene Coater from Specialty Coating Systems

Despite its advantages, parylene coating on its own resulted in malfunction of all sensors. After several experiments, it was determined that the parylene coating failure was caused by parylene flowing into the crevices of a trimmed sensor.

To take advantage of the benefits of parylene, a multi-layer approach to water insulation was designed. A flow chart of the entire process is shown in Figure 25.

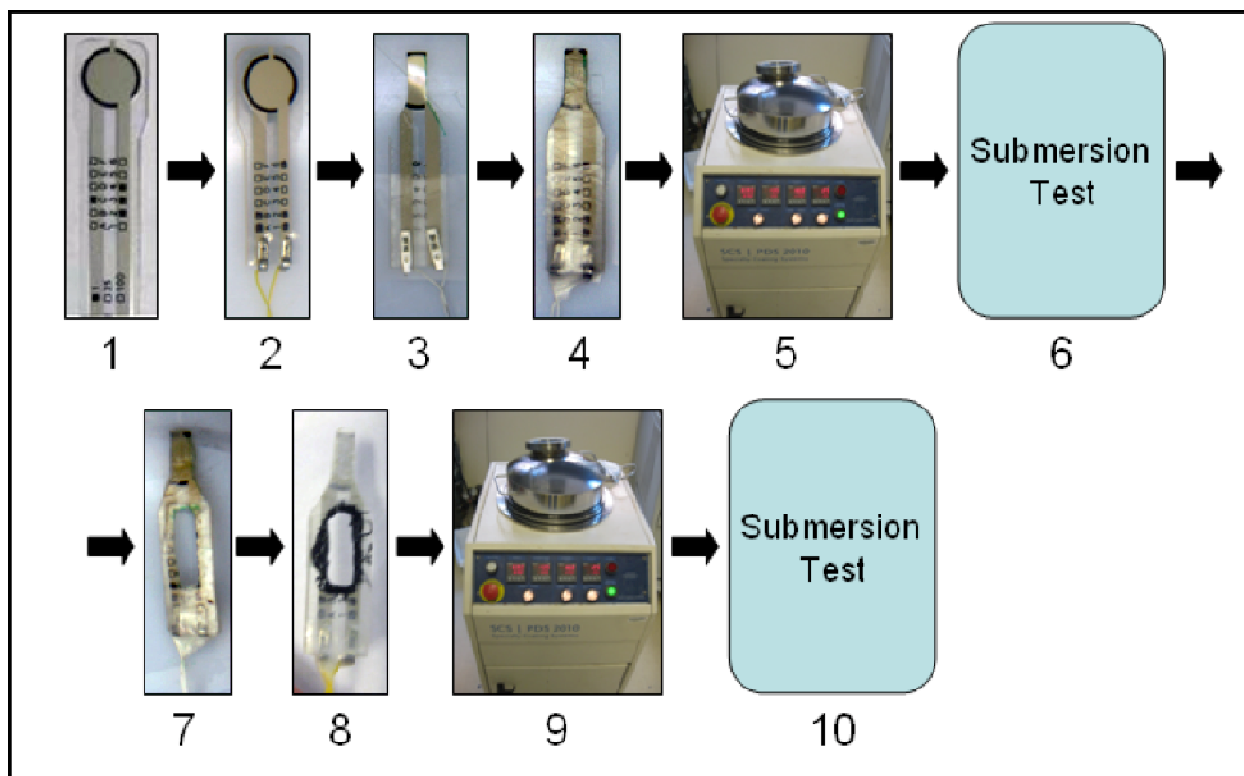


Figure 25. Flow chart for sensor insulation process. (1) Start with full sensor. (2) Cut bottom and crimp wires (3) Trim top of sensor to size. (4) Wrap trimmed sensor completely using parafilm. (5) Coat in parylene. (6) Perform submersion tests. (7) Trim box out of center. (8) Coat box using Silithane 803. Allow it to dry overnight. (9) Add a second coat of parylene. (10) Perform a second submersion test.

After trimming the sensor to size and crimping the wire connections, the sensor was wrapped in overlapping strips of Parafilm (Pechiney Plastic Packaging) using the “tennis racket” method. This parafilm layer protected the sensor from seeping parylene.

Parylene functioned as the second layer to ultimately protect the sensor from water and provide mechanical support for the Parafilm. For the box cut-out, Parafilm could not be used because of the harsh corners. However, thickness was also not a constraint in this area. Several paste adhesives were used in experiments for this box-cut out, including PSI-326 (Polymeric Systems, Inc), Silithane-803 (Polymeric Systems, Inc), and RTV-108 (Momentive). Ultimately Silithane-803 provided the most effective seal.

After coating the box cut-out using Silithane-803, another layer of Parylene was added. After each stage of the process, each sensor was re-tested using the LabVIEW User Interface/DAQ. After each Parylene coating step, the sensors were subjected to water, first using a paper towel and then a more rigorous submersion test (Figure 26). Due to variability in the layered coating process, not all sensors survived these submersion tests. However, the yield was high enough to fabricate a sufficient number of sensors for later experiments.

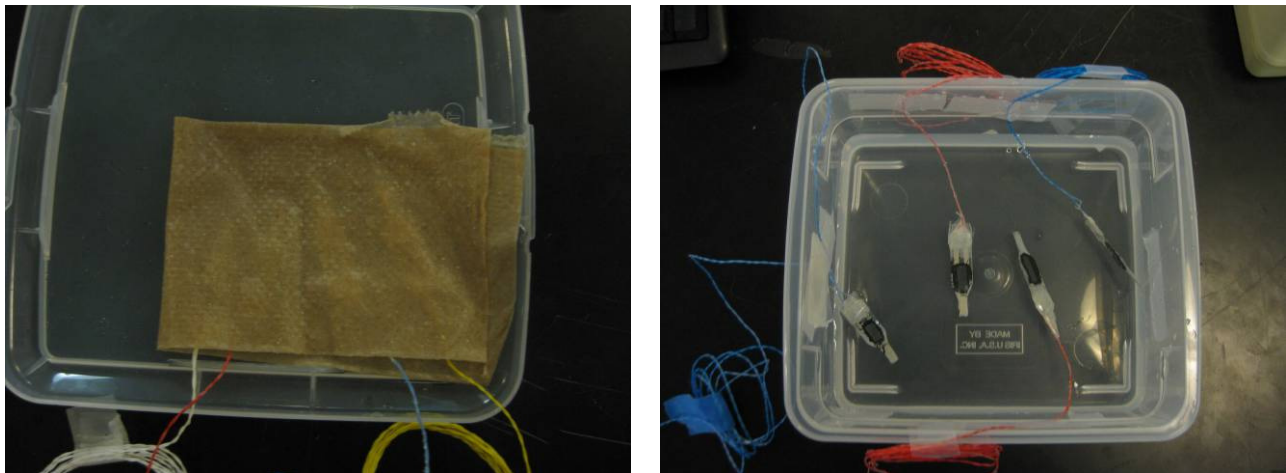


Figure 26. (Left) Sensors wrapped in a wet paper towel. (Right) Sensors submerged in a water bath

Prior to animal experiments, further tests were performed to validate the waterproofing process.

#### 4.1.4 Validation of Waterproof Sensors

Sensors insulated using the previously described process were validated through two experiments. In the first, a peg board was submerged in a water tank (Figure 27). Sensors were then mounted onto the ends of a robotic graspers and the da Vinci used to perform an underwater peg transfer.

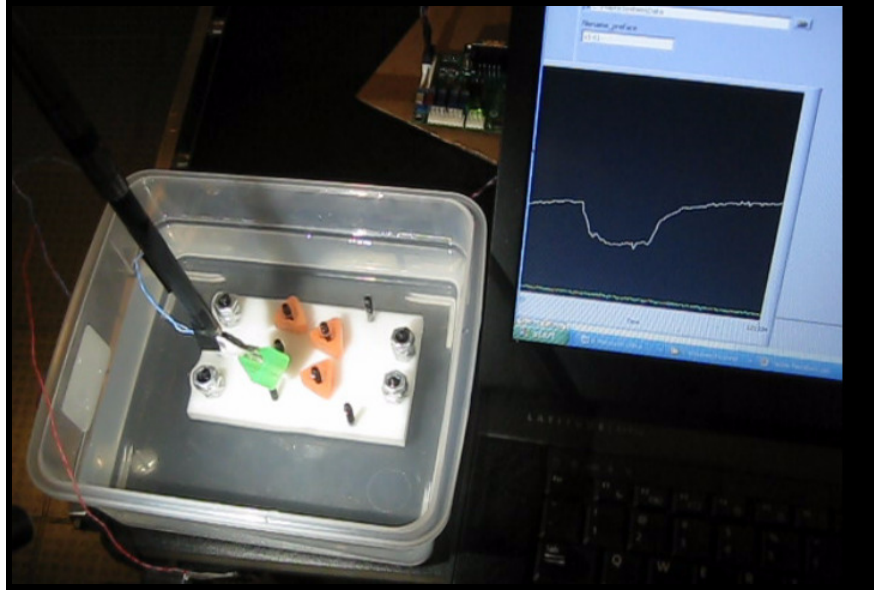


Figure 27. Waterproof sensors were validated by performing an underwater peg transfer.

In the second method, sensor-equipped graspers were used to grasp small intestine in a leporine cadaver. Functionality of the sensors during the grasping of tissue was validated, and sensor readings recorded (Figure 28).

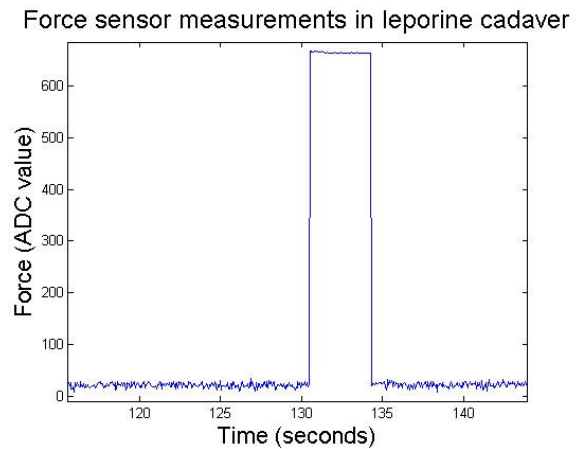


Figure 28. (Left) Sensor-equipped graspers on tissue in a leporine cadaver. (Right) Grip force recordings.

These experiments demonstrated the initial feasibility of using sensors coated with this process for subsequent studies in animal models.

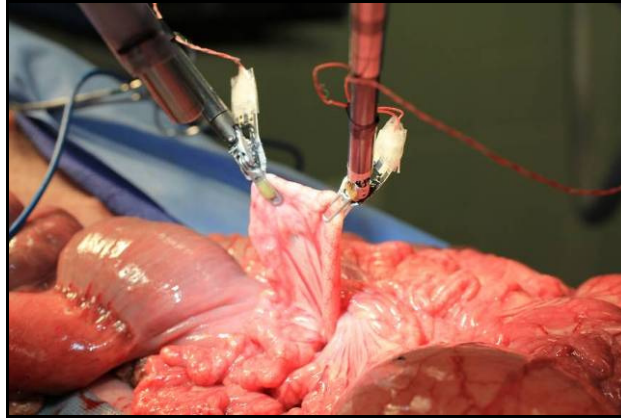


Figure 29. Moisture insulated sensors used for live tissue experiments

Following these validation studies, a dry run experiment was performed to evaluate and iterate on the animal study protocol. During this dry run, moisture insulated sensors functioned for the length of the four hour experiment (Figure 29).

A characterization was performed to determine the impact of the coating layers to sensor sensitivity (Figure 30). Known forces were applied to coated and uncoated sensors using an Instron mechanical loading system, with all other aspects of the feedback system (specifically the hardware potentiometer position) remaining unchanged.

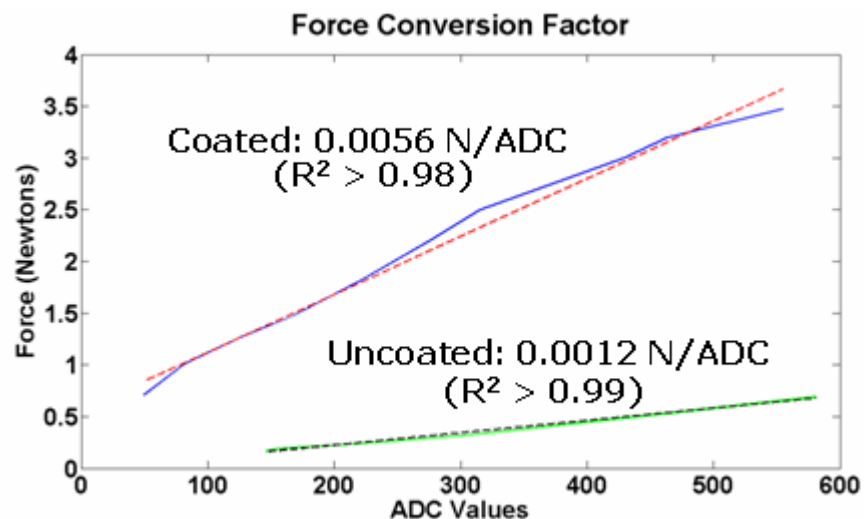


Figure 30. Characterization of coated and uncoated sensors. Dashed lines are a linear fit.



During this characterization, it was determined that the coating increased the dynamic range by a factor of four to five. More importantly, this increase was linear over the range of the system, and so could be accounted for by adjusting the gain of the electrical hardware. During this particular characterization, the hardware gain had been adjusted so that coated sensors could detect light forces (1 N).

## **4.2 *Balloon Actuators***

The primary engineering effort in the initial tactile feedback system was devoted towards developing an optimal actuator configuration for robotic surgery [4]. This six-tube actuator design was integrated successfully with the components of the new tactile feedback system without significant modification. The only additional actuator work required was to develop a second actuator configuration that was compatible with integration into a non-robotic laparoscopic instrument..

### **4.2.1 Initial Version: Six Tube Actuator for Robotic Surgery**

Pneumatic actuators provided pressure stimuli to fingertips using hemispherical silicone balloons, targeting the SA mechanoreceptors through constant deformation of the finger pad. The actuators were composed of a macromolded polydimethylsiloxane (PDMS) substrate housing a  $3 \times 2$  array of pneumatic channels and a thin film silicone membrane (Figure 31). Previously, each actuator element was independently controlled, resulting in six tube connections. These actuators were mounted onto the da Vinci master controls using Velcro straps and used in the live tissue robotic surgery feedback study (Section 6). These actuators were also integrated with remote surgery systems (Section 7).



Figure 31. Initial version of actuators

These actuators were beneficial in that each of the six elements could be independently inflated. However, this function could only be utilized with a matching six element sensor array. Because the previously designed sensor array could not fit onto a surgical grasper, a single element sensor was used. For robotic and remote surgery applications, each of the six actuator elements was connected through external pneumatic fittings so that all six elements inflated in unison in response to the single element sensor.

For the non-robotic laparoscopic surgery application (Section 5), the six tubes could not integrate effectively with the instrument handle, and so a new single-tube actuator was designed.

#### **4.2.2 Single Tube Actuator for Laparoscopic Grasper**

A single-tube actuator was designed by linking the vertical chambers with an internal horizontal tunnel (Figure 32). These actuators were fabricated through transfer molding in the same process as the six-tube actuators, except by using the newly designed actuator mold.

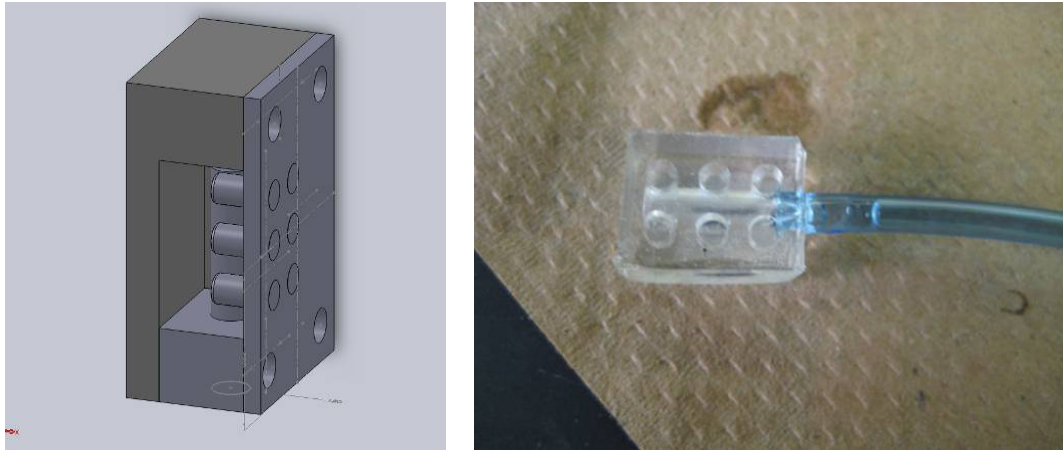


Figure 32. (Left) CAD Drawing of mold for single tube actuator. (Right) Single tube actuator during fabrication

In order to improve the way that the actuator joined with the substrate, a portion of the tubing was halved (Figure 33) and rotated so that the open area connected with the vertical channels and air could flow to the balloon elements. The bottom half was used keep the actuator and tube connection supported while the RTV adhesive was curing.

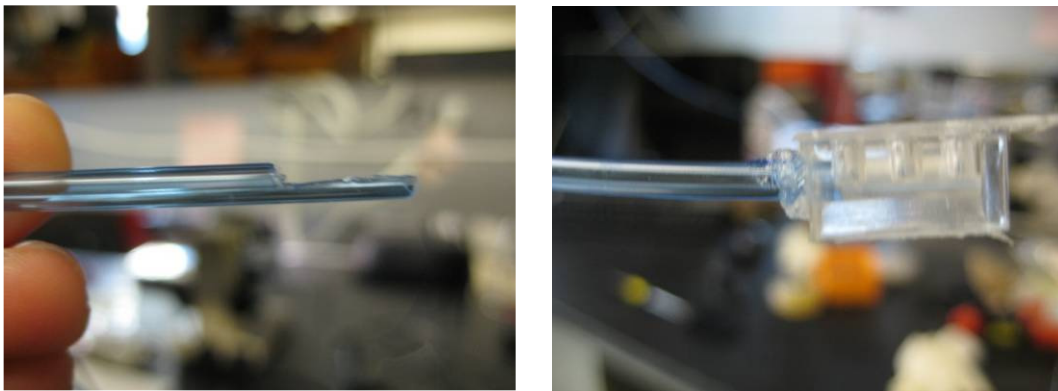


Figure 33. The single tube is cut so that it joins easily and supports the actuator substrate

This size of the single-tube actuator was set to fit into the custom handles of the non-robotic laparoscopic grasper and therefore was taller than the original robotic surgery actuators. For this reason the original six-tube actuator design was used for the robotic and remote surgery applications. The original six-tube actuator mold and the new single-tube actuator mold are both shown in Figure 34.



Figure 34. (Left) Single-Tube actuator mold for laparoscopic surgery  
(Right) Six-Tube actuator mold for remote and robotic surgery

### **4.3 Pneumatic System**

The pneumatic system receives signals from the electrical system and correspondingly routed air pressure levels to the balloon actuators. The initial version used electro-pneumatic regulators, but caused unintentional vibration stimuli that was distracting to surgeons or other users. Two more iterations were developed using different configurations of digital valves. These new designs addressed the shortcomings of the previous system and achieved three-level and five-level inflation respectively.

#### **4.3.1 Initial Version (Electro-Pneumatic Regulator)**

The initial version of the pneumatic system utilized ITV-0010 electro-pneumatic regulators (Figure 35) which converted analog voltages into variable pressure outputs.

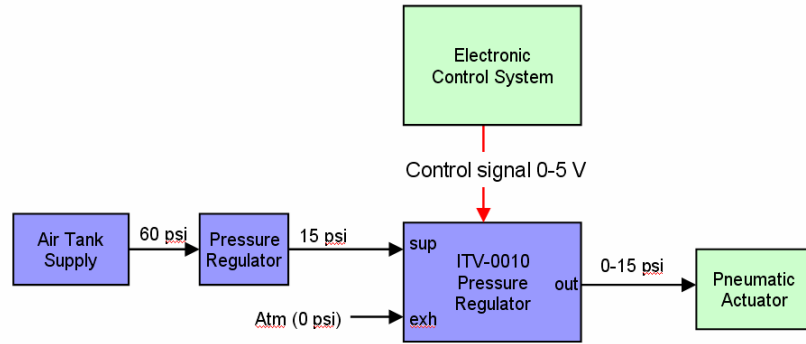


Figure 35. (Left) SMC ITV-0010 pressure regulators mounted in the da Vinci Surgical System (Right) Functional Block diagram of initial pneumatic system

This design suffered from several drawbacks, including unintentional vibratory feedback and excessive sound that often distracted operators from the surgical task. Two new iterations of the system were designed to address these drawbacks. Additional objectives included a reduction of the system footprint while maintaining the five discrete inflation levels available in the previous system.

### 4.3.2 Three-Level Digital Valve System

In the second version of the pneumatic system, the analog electro-pneumatic regulators were replaced with on/off solenoid valves that could be controlled with digital signals rather than analog voltages (Figure 36, Figure 37).



Figure 36. Three-Level Valve Pneumatic System

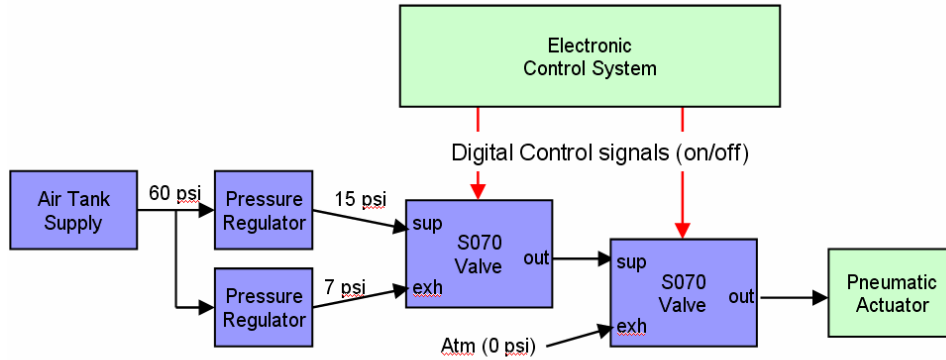


Figure 37. Block Diagram of Three-Level Valve Pneumatic Systems

This smaller system eliminated the unintentional vibrations and also the auditory noise, but reduced the number of output inflation levels from five to three. Additionally, while complete deflation functioned properly (Level 2  $\rightarrow$  Level 0), this system could not successfully perform intermediate deflation (Level 2  $\rightarrow$  Level 1).

### 4.3.3 Five-Level Digital Valve System

The third iteration of the pneumatic system offered two major changes. First, the standard pressure regulators were replaced with high precision regulators (SMC IR1000-N01). This allowed for intermediate deflation and increased repeatability in actuator outputs. Second, a new tiered arrangement of solenoid valves increased the resolution of actuator output from three to five distinct levels (Figure 38, Figure 39).

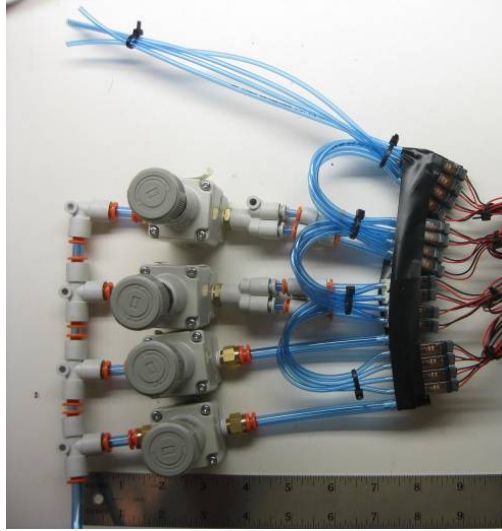


Figure 38. Version 3 of pneumatic system (five-level) with high precision regulators and solenoid valves.

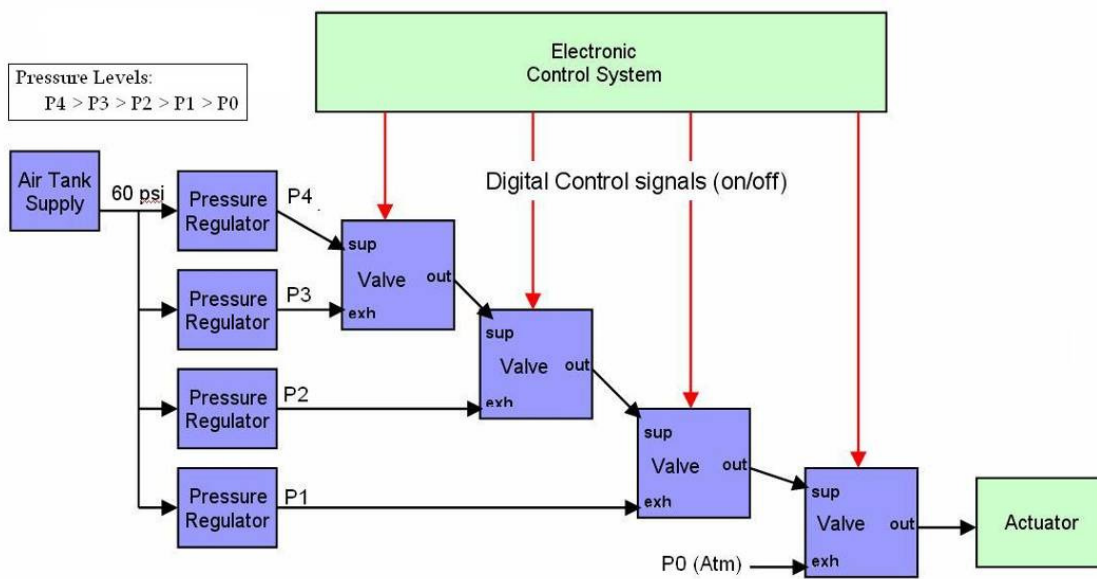


Figure 39. Block diagram for Five-Level Valve Pneumatic System

The resulting system was smaller, operated more quickly than the initial version (<60 ms response), and provided more repeatable inflation. It maintained five discrete inflation levels, while effectively eliminating vibratory and auditory noise.

## 4.4 Electronic System

The purpose of the electronic system was to acquire and interpret the values from the force sensors, process them, and control the pneumatic system. The initial version used a Texas Instruments Evaluation circuit board and suffered from several limitations, especially in its ability to interface with future developments of the technology.

Therefore, a new, two-part wireless electronic system was designed.

### 4.4.1 Initial Version (Texas Instruments Evaluation Board)

The previous version of the control hardware utilized a two-part circuit for each grasper, which included a DSP evaluation board from Texas Instruments (TI ezDSP2808) and a signal conditioning board connected using a ribbon cable (Figure 40).

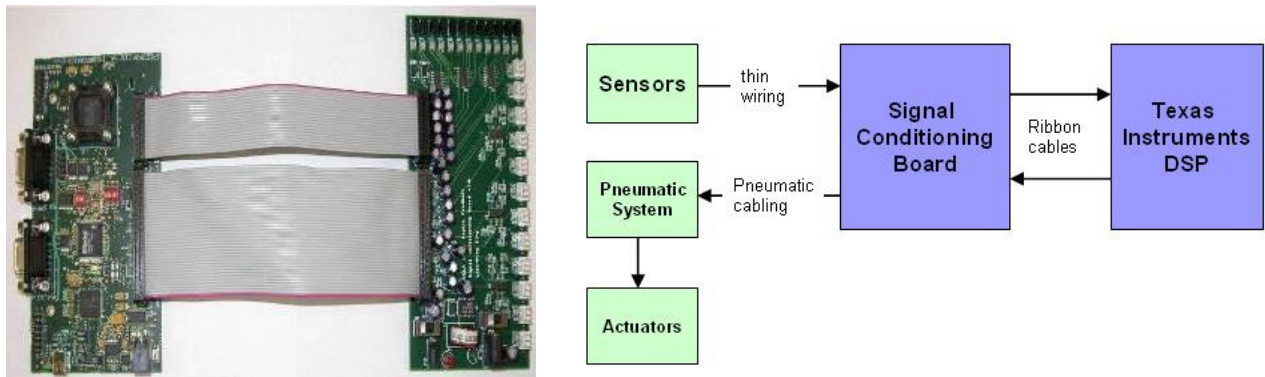


Figure 40. (Left) Two part control system with using DSP Evaluation Board (TI ezDSP2808) and a custom signal conditioning board. (Right) Block diagram for Version 1 Control Hardware

This system was suitable for the initial evaluation of other tactile feedback components and allowed for rapid prototyping, but did not allow for further improvement of the technology. The system was designed specifically for robotic surgery and interfaced only with the initial version of the pneumatic system. Adjustment of control parameters required disconnecting the electronic system and reprogramming the Texas Instruments microcontroller. Data collection required a third circuit board and an external data acquisition system.



Additional practical concerns limited this system's use in the surgical setting. This included excessive wiring that stretched from the da Vinci robot system to the da Vinci master control and the need for three separate power supplies.

#### 4.4.2 Two-Part Wireless System (dsPIC / Bluetooth)

A new two-part wireless electronic system was designed to improve upon the previous system (Figure 41) [155]. The required functionality was split into two custom printed circuit boards (PCBs): a transmitter that interfaced with the sensors, and a receiver that interfaced with the pneumatics and actuators. These two circuits communicated over a Bluetooth serial connection. Separating the control components into two boards eliminated the external wiring between the da Vinci robot and control console.

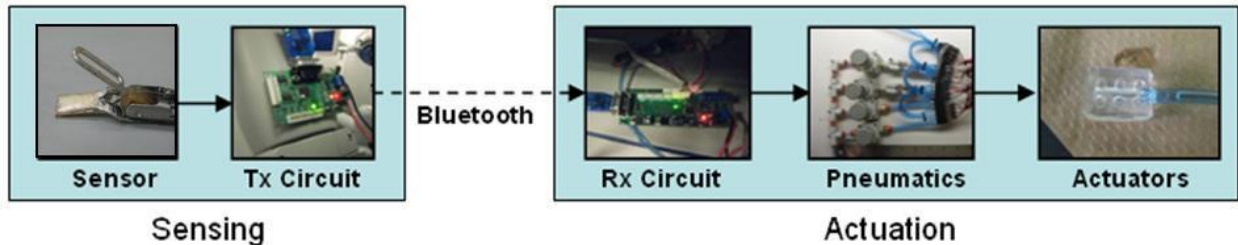


Figure 41. Block diagram for second version of electrical control system.

The transmitter board (Figure 42, Figure 43) measured sensor outputs, encoded this information, and transmitted over Bluetooth.

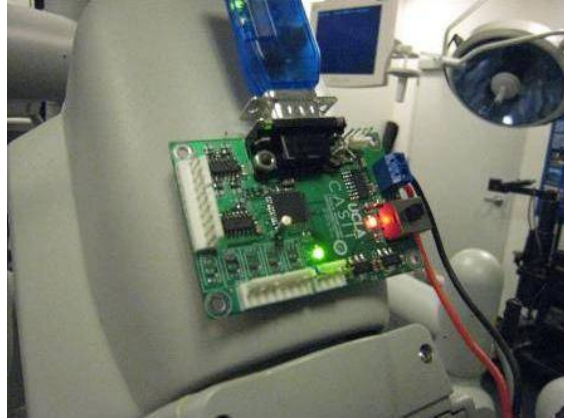


Figure 42. Transmitter mounted on the da Vinci robot

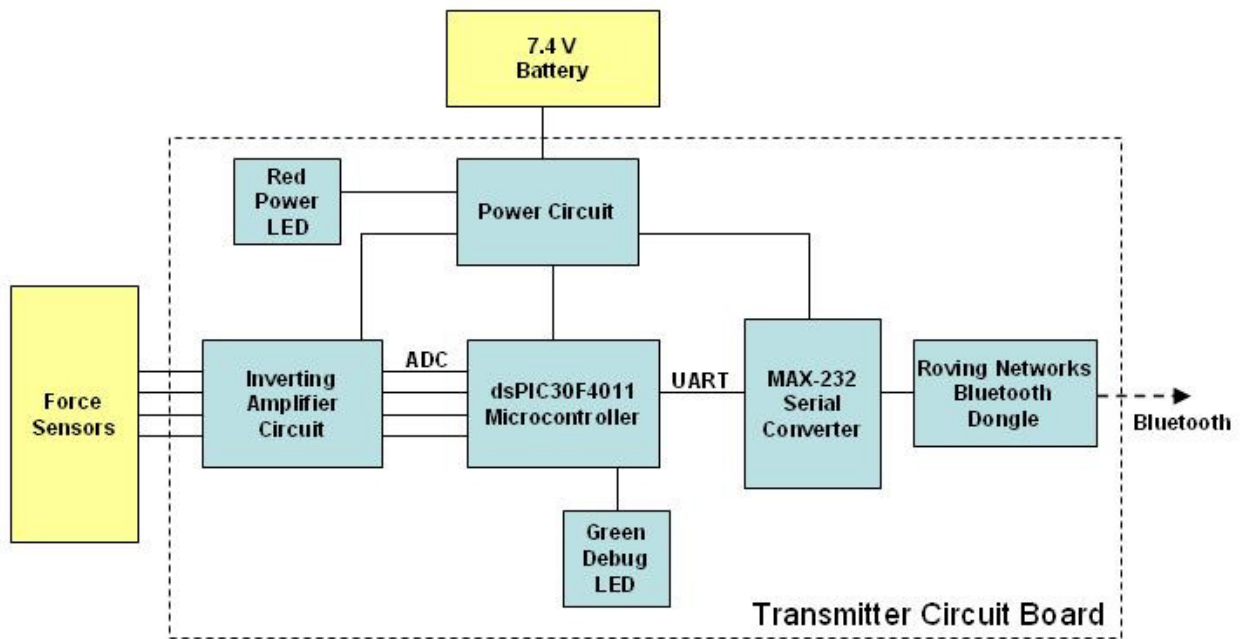


Figure 43. Transmitter Circuit Board, System Block Diagram

Sensor resistances were converted to voltages using operational amplifiers in an inverting amplifier circuit. These voltages were read into the dsPIC Microcontroller (MCU) using the built-in analog-to-digital controller (ADC). The MCU software encoded this information into a data message and output it over the Universal Asynchronous Receiver/Transmitter (UART) through a MAX-232 Serial Converter to a Roving Networks Bluetooth Dongle (RN-270). The

Bluetooth dongle converted the RS-232 serial transmission into a wireless Bluetooth transmission.

The receiver board (Figure 44, Figure 45) decoded the Bluetooth message and sent control signals to the pneumatic system.

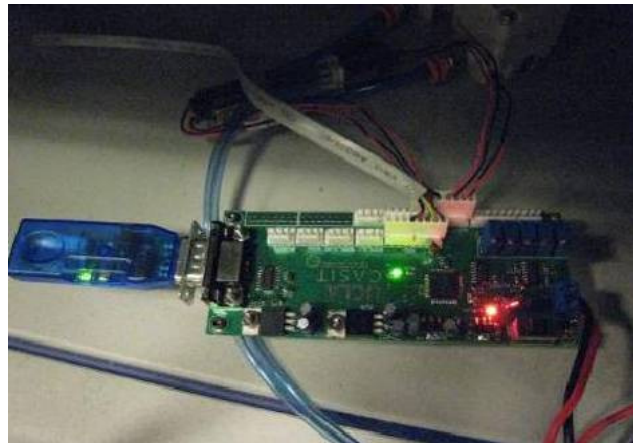


Figure 44. Receiver circuit placed near the da Vinci console

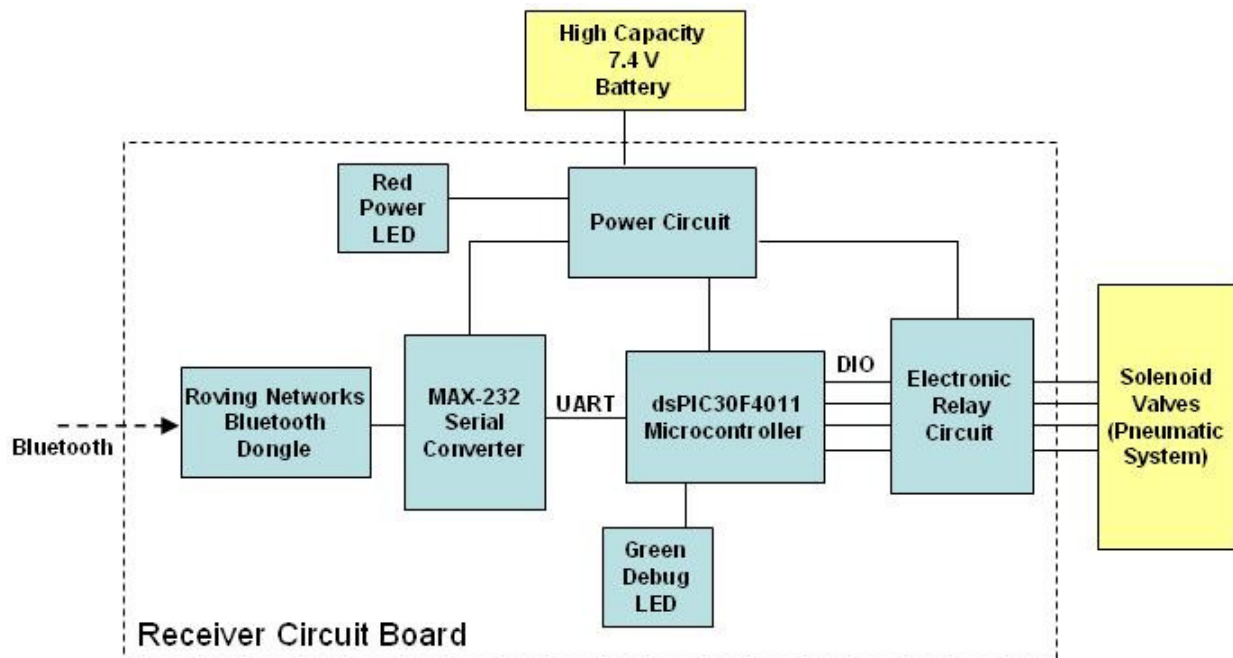


Figure 45. Receiver Circuit Board, System Block Diagram

The receiver used a Bluetooth dongle that had been paired with the one on the transmitter. The data was read into the dsPIC using the UART. The dsPIC's software decoded

this data message and activated the appropriate digital outputs lines on the Digital Input/Output module (DIO). The dsPIC could not provide sufficient current to drive the solenoid valves, so the digital outputs instead acted as switches on an electronic relay circuit.

Both circuit boards used a dsPIC30F4011 microcontroller. This microcontroller was chosen because it included digital outputs for actuator control, two UART channels (one for Bluetooth communication, one for PC interface), eight analog inputs for sensors (at least four were needed for robotic surgery), and up to five analog outputs for backwards compatibility with the first version of the pneumatic system.

The transmitter board functioned using a single 7.4 V battery. The receiver board required more power to drive the electronic load of the pneumatic valves, and could use either a high capacity 7.4 V battery or an external DC power supply.

This version of the electronic system was four times smaller than the previous version, two times less expensive, more versatile, interfaced with all versions of the pneumatic system, eliminated excessive wiring, was flash programmable, and connected readily with a PC for data acquisition.

## ***4.5 User Interface***

A user interface (UI) was developed using National Instruments LabVIEW® to simplify data acquisition and system troubleshooting. Later, features were added to display force values, tag events during data collection, control actuators directly, activate/deactivate tactile feedback during runtime, and adjust software thresholds without the need to reprogram the microcontroller.

The system also allowed for the saving and loading of threshold profiles for particular subjects or subject populations, such as increasing grip sensitivity for experts, although adjusting the hardware potentiometers ended up being more effective.

The UI software ran on a Windows PC and interfaced with the receiver circuit using a KeySpan® USB to RS-232 Converter. It included windows for data collection (Figure 46) and parameter adjustment (Figure 47).

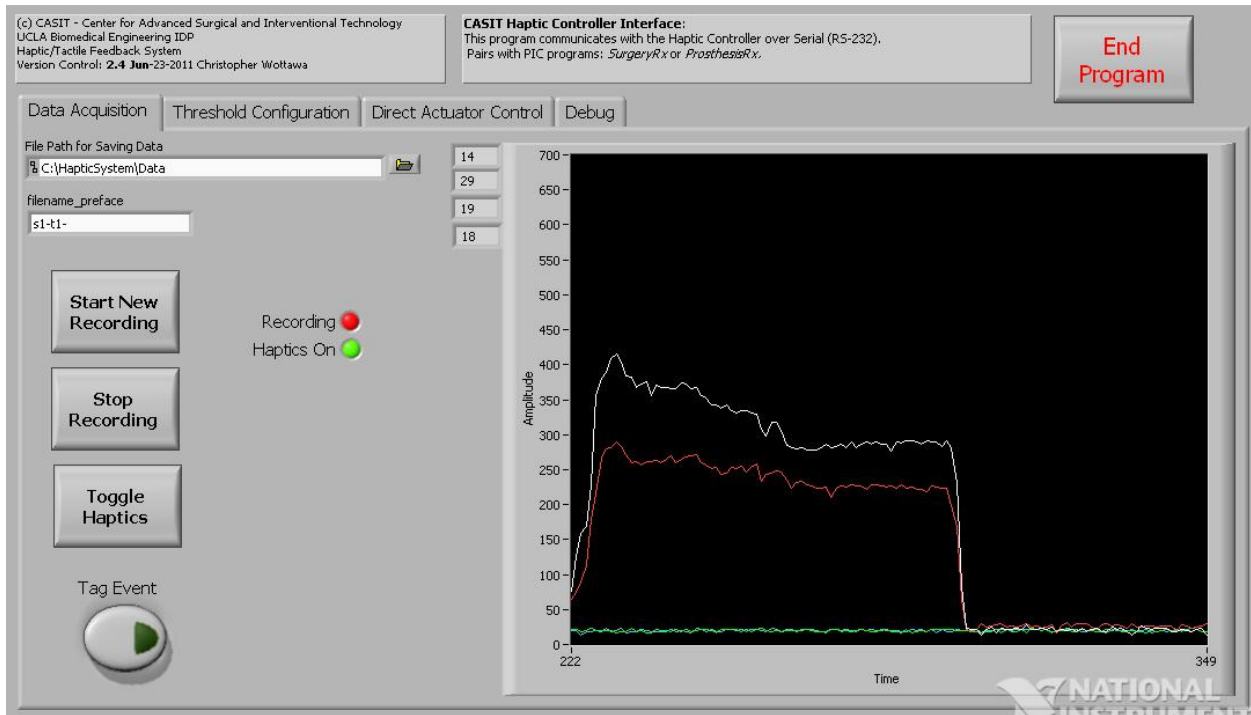


Figure 46. Haptic Controller Interface – Data Collection Window

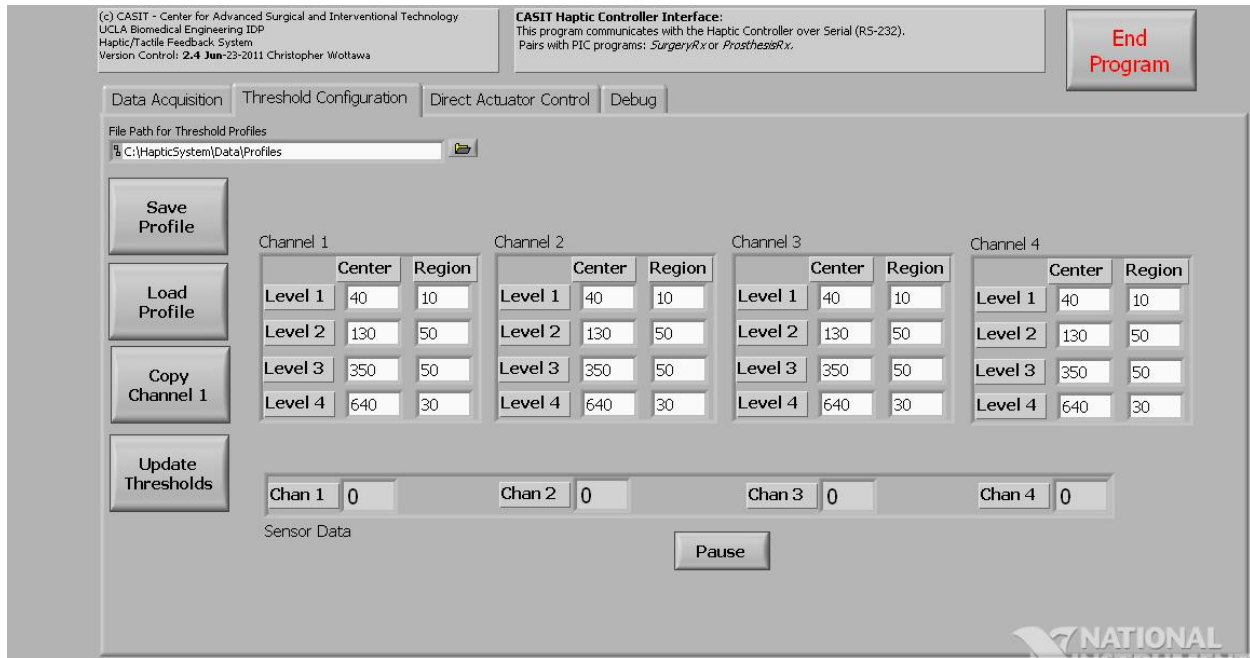


Figure 47. Haptic Controller Interface – Parameter Adjustment Window

This system was used for data collection during the non-robotic laparoscopic grasper grip force study (Section 5.2) and experienced no errors or slow-downs.

During the robotic surgery animal studies (Section 6.2), it was found that the UI software caused a drop in system performance. To account for this, a reduced version of the UI software was designed that eliminated all but data display and logging. The reduced version was connected directly to the Tx circuit rather than the Rx circuit for data collection during the animal studies.

This reduced UI software was also used as a starting point during development of the remote tactile feedback system (Section 7.1).

## 4.6 Control Software

New control software was designed to support the wireless embedded hardware and pneumatic components. This included a custom message protocol and support for simultaneous

interleaved communication between the two control circuits and the user interface. Additionally, this software improved upon existing algorithms by eliminating level transition jitter.

A hierarchical block-based approach was utilized to maximize the re-use of code and allow components to be shared among surgical and other tactile feedback applications.

Control software was developed in PICC (a version of C specific to PIC MCU's) and ran on the dsPIC30F4011. Development of the communication protocol was done in concert with the user interface software in order to maintain consistency across platforms.

### 4.6.1 Functional Overview

The surgery tactile feedback system used two main PICC programs (*HapticTx* and *SurgeryRx*), and one library (*CASIT\_SerialComm*). These programs achieved four main functions: Data Collection, Communication, Data Processing, and Actuator Control, as shown in Figure 48.

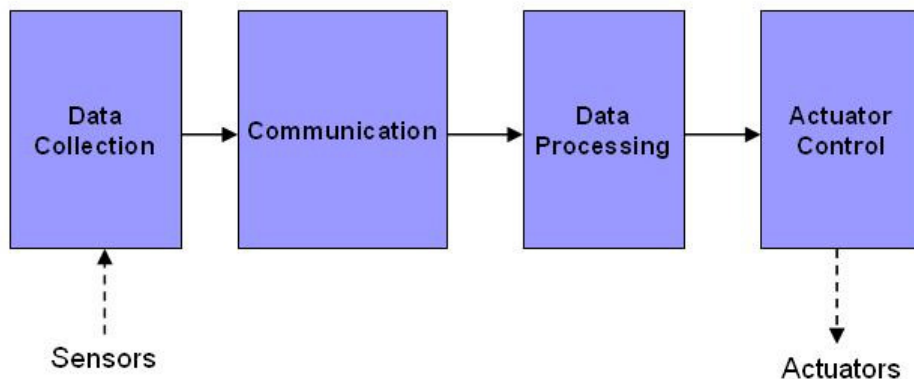


Figure 48. Control Software, top level functional block diagram.

### 4.6.2 Data Collection

The Data Collection functional block (Figure 49) controlled the reception of sensor data over the microcontroller's built-in Analog-to-Digital Converter (ADC), the subsequent

construction of a data message, and transmission of this data message over the Bluetooth module. This software operated on the transmitter (Tx) circuit board.

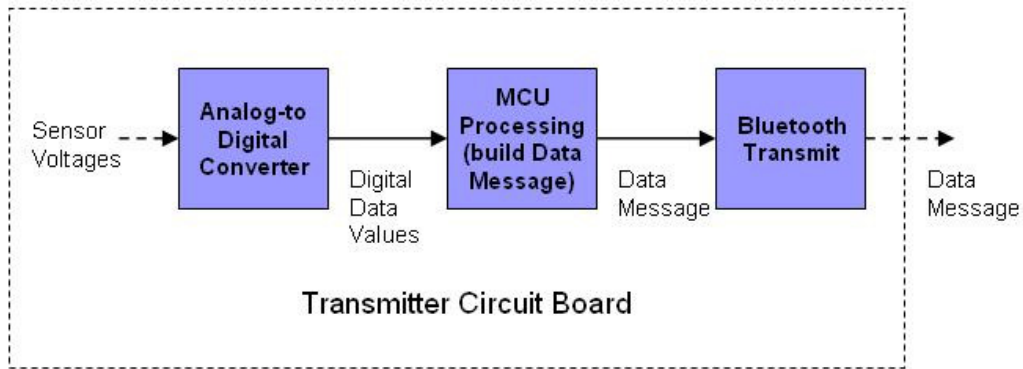


Figure 49. Data Collection Block Diagram

### 4.6.3 Communication

A communication algorithm was required due to the wireless hardware and integration with remote surgery. This software block organized communication between the transmitter (Tx) circuit, the receiver (Rx) circuit, and the user interface (PC) (Figure 50).

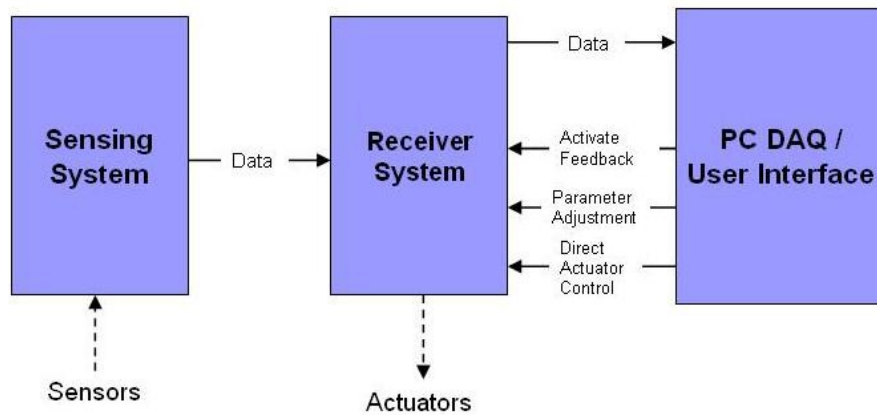


Figure 50. Communication block. Arrows represent different message types.

The communication protocol used a hierarchical approach to generalize software (Figure 51).





Figure 51. Layered code Infrastructure

The *Serial Comm Layer* included functions for directly sending and receiving characters over the serial ports and Bluetooth interface, as well as error checking for all message types. The *Message Layer* built upon the *Serial Comm Layer* and contained functions for constructing and handling specific message types. This *Message Layer* can be shared among all tactile feedback applications. The *Application Layer* chose which message types to send and when, and differed depending on the application. Four types of messages have been implemented (Table 2).

Table 2. Communication Protocol Message Types

Message Type	Content	Uses
Data ("Sensor")	Raw Data from all sensor channels	<ul style="list-style-type: none"> <li>• Recording Data</li> <li>• Displaying Data</li> <li>• Controlling Pneumatics</li> </ul>
Direct Actuator Control ("Level")	Desired output level for all actuator channels	<ul style="list-style-type: none"> <li>• Perceptual Testing</li> <li>• Troubleshooting Pneumatics</li> <li>• Remote Surgery System</li> </ul>
Parameter Adjustment ("Threshold")	Desired Threshold Levels	<ul style="list-style-type: none"> <li>• Run-time Threshold Adjustment</li> <li>• Grip Force Studies</li> </ul>
("Activate")	Desired Tactile Feedback State (ON/OFF)	<ul style="list-style-type: none"> <li>• Run-time activation/deactivation</li> <li>• Grip Force Studies</li> </ul>

Communication messages were constructed as a string of ASCII characters transmitted over the serial UART. All messages used the following format:

Y[type][length][data][checksum]Z

The letters *Y* and *Z* define the start and end points of the message.

*Type* is a single character that defined one of the four message types:

- L – Level Packet: contained data for desired level of each actuator element

- S – Sensor Packet: contained digitized force data values, typically a number between 0 and 660, representing an ADC reference voltage between 0 and 3.3.
- T – Threshold Packet: contained desired threshold levels, including center points and region sizes.
- A – Activation Packet: contained the desired activation state of feedback (ON/OFF).

*Length* contained the number of characters that were sent with the message. For a Sensor message, this number is typically 19 when four channels are used and 13 when only two are used. By checking the length field with the number of characters received, errors could be avoided despite dropping characters in the transmission.

*Data* was the content of the message and could be either sensor values or desired parameters. The format of the data was dependent on the message type.

*Checksum* is a two character decimal representation of the sum of all of the characters in the message and is used for error checking. By calculating the checksum on the receiving end and comparing it with the value that was sent, it could be determined whether any bits were flipped during the transmission.

#### **4.6.4 Data Processing: Jitter Reduction Algorithm**

The data processing block (Figure 52) converted sensor data values into desired inflation levels.

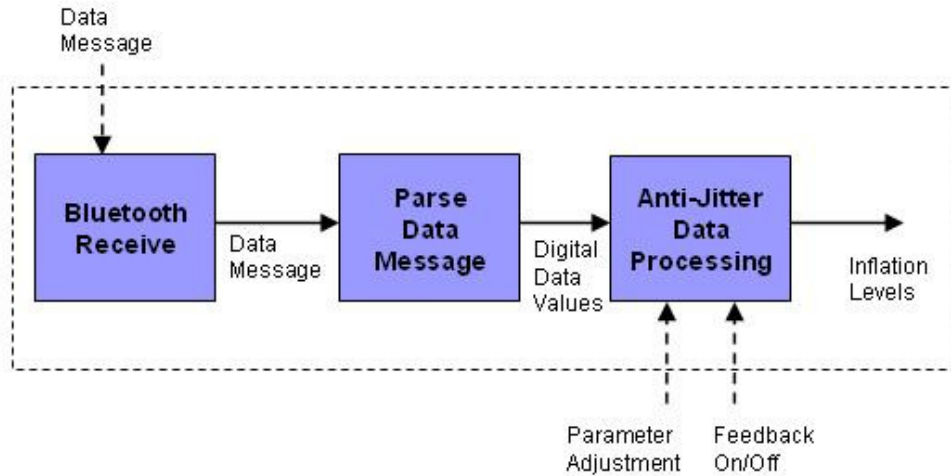


Figure 52. Data Processing Block

Initially, this was done with a simple threshold algorithm (Figure 53). In this algorithm, the received sensor value was simply compared with a set of thresholds, and the level determined. Level transition jitter occurred when the sensor value fluctuated around the threshold level, resulting in rapid transition between two adjacent levels. As a result, balloon actuators rapidly inflated and deflated.

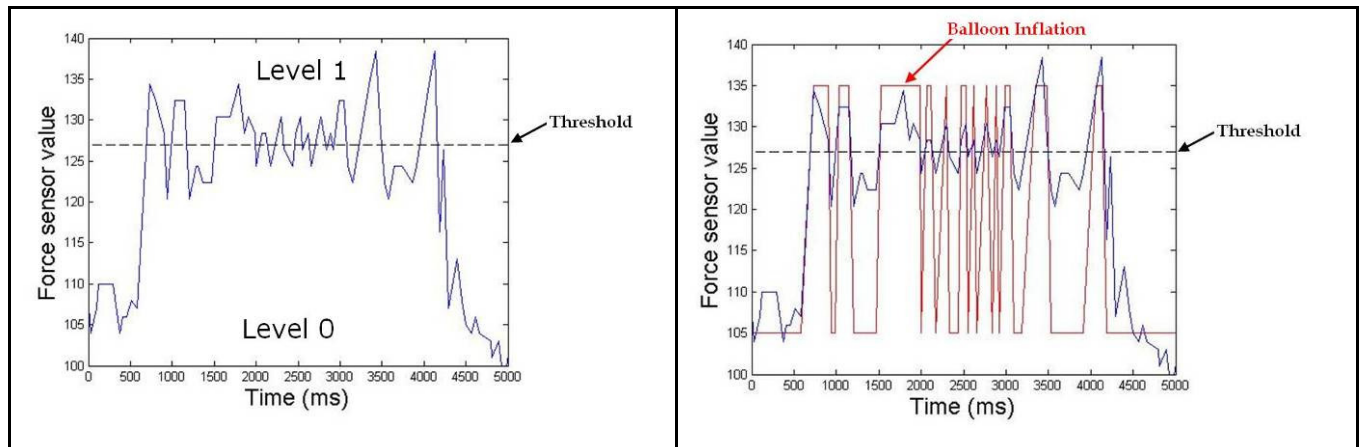


Figure 53. Simple threshold algorithm suffers from sporadic balloon inflation/deflation when the sensor signal hovers around the level transition threshold.

To address this issue, an anti-jitter algorithm was implemented, where rising thresholds were separated from falling thresholds (Figure 54). The inflation level was only increased when

sensor values crossed the rising threshold, and was only decreased when it fell below the falling threshold. This algorithm eliminated level transition jitter.

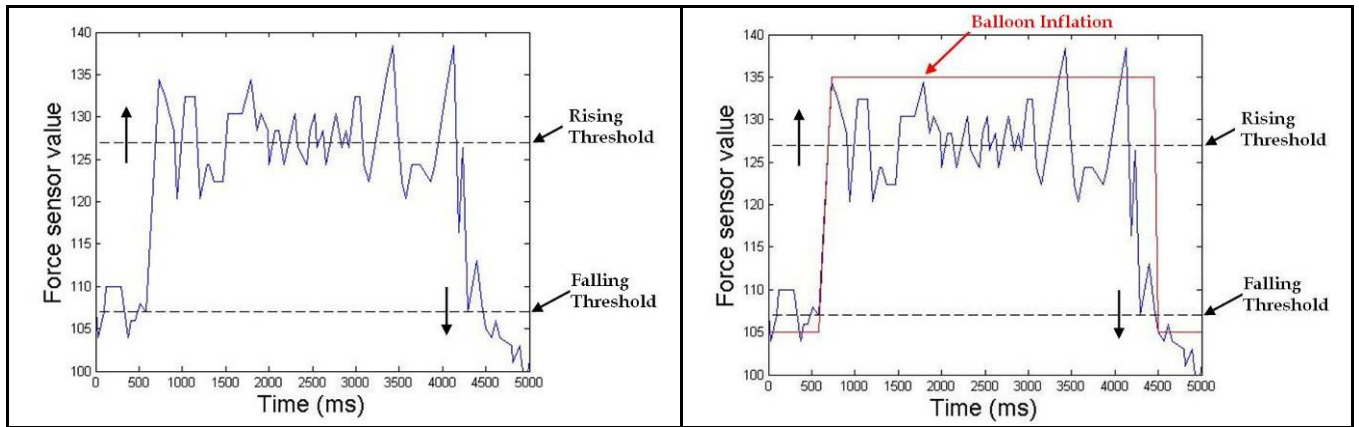


Figure 54. Anti-jitter algorithm separates the rising and falling thresholds, resulting in smoother balloon behavior.

#### 4.6.5 Actuator Control

The actuator control block (Figure 55) converted the desired inflation levels into a set of digital output signals that directly interface with the pneumatic system.

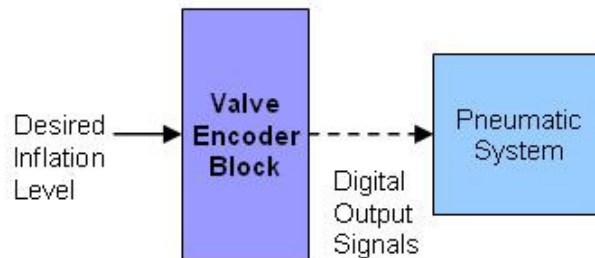


Figure 55. Actuator Control Block

This valve encoder block was organized around the physical arrangement of the pneumatic system and actuators, and their connections with the receiver circuit.

#### 4.6.6 Complete System

A complete block diagram of the software system is shown in Figure 56.

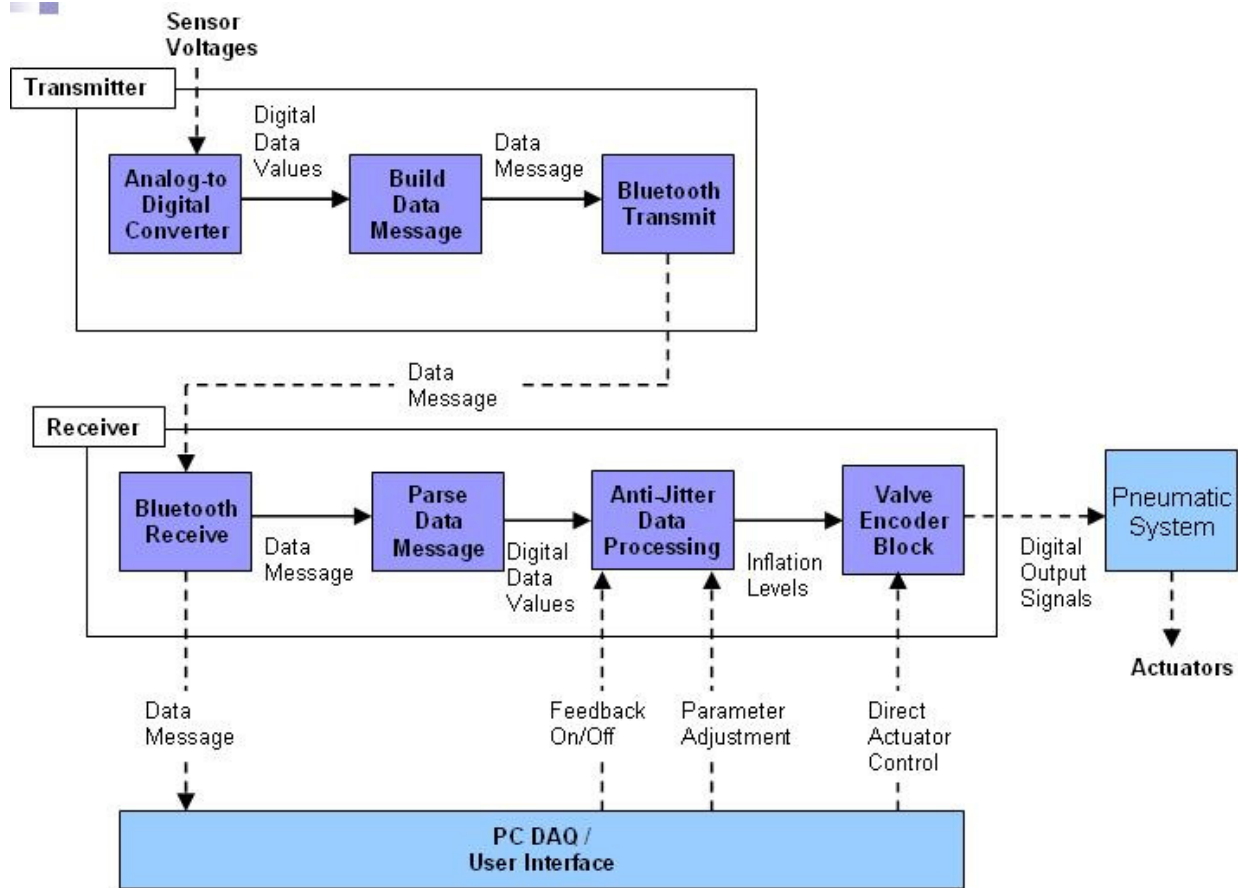


Figure 56. Full Block Diagram of Control Software

#### 4.7 Summary of System Improvements

In 2008, this research inherited a functioning tactile feedback system. An iterative redesign was performed on all aspects of the system. This was necessary in order to address some of the initial system’s shortcomings, improve its performance, and to allow the necessary expansion to other applications and use in live tissue.

The pneumatic system was redesigned to remove unintentional vibration and provide direct inflation feedback as originally intended, without sacrificing the number of discrete inflation levels. A new two-part, wireless electronic system was developed that was smaller, cheaper, and more versatile for other minimally invasive and tactile feedback applications. New

control software was written to support wireless communication, the new hardware, and the new pneumatic system. This software utilized an anti-jitter threshold algorithm and a custom message protocol to handle wireless communication. A user interface was designed that allowed for easier data collection and run time adjustment of control parameters. The sensor mounting process was improved, and a new process was developed for protecting sensors from moisture damage, thus enabling *in-vivo* use.

A primary focus of the initial system was optimizing the actuator configuration for maximum perceptibility. This six-tube actuator design was retained for the robotic and remote surgery applications. A new single-tube actuator was designed for integration with a non-robotic laparoscopic instrument.

Together these improvements allowed the integration of tactile feedback into additional applications and a further evaluation of its benefit in minimally invasive surgery.

The following sections describe the evaluation of tactile feedback in three new applications: non-robotic laparoscopic surgery (Section 5), robotic surgery for potential clinical benefit in an animal model (Section 6), and remote surgery (Section 7).

## 5 Evaluation of Tactile Feedback in Laparoscopic Surgical Training

In robotic surgery, tactile feedback is entirely absent. In laparoscopic surgery, tactile feedback during grip is attenuated and limited to the resistance felt in the tool handle. In previous robotic surgery studies it was determined that adding supplemental tactile feedback significantly reduced grip force [153]. The purpose of this task was to determine if that same effect could be observed in non-robotic laparoscopic surgery.

The improved tactile feedback system was first integrated into a non-robotic laparoscopic grasper [156]. This system was used to perform a study to evaluate the role of tactile feedback during laparoscopic training [157].

### 5.1 Laparoscopic Grasper Tactile Feedback System Integration

Laparoscopic grasper integration focused on the mounting of sensors and actuators and construction of an enclosure for pneumatic and electrical components. The completed laparoscopic grasper is shown in Figure 57.

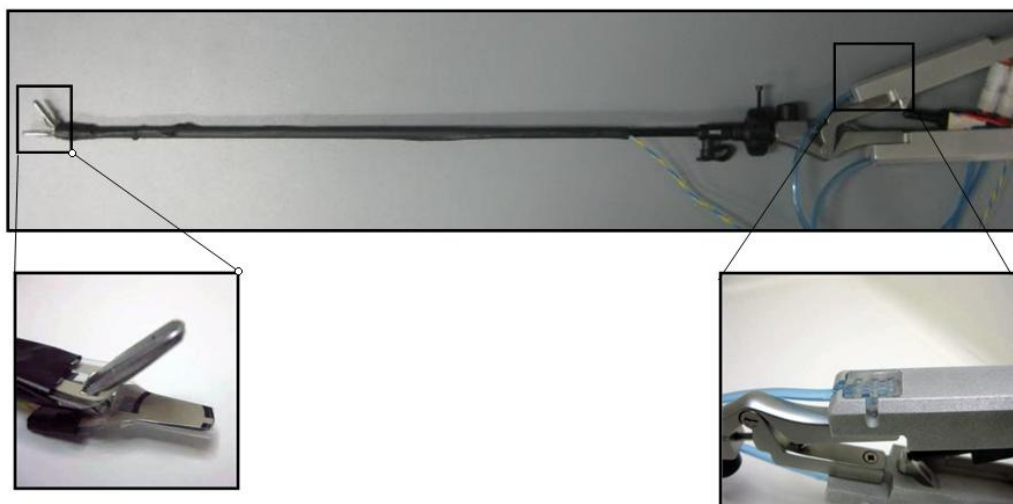


Figure 57. (Top) Completed Laparoscopic grasper. (Bottom left) Piezoresistive force sensors mounted onto the grasper tip. (Bottom Right) Single-tube actuators mounted flush in the handles.

New handles were designed and fabricated for the purpose of effectively integrating the tactile actuators into commercial laparoscopic tools. Actuators sat in small rectangular pockets in the tool handles in such a way that the balloon actuator surface was flush with the surface of the tool handle.

The actuators were placed to provide an ergonomic contact surface to the thumb and forefinger of the surgeon. Grooves were cut to allow for easy routing of the pneumatic tubing. Wires secured to the grasper shaft using heat shrink tubing.

Single element force sensors were mounted onto the tips of a grasper, and new actuators designed to fit into a laparoscopic handle so that all balloon elements inflated synchronously.

The control and pneumatic systems were housed in a portable plastic enclosure, mounted vertically to support the air canister (Figure 58).



Figure 58. Tactile feedback system mounted in a plastic project enclosure.

The complete system was validated by having users perform single handed peg transfers in a typical Fundamentals of Laparoscopic Surgery (FLS) box trainer using the tactile feedback



system. Qualitatively, these users indicated perceptible inflation while gripping the rubber objects.

## **5.2 Laparoscopic Grasper Grip Force Study**

Once integration was complete, a study was performed to determine the effect of tactile feedback on a subject's grip force during peg transfer training tasks using a non-robotic laparoscopic grasper (Figure 59) [157].



Figure 59. Tactile Feedback system integrated into a non-robotic laparoscopic grasper.

The purpose of the experiment was to test the hypothesis that providing tactile feedback would result in subjects gripping objects with reduced levels of force. Using safe levels of force during laparoscopic surgery could reduce the incident of tissue damage and decrease the learning curve associated with complex minimally invasive techniques.

### **5.2.1 Methods**

Eleven novice (no experience with laparoscopic surgery) and four expert (FLS certified) subjects used laparoscopic instruments with integrated tactile feedback to perform single-handed

peg transfer tasks in three blocks of trials. Prior to the task, novice subjects were trained by an expert to pick up rubber pieces using the instrument and instructed to use just enough force to complete the task. Subjects were allowed to practice for five minutes to demonstrate that they could perform the task.

In the first block, the subjects were tested with the tactile feedback system inactivated to determine baseline force. In the second block, the tactile feedback system was activated and the trials repeated. In the third block, the tactile feedback system was again deactivated to determine possible short term learning effects. In each block of trials, the novice subjects performed six peg transfers using their dominant hand followed by six transfers using their non-dominant hand. Expert subjects performed 18 peg transfers with each hand. The forces at the tips of the grasper were recorded during each grasping event. This protocol was nearly identical to the one that was used in the previous robotic surgery study [153].

Each data set consisted of continuous, time-stamped, grip force measurements (Sample rate = 20 Hz). In each data set, grip events were manually tagged during the course of the trial using the data acquisition aspect of the user interface (National Instruments LabVIEW®). Peak and average forces were calculated for each grasping event. Blocks of trials were compared using a Wilcoxon signed rank test, where each subject served as their own control. Because twelve comparisons were being evaluated (three conditions, dominant/non-dominant hand, average/peak force) the Bonferroni correction was used, and a p-value of  $0.05/12 = 0.004$  considered for significance.

Grip force data was originally recorded as a raw 10-bit ADC value. An Instron® mechanical loading system was used to determine the conversion factor from ADC value to Force (Newtons). For novice subjects, there was a trade-off between saturating the force sensor

signal and failing to detect light forces. Gain was adjusted so that these light signals were always detected, but as a result force sensor signals saturated during times of higher force, such as when the tactile feedback system was deactivated in the first trial. This had an effect on the variance of peak and average forces and therefore non-parametric statistical methods were used.

## 5.2.2 Results

For novice subjects, the sets of trials with tactile feedback (Trial 2) showed significantly reduced grip force when compared to those without tactile feedback (Trials 1 and 3) (Figure 60). The results of hypothesis testing using the Wilcoxon signed rank test are shown in Table 3.

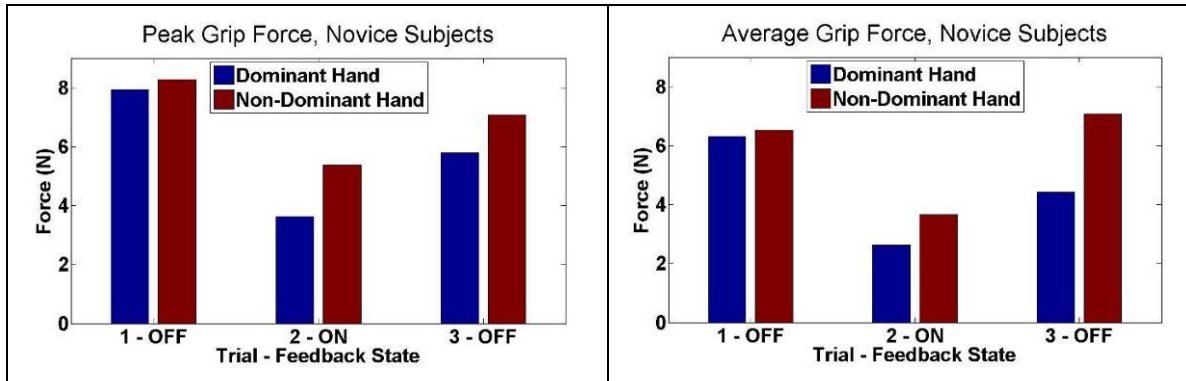


Figure 60. Novice subjects: peak and average grip force results

Table 3. Non-Robotic Training Study: Hypothesis Testing for Novices

Peak force	<i>p</i> value	Average force	<i>p</i> value
<b>Dominant hand</b>			
Trial 1 (OFF) versus trial 2 (ON)	<0.001	Trial 1 (OFF) versus trial 2 (ON)	<0.001
Trial 2 (ON) versus trial 3 (OFF)	<0.001	Trial 2 (ON) versus trial 3 (OFF)	<0.001
Trial 1 (OFF) versus trial 3 (OFF)	0.014	Trial 1 (OFF) versus trial 3 (OFF)	0.032
<b>Nondominant hand</b>			
Trial 1 (OFF) versus trial 2 (ON)	0.002	Trial 1 (OFF) versus trial 2 (ON)	0.003
Trial 2 (ON) versus trial 3 (OFF)	<0.001	Trial 2 (ON) versus trial 3 (OFF)	0.002
Trial 1 (OFF) versus trial 3 (OFF)	0.067	Trial 1 (OFF) versus trial 3 (OFF)	0.054

For the four expert subjects there were no significant differences between any trials due to tactile feedback (Figure 61).

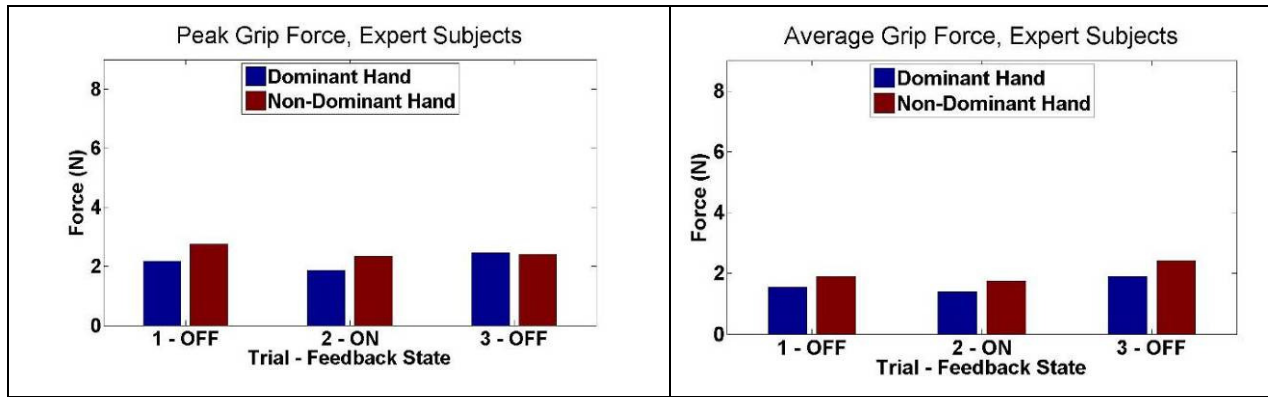


Figure 61. Expert subjects: peak and average grip force results.

Hypothesis testing results for expert subjects is shown in Table 4. As before, differences were considered significant if the p-value was less than 0.004.

Table 4. Non-Robotic Training Study: Hypothesis Testing for Expert Subjects

Peak force	<i>p</i> value	Average force	<i>p</i> value
<b>Dominant hand</b>			
Trial 1 (OFF) versus trial 2 (ON)	0.159	Trial 1 (OFF) versus trial 2 (ON)	0.349
Trial 2 (ON) versus trial 3 (OFF)	<0.001	Trial 2 (ON) versus trial 3 (OFF)	<0.001
Trial 1 (OFF) versus trial 3 (OFF)	0.023	Trial 1 (OFF) versus trial 3 (OFF)	0.002
<b>Nondominant hand</b>			
Trial 1 (OFF) versus trial 2 (ON)	0.050	Trial 1 (OFF) versus trial 2 (ON)	0.375
Trial 2 (ON) versus trial 3 (OFF)	0.833	Trial 2 (ON) versus trial 3 (OFF)	0.741
Trial 1 (OFF) versus trial 3 (OFF)	0.049	Trial 1 (OFF) versus trial 3 (OFF)	0.375

After Trial 2, average and peak grip forces increased significantly ( $p < 0.004$ ) for the dominant hand. This could be due to fatigue after a large number of trials or acclimation and reliance on the feedback.

### 5.2.3 Discussion

The results indicate that supplementary tactile feedback using this system helped novice subjects perform the laparoscopic training task with reduced grip forces. These results are similar to those that were found for robotic surgery where tactile feedback is entirely absent.

Limited tactile feedback is present in laparoscopic surgery and is conveyed through changes felt in the mechanical resistance of the tool handle. Novices are not as sensitive to these changes as experts and tactile feedback appears to augment perception of these changes. While there were minor improvements due to learning, the improvement due to tactile feedback was more appreciable.

Tactile feedback using this system did not affect the already low grip forces applied by expert subjects. This may be due to the presence of significant kinesthetic memory for fine control of grip using laparoscopic instruments, enhanced sensitivity to subtle changes in the forces used to grasp objects, or both.

This study suggested that tactile feedback may be beneficial for laparoscopic training of novice surgeons or for those learning new techniques [157].

## **6 Evaluation of Tactile Feedback in Robotic Surgery for Potential Clinical Application using an Animal Model**

Until now, tactile feedback systems and system components have not been compatible for use in clinical robotic surgery environments and therefore the potential benefit of tactile feedback in robotic surgery has been difficult to study. Through work with insulating sensors from moisture (Section 4.1.3), this research has developed the first tactile feedback system that could be used in live tissue.

The objective of this next task was to integrate the improved tactile feedback system with the da Vinci Surgical System and perform a study to evaluate the system and effects of tactile feedback in live tissue.

In a previous study [151], it was found that tactile feedback helped reduce grip force in a dry environment. The purpose of this study was to determine if there would be a similar result when handling tissue. An additional objective of this study was to validate operation of the system in a live tissue environment and to identify further technical limitations.

### ***6.1 System Preparation and Integration with da Vinci Surgical System***

The improved tactile feedback system was integrated into the da Vinci Surgical System®. Waterproof sensors were mounted onto the robotic graspers using a layer of thin adhesive (Figure 62). Stronger adhesives imparted additional stress on the sensors, locking them in an activated position.



Figure 62. Waterproof sensor mounted on robotic grasper

The transmitter circuit and its battery pack were attached to the da Vinci robot near the sensors using Velcro (Figure 63).

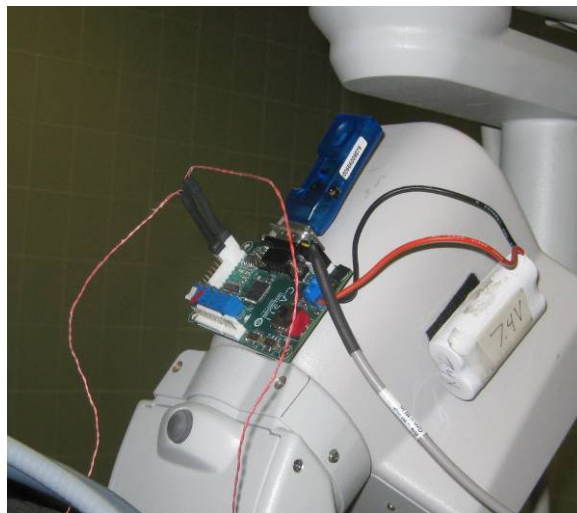


Figure 63. The transmitter circuit mounted on the da Vinci robotic system.

Six-tube actuators were mounted onto the da Vinci master controls (Figure 64). Each of the six actuator elements were connected externally through pneumatic fittings so that all elements would inflate together. Since one sensor and two actuators were used for each hand, the two actuators were also connected externally through pneumatic splitters.

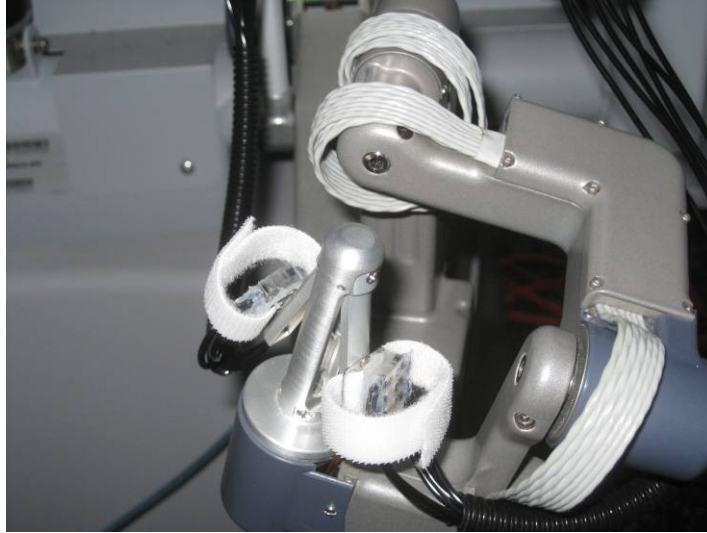


Figure 64. Actuators mounted on the da Vinci master controls.

The pneumatic system and receiver circuit were housed in a plastic enclosure and positioned near the da Vinci console (Figure 65). Because of the wireless connection between transmitter and receiver, no extra wires were needed between the da Vinci robot and control console.



Figure 65. The receiver circuit and pneumatic system housed in a plastic enclosure and positioned near the da Vinci console, along with a back-up air canister.



Prior to the study, sensors were calibrated by grasping a foam block and adjusting transmitter circuit potentiometers. The potentiometers were further adjusted after a practice run on the actual bowel thirty minutes prior to the animal experiment. Due to the dynamic range of the electronics, there was a balance between detecting small forces and saturating at larger forces. When these objectives came into conflict, the system was adjusted with preference for small force detection, and this resulted in frequent saturation, which artificially decreased the variance between these measurements. For this reason, subsequent hypothesis testing was performed using non-parametric statistical methods.

Pneumatic regulators were adjusted to provide the pressure outputs shown on Table 5 as determined by surgeon feedback. These pressure outputs created the largest impulse from level 0 to level 1, indicating a force sufficient to hold the object. Burst pressure varied by actuator, but was experimentally determined to be approximately 50 PSI.

Table 5. Pressure Outputs for Live Tissue Experiments

Level 0	0 PSI
Level 1	25 PSI
Level 2	30 PSI
Level 3	35 PSI
Level 4	40 PSI

Software thresholds were adjusted so that the minimal force required to hold the tissue would cause a transition to level 1, but also to avoid pneumatic activations caused by system noise (Table 6). These thresholds were adjusted based on surgeon feedback.

Table 6. Live Tissue Experiment Software Thresholds

<b>Transition Point</b>	<b>Center Point (ADC Units)</b>	<b>Anti-Jitter Region Size (ADC Units)</b>
Level 0/1	80	20
Level 1/2	160	30
Level 2/3	350	30
Level 3/4	600	30

Integration of the tactile feedback system into the da Vinci robot was evaluated by grasping foam blocks using the system and observing actuator inflation in response to grasping events.

## ***6.2 Robotic Surgery Grip Force Study in an Animal Model***

A study was performed to evaluate the effects of tactile feedback on grip force and tissue damage during robotic surgery procedures in a porcine model. This was done by having expert and trainee subjects run a pig bowel, and assessing the measured grip force and observed tissue damage with and without the feedback system. It was hypothesized that tactile feedback would result in both reduced grip force and a reduction in tissue damage.

### **6.2.1 Methods**

Nineteen subjects (seven surgeons and twelve surgical residents) used the da Vinci surgical system to pass porcine bowel from one grasper to the other (“run the bowel”), until they had grasped the bowel ten times with each grasper (Figure 66). An expert robotic surgeon explained the task, and then verbally guided subjects during the procedure by counting grasps and instructing them when to begin and end (Figure 67).

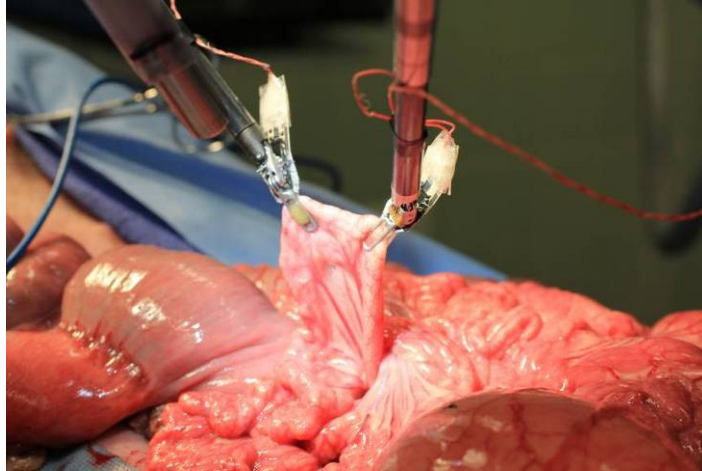


Figure 66. The da Vinci with tactile feedback being used to run porcine bowel



Figure 67. Observing surgeon during the dry run of the live tissue study

Subjects were also classified as *experts* and *novices*, where experts had performed six or more robotic surgery cases and novices had performed five or fewer (most often, none). One senior urology resident and four attending surgeons were considered experts based on their answers to the exit surveys. The remaining fourteen subjects were considered novices.

For each subject, the bowel run was performed three times in the following conditions: (T1) tactile feedback off, (T2) tactile feedback on, and (T3) tactile feedback off. This staggered structure was designed to help establish short term learning effects using the system.

When the subject had completed all three blocks of trials, the observing surgeon harvested the grasped bowel using electrocautery. The bowel segment was photographed prior to being fixed in formalin in preparation for histopathological sectioning and inspection. Specimens were embedded in paraffin and stained using standard Hematoxylin and Eosin stain.

A porcine model was used because it is a well-established model for abdominal surgery. A total of four pigs were used for all studies, one for a dry-run experiment, and three for the study at 5-10 subjects per pig. Experiments were performed in the UCLA Division of Laboratory Animal Medicine (DLAM) Surgery Suite with help and supervision from attending veterinarians. The study was approved by the Animal Research Committee (ARC) under protocol number 2008-172-12A. Work with human subjects was approved by the Institutional Review Board (IRB) under protocol #11-000077.

The study was performed on three separate dates to facilitate scheduling of surgeons and residents.

Following the study, subjects filled out a questionnaire (Figure 68).

Tactile Feedback Study Questionnaire      Date \_\_\_\_\_      Time: \_\_\_\_\_

Background

Which best describes your surgery experience?

Intern      Resident      Attending      Other \_\_\_\_\_

What is your field of expertise (i.e. general surgery, urology)? \_\_\_\_\_

How many robotic surgery cases have you performed?

None      None, but I have received training      1-5      6-20      More than 20

Are you FLS Certified?

Yes      No

Are you left or right-handed?

Left      Right

Tactile Feedback Study

1) Tactile Feedback helped me perform the task

Strongly Disagree      Disagree      Neither Agree Nor Disagree      Agree      Strongly Agree

2) Tactile feedback had no effect on my performance

Strongly Disagree      Disagree      Neither Agree Nor Disagree      Agree      Strongly Agree

3) With tactile feedback, I grasped tissue with less force.

Strongly Disagree      Disagree      Neither Agree Nor Disagree      Agree      Strongly Agree

4) The balloon inflations were easy to feel.				
Strongly Disagree	Disagree	Neither Agree Nor Disagree	Agree	Strongly Agree
5) I found myself ignoring the balloon inflations				
Strongly Disagree	Disagree	Neither Agree Nor Disagree	Agree	Strongly Agree
6) The balloon inflations were intuitive				
Strongly Disagree	Disagree	Neither Agree Nor Disagree	Agree	Strongly Agree
7) The inflations became more difficult to feel over time.				
Strongly Disagree	Disagree	Neither Agree Nor Disagree	Agree	Strongly Agree
8) Avoiding drops was my highest priority				
Strongly Disagree	Disagree	Neither Agree Nor Disagree	Agree	Strongly Agree
9) Delicate grasping was my highest priority				
Strongly Disagree	Disagree	Neither Agree Nor Disagree	Agree	Strongly Agree
<u>Comments and Suggestions:</u> Please share any other comments or suggestions that you may have about tactile feedback or improving the system. Thank you for your help with our research!				

Figure 68. Questionnaire for Robotic Surgery Tactile Feedback Study

Grip force was measured during each of these trials using the grasper-mounted force sensors and logged using the data acquisition aspect of the user interface (National Instruments LabVIEW®). These sensors had a saturation point at ADC Value = 660, and a minimum detectable value at ADC = 60. An Instron® mechanical loading system was used to determine the conversion factor from ADC value to Newtons by measuring ADC output in response to

known loads. The results of this characterization showed a linear relationship ( $R^2 > 0.98$ ) between the ADC value and Force (Newtons), a saturation point at approximately 4.5 Newtons (ADC=660), and a minimum detectable force at 0.9 Newtons (ADC=60) (Figure 69).

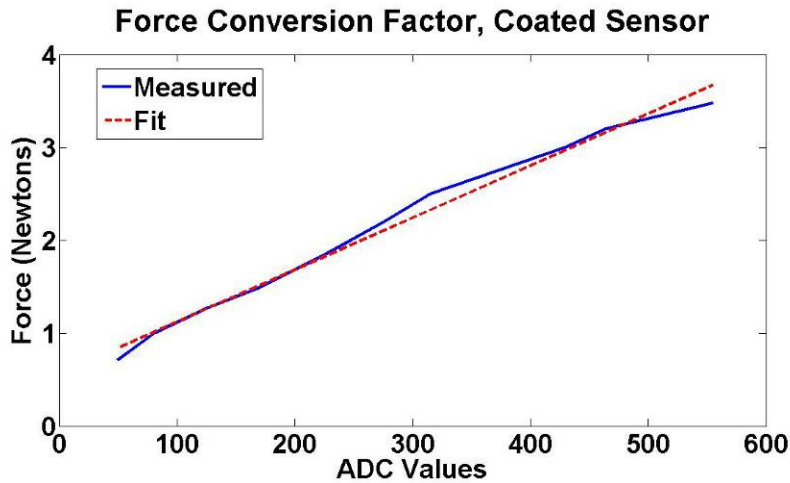


Figure 69. Linear relationship between ADC values and force for coated sensors and live tissue study potentiometer settings

Grasping events were extracted through rising and falling thresholds and manually verified during data analysis. During post-processing, false positives were removed and missed events added. Time-averaged force was calculated for each grasping event using a Riemann sum divided by the event's duration.

Tissue damage was evaluated by gross inspection of the damaged areas of bowel by a blinded pathologist, along with controls. The pathologist counted the number of sites of observable damage and scored each damage site as either level 1 (light), level 2 (medium), or level 3 (heavy) damage.

Prior to the experiments, a dry run was performed by research collaborators. Pathological inspection of the histology of the dry run tissue was performed by two blinded analysts. These evaluations found that the histological examination matched closely with a previously performed gross exam (Figure 70). From this, it was concluded that damage could be evaluated from gross inspection.



Figure 70. Example of damaged bowel. (Left) Gross exam indicated hemorrhagic tissue (Right) Corresponding histology image shows focal hemorrhage in muscularis propria

At the end of the experiment, data consisted of tissue damage scores and a vector of time-averaged grip forces for each subject.

## 6.2.2 Statistical Analysis and Results

Both the grasping forces data and tissue damage results showed non-normal distributions. For the grasping force, this was due to frequent saturation on high end of the scale. For tissue damage, this was due to a majority of segments ranked with zero or one site of damage. For these reasons all statistical analyses were performed using non-parametric methods.

Five statistical analyses were performed on the data from the live tissue experiment:

- (1) Population Analysis of Force Data
- (2) Population Analysis of Tissue Damage Scores
- (3) Analysis of Force / Damage Correlation
- (4) Classification of Subjects by Force Data (Subject-By-Subject Analysis)
- (5) Analysis of Survey Answers



In the population analysis of force data, Friedman's Test was performed to distinguish differences in grip force between the conditions (T1 – OFF, T2 – ON, and T3 – OFF), for each subject group (All Subjects, Novices, Experts, Attendings, and Residents).

In the tissue damage analysis, a Wilcoxon Signed Rank Test was performed to distinguish differences in the number of sites of tissue damage for each subject group.

To test the correlation between force and damage, a linear regression test was used on the mean forces used across a segment of bowel and its damage score.

In the subject-by-subject analysis, each subject was analyzed independently using the Wilcoxon Rank Sum Test and then categorized based on the combination of their individual p-values for each of the pair-wise comparisons (T1/T2, T2/T3, T1/T3).

Finally, survey data was analyzed by calculating and comparing the mean scores for each of the questions for each of the subject groups.

### ***Force Data: Population Analysis***

Because of the non-Gaussian distribution of the data, it was analyzed by median and interquartile range and displayed using box-and-whisker plots. Mean force plots are displayed alongside for comparison. The force data for each of the subject groups is shown in Figure 71 - Figure 75.

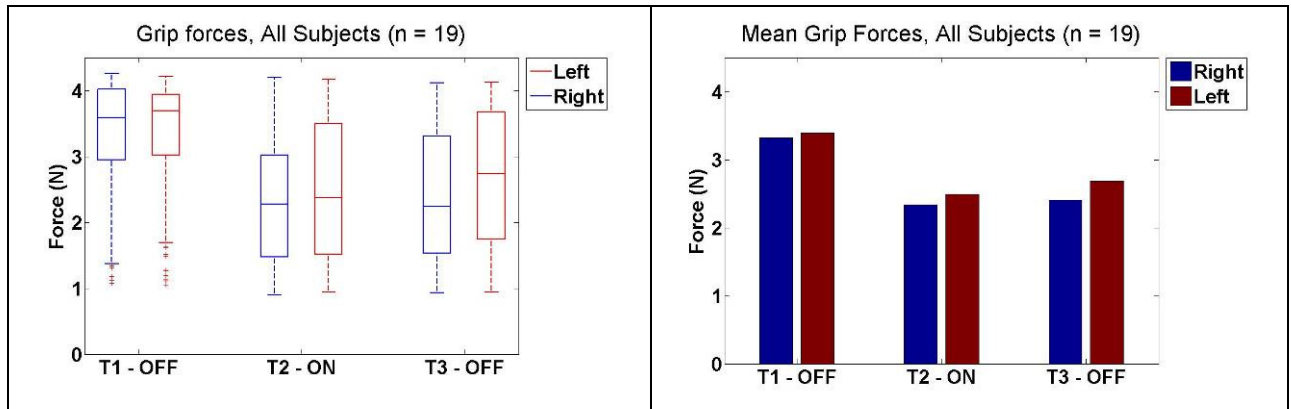


Figure 71. Live tissue grip force results, all subjects.

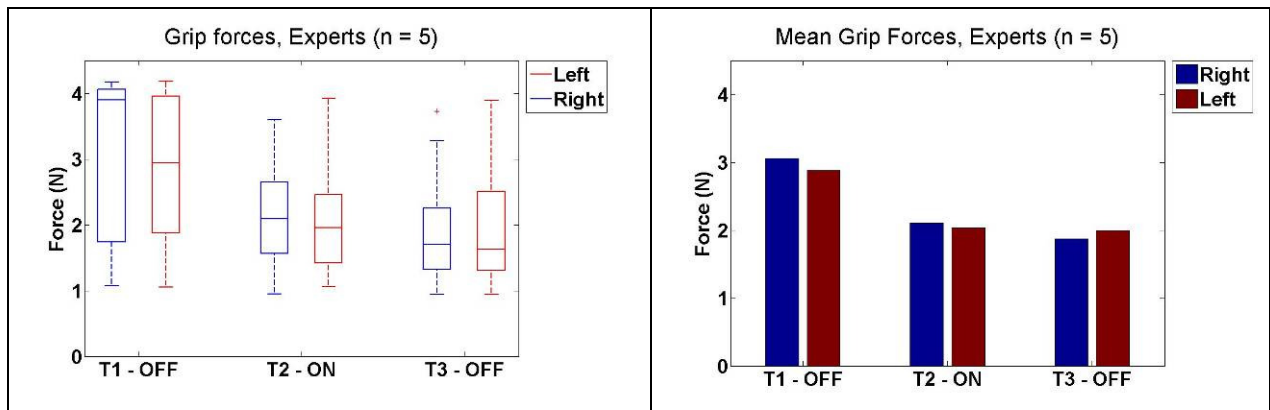


Figure 72. Live tissue grip force results, expert subjects

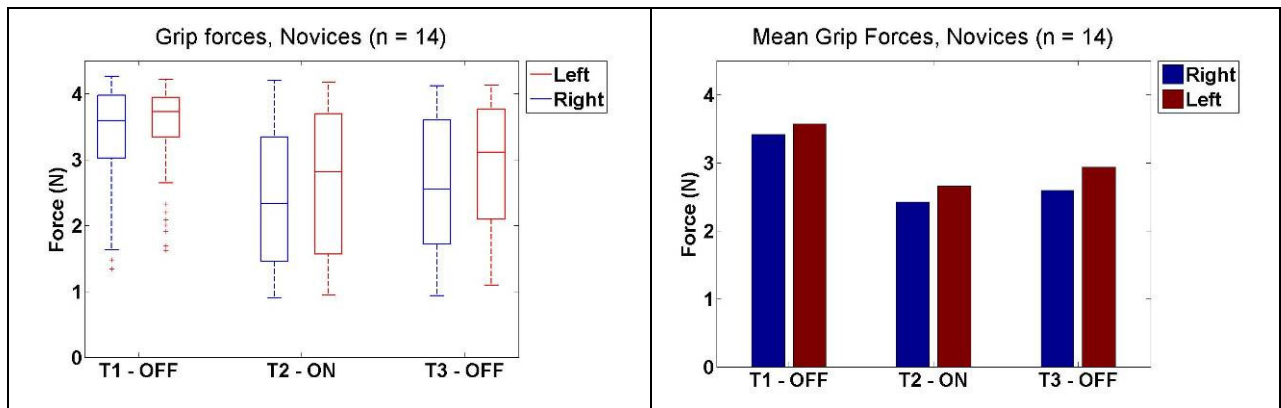


Figure 73. Live tissue grip force results novice subjects

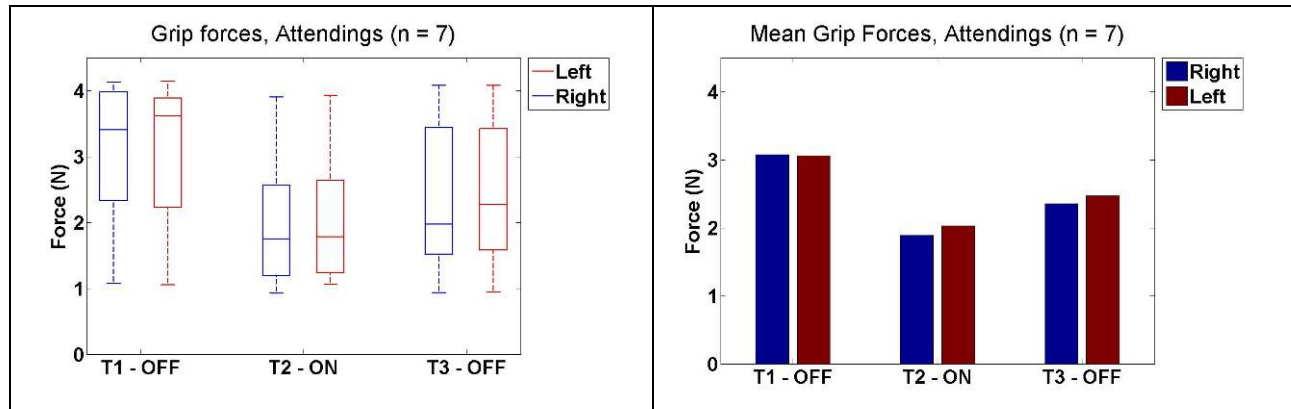


Figure 74. Live tissue grip force results, attending surgeons.

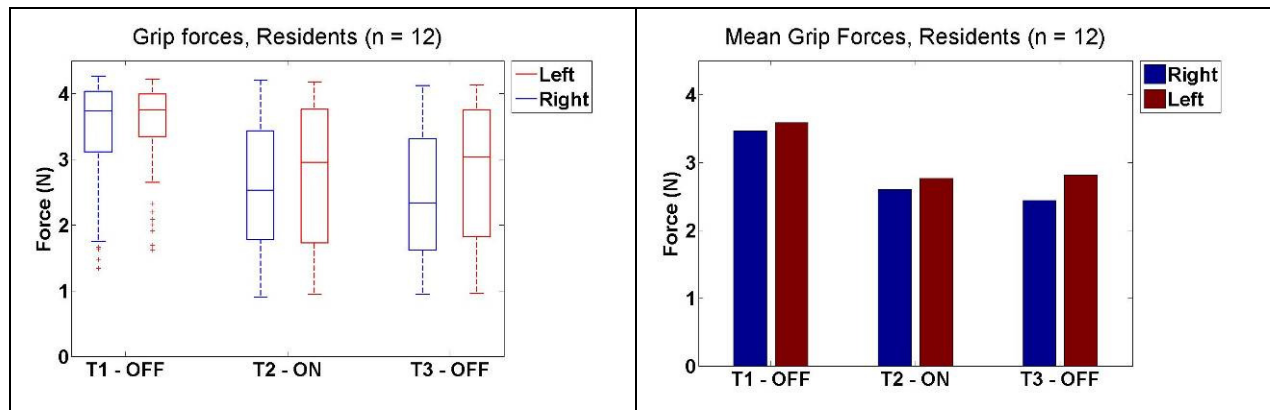


Figure 75. Live tissue grip force results, surgical residents

Subjects in each of the five groups (All Subjects, Experts, Novices, Attendings, Residents) were compared using Friedman’s Test, with seven repetitions for each subject. Friedman’s Test is a non-parametric test similar to the parametric repeated measures ANOVA that detects differences across two or more measures. When the number of grasping events was different for each subject, seven events were randomly selected from those available.

The following hypotheses were tested:

$H_{1,a}$ : There were significant differences across all three measures

$H_{2,a}$ : There were significant differences between condition 1 (T1) and condition 2 (T2)

$H_{3,a}$ : There were significant differences between condition 2 (T2) and condition 3 (T3)

$H_{4,a}$ : There were significant differences between condition 1 (T1) and condition 3 (T3)

To test all four hypotheses, Friedman's test was run four times: once across all three measures, and then three pair-wise comparisons. Because four comparisons were made, a Bonferonni correction was used and  $P < 0.0125$  considered for significance. Table 7 shows the resulting p-values.

Table 7. P-Values for force data hypothesis testing using Friedman's test

Group	Hand	P (All)	P (T1 / T2)	P (T2 / T3)	P (T1 / T3)
All Subjects (n = 19)	Right	1.33e-018***	1.22e-016***	0.826	4.01e-013***
	Left	3.15e-014***	3.15e-011***	0.455	7.66e-012***
Experts (n = 5)	Right	5.68e-006***	4.22e-006***	0.0814	0.000228***
	Left	6.03e-005***	0.000228***	0.71	0.000115***
Novices (n = 14)	Right	4.18e-014***	1.56e-012***	0.339	3.31e-010***
	Left	8.11e-010***	1.75e-008***	0.0877	1.74e-007***
Attendings (n = 7)	Right	5.42e-006***	5.54e-008***	0.106	0.0357
	Left	4.92e-008***	4.49e-007***	0.00735*	2.38e-005***
Residents (n = 12)	Right	1.43e-015***	8.83e-012***	0.319	3.69e-013***
	Left	4.76e-008***	5.71e-006***	0.113	2.42e-007***

The data showed a significant decrease in grasping force from T1 to T2 for all groups ( $P < 0.0125$ ) for both the dominant and non-dominants hands. All groups showed no significant differences in the distributions between T2 and T3 indicating that, overall, the lower forces were retained. This implies that the benefit from T1 to T2 could be caused by either the addition of tactile feedback or an increased familiarity to the task, or both.

The box and whisker plots showed that for all groups except for experts, the median and interquartile range of forces for T1 were clustered near the saturation point, whereas experts showed both higher and lower forces in T1. T2 also showed a large degree of variability across all subject groups, indicating that the feedback system had impact on some subjects, but not others. T3 showed a similar degree of variability, indicating that the retention of low force values also varied by subject.

For this reason, a subject-by-subject analysis was also performed.

### ***Tissue Damage: Population Analysis***

Tissue damage was quantified by a blinded pathologist who counted the number of sites of damage on each section of bowel and rated each site as L1 (light), L2 (medium), or L3 (heavy) damage (Figure 76). An example of light (L1) damage was a faint or superficial hemorrhage. An example of medium (L2) damage was a 2 – 3 mm raised hematoma or an intermediate (grade 2) lesion. An example of heavy (L3) damage was disrupted serosion or a hemorrhagic area with a 2 mm scab and 6 mm area of discoloration.

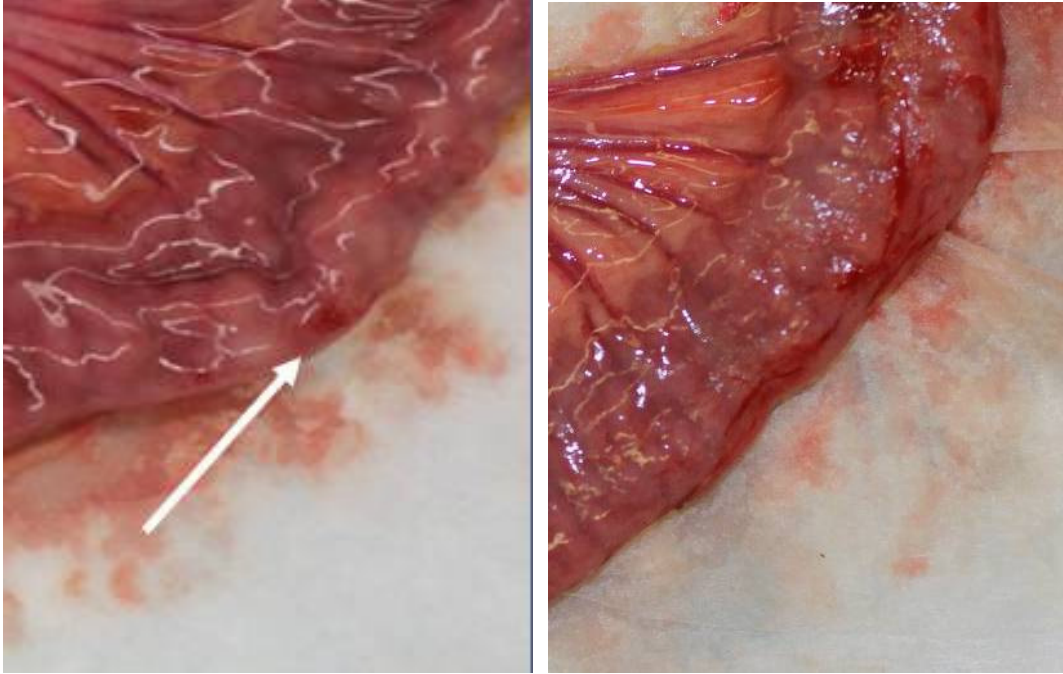


Figure 76. (Left) An example of light (L1) damage. (Right) An example of heavy (L3) damage where pathologist noted a possible disrupted serosion

Statistical methods were performed to test the following hypotheses

*H<sub>1,a</sub>: There were significant differences in total number of damage sites between at least two of the three measures.*

*H<sub>2,a</sub>: There were significant differences in total number of damage sites between condition 1 (T1) and condition 2 (T2)*

*H<sub>3,a</sub>: There were significant differences in total number of damage sites between condition 2 (T2) and condition 3 (T3)*

*H<sub>4,a</sub>: There were significant differences in total number of damage sites between condition 1 (T1) and condition 3 (T3)*

Damage scores were compared using Friedman's test across all three measures (T1, T2, and T3) with one repetition per subject. Pair-wise comparisons were made using a Wilcoxon Signed Rank Test (non-parametric) as data was matched, but not normally distributed. There was not enough statistical power to analyze the different levels of damage independently, so significance testing was performed on the total number of damage sites. Because four

comparisons were made, Bonferonni's correction was used and  $P < 0.0125$  considered for significance.

Charts showing the mean number of damage sites for each of the experience levels is shown in Figure 77 – Figure 81 and the p-values from the hypothesis testing is shown in Table 8.

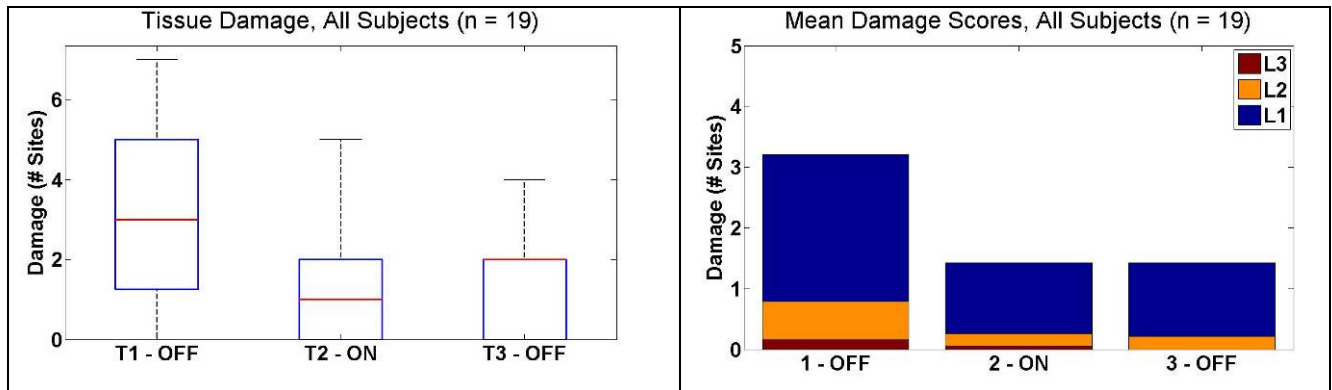


Figure 77. Tissue damage results, all subjects

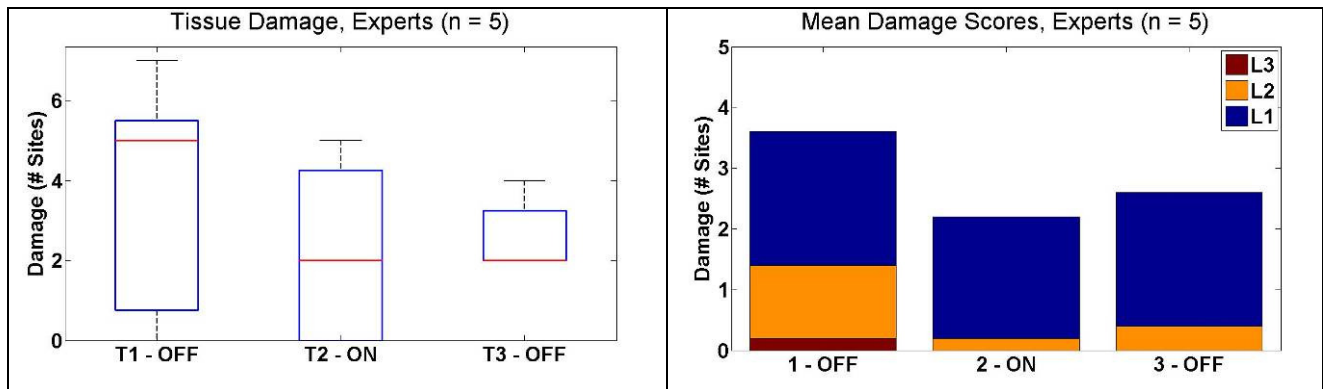


Figure 78. Tissue damage results, expert subjects

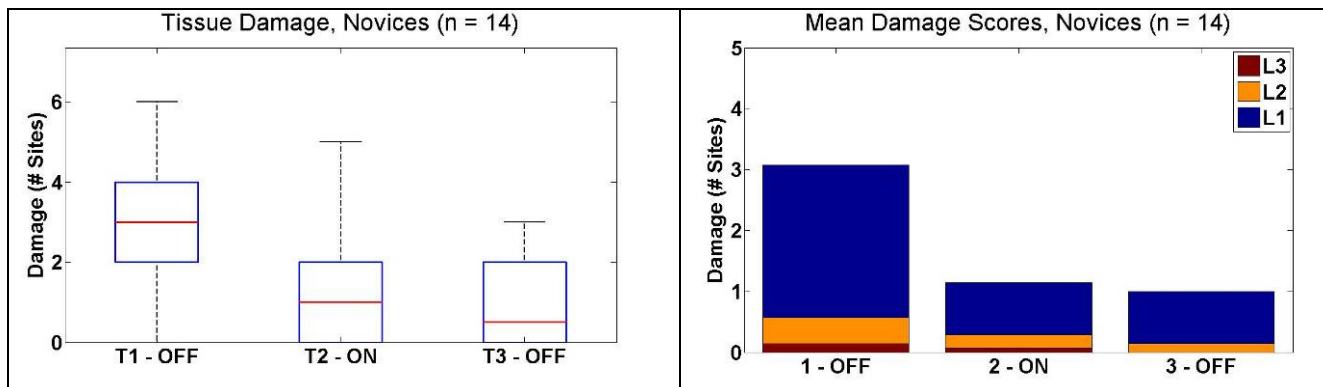


Figure 79. Tissue damage results, novice subjects

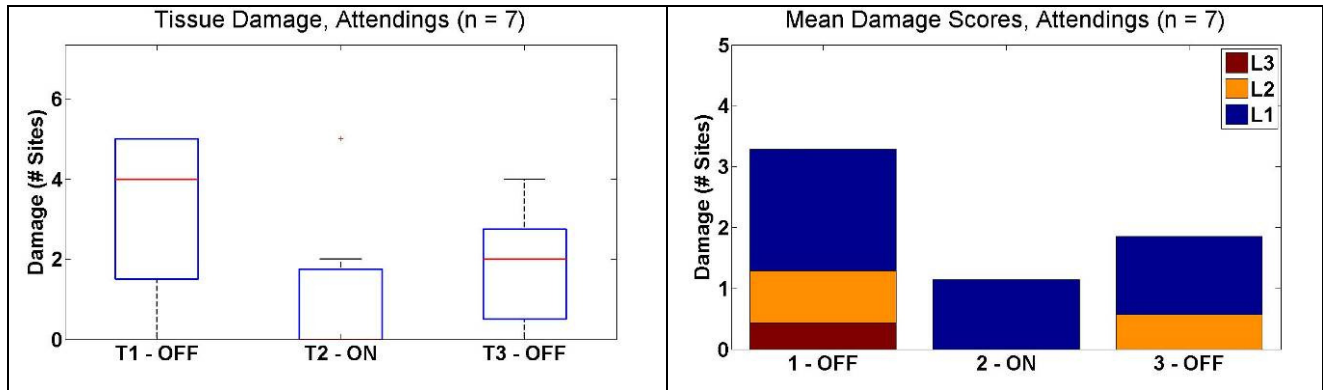


Figure 80. Tissue damage results, attending surgeons

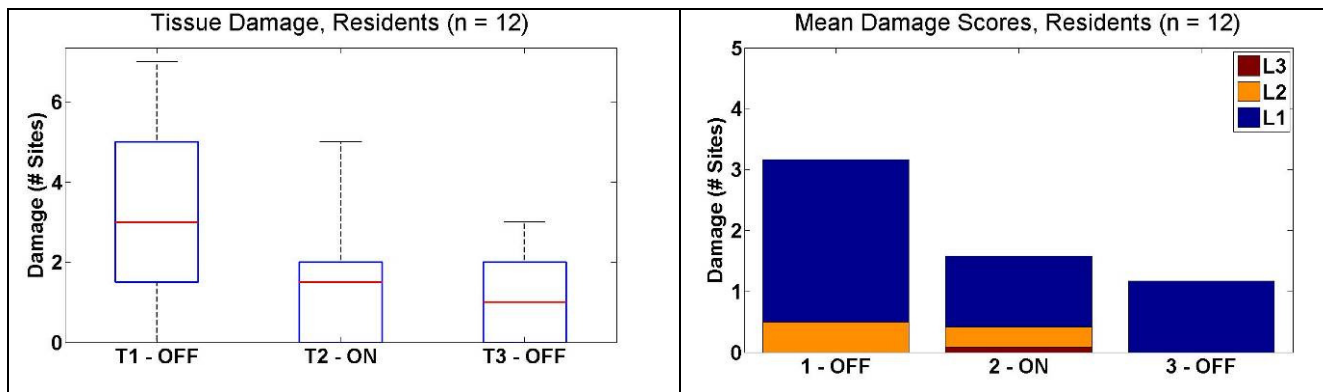


Figure 81. Tissue damage results, only surgical residents

Table 8. P-Values for tissue damage hypothesis testing.

Group	P (All) <sup>a</sup>	P (T1 / T2) <sup>b</sup>	P (T2 / T3) <sup>b</sup>	P (T1 / T3) <sup>b</sup>
All Subjects (n = 19)	0.00082012 <sup>**</sup>	0.0017553 <sup>**</sup>	0.95728	0.017142
Experts (n = 5)	0.46547	0.25	1	0.6875
Novices (n = 14)	0.0011183 <sup>**</sup>	0.0046387 <sup>*</sup>	0.69336	0.0097656 <sup>*</sup>
Attendings (n = 7)	0.11456	0.0625	0.5	0.25
Residents (n = 12)	0.0049443 <sup>*</sup>	0.018555	0.36328	0.035156

<sup>a</sup> Friedman's Test, one rep per subject



## <sup>b</sup>Wilcoxon Signed Rank Test

Each subject group showed a decrease in mean number of damage sites between T1 and T2, but statistical significance was only obtained for all subjects (n=19) and novice subjects (n=14). This is more likely due to a lack of statistical power as these two groups had the largest number of subjects.

The *All Subjects* group showed a significant decrease in the number of damage sites between T1 and T2 ( $P < 0.002^*$ ). The test showed no significant differences between T2 and T3 ( $P > 0.9$ ). In the comparison between T1 and T3, the p-value was 0.017, which would not be significant with the Bonferonni correction, but is close. These results are similar to the force damage results, and indicate that the decrease in damage could be due to tactile feedback or familiarity with the task.

### ***Force / Damage Correlation Analysis***

An analysis was performed to determine if there was a significant correlation between mean force and the number of observed sites of tissue damage. This was done by calculating the mean grasping force applied to a section of bowel, matching it with that bowel's damage score, and performing a linear regression on the results. (Figure 82).

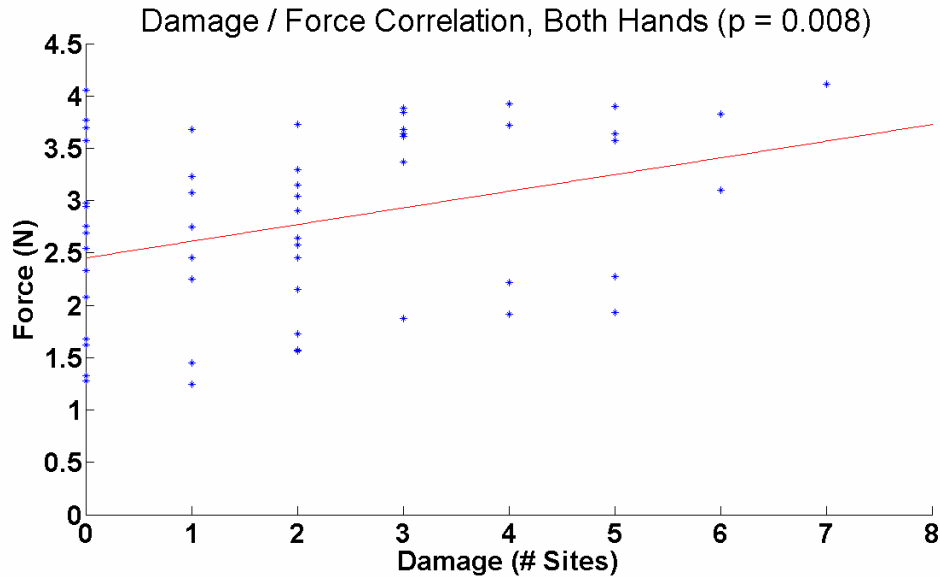


Figure 82. Correlation analysis of damage and mean grasping force.

The results showed a significant correlation ( $P= 0.008$ ) between the mean force across both hands and the number of sites of damage. This suggests that that using consistently higher levels of force may lead to higher incidence of damage. For bowel segments with fewer than two damage sites, there appeared to be similar occasions of low and high force. Bowel segments with three or more sites of damage occurred more often when higher forces were used.

This data suggests that decreasing grip force may have a beneficial on damage to tissue.

### ***Force Data: Subject-By-Subject Analysis***

The initial results indicated a large amount of variability between subjects. An additional analysis was performed to compare each subject individually. In this case, time-averaged grip force values were compared using a Wilcoxon Rank Sum test, a non-parametric test between groups of independent samples. Pair-wise comparisons were made to test the following hypotheses for each subject:

*H<sub>1,a</sub>: There were significant differences between condition 1 (T1) and condition 2 (T2)*

*H<sub>2,a</sub>: There were significant differences between condition 2 (T2) and condition 3 (T3)*

*H<sub>3,a</sub>: There were significant differences between condition 1 (T1) and condition 3 (T3)*

At the end of this analysis each subject had a vector of three p-values. Based on these p-values, subjects were classified into one of the following six groups:

(1) *No Effect*: Subject showed no significant differences between T1 and T2, and the mean forces in all conditions were greater than 2.5 N.

(2) *Already Low*: Subject showed no significant differences between T1 and T2, and the mean forces in all conditions were less than 2.5 N.

(3) *Higher*: Subject used more force with tactile feedback. ( $T_2 > T_1$ )

(4) *Lower and Completely Retained*: Subject used less force with tactile feedback. When system was turned off in T3, this low force was completely retained. T2 and T3 were indistinguishable.

(5) *Lower & Not Retained*: Subject used less force with tactile feedback. When the system was turned off in T3, the force raised up to the level of T1. T1 and T3 were indistinguishable.

(6) *Lower and Partially Retained*: Subject used less force with tactile feedback. When the system was turned off in T3, the force increased, but not as high as T1. T1, T2, and T3 were different, and  $T_1 > T_3 > T_2$ .

Each hand was analyzed independently, so for 19 subjects, there were 38 cases. There were occasions where a subject's dominant hand was placed in one group and non-dominant hand placed into another group.

The following section describes the criteria for placing a subject-hand into each of the aforementioned groups.  $H(T1/T2)$  refers to the hypothesis comparing  $T1$  and  $T2$ .  $H = 0$  implies there is evidence for the null hypothesis whereas  $H = 1$  implies evidence to reject the null hypothesis.

Subjects were classified as *No Effect* if  $H(T1/T2) = 0$ , and mean forces in all conditions were over 2.5 N. An example is shown in Figure 83.

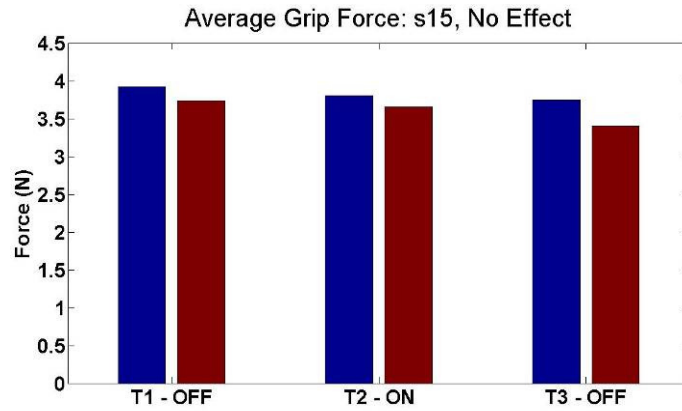


Figure 83. An example of a subject with no effect due to tactile feedback.

Subjects were classified as *Already Low* if  $H(T1/T2) = 0$ , and the mean forces in all conditions were under 2.5 N. An example of an expert subject is shown in

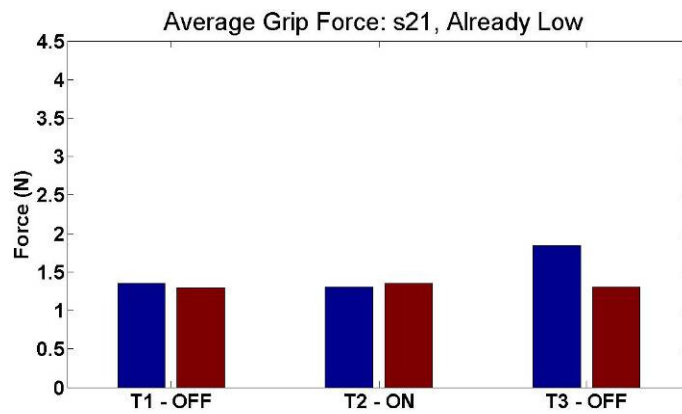


Figure 84. An expert subject with already low forces

Subjects were classified as *Higher* if  $H(T1/T2) = 1$ , but  $\text{mean}(T2) > \text{mean}(T1)$ . This occurred for both hands on one of the nineteen subjects. The mean force data for this subject is shown in Figure 85.

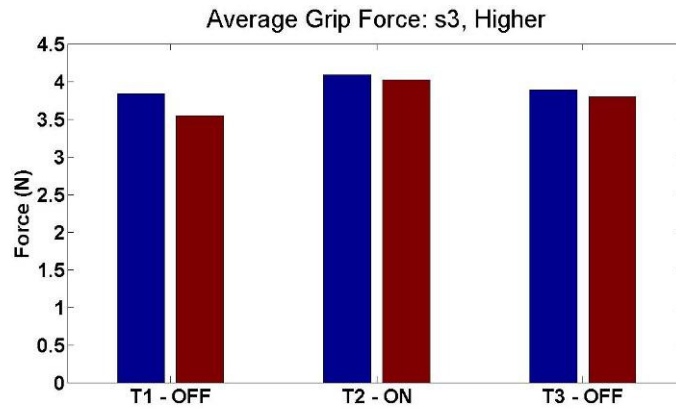


Figure 85. One subject showed higher forces with tactile feedback

Subjects were classified as *Lower and Completely Retained* in the following two cases:

(1)  $H(T1/T2) = 1$ ,  $H(T2/T3) = 0$ ,  $H(T1/T3) = 1$ . T2 was indistinguishable from T3 and they were both lower than T1.

(2)  $H(T1/T2) = 1$ ,  $H(T2/T3) = 1$ ,  $H(T1/T3) = 1$ , and  $T3 < T2$ . T3 is lower than T2.

These cases implied that a subject learned throughout the course of the experiment. It is unclear whether the improvement is due to tactile feedback or subject's increasing familiarity with the task or some combination. An example of a subject's data is shown in Figure 86.

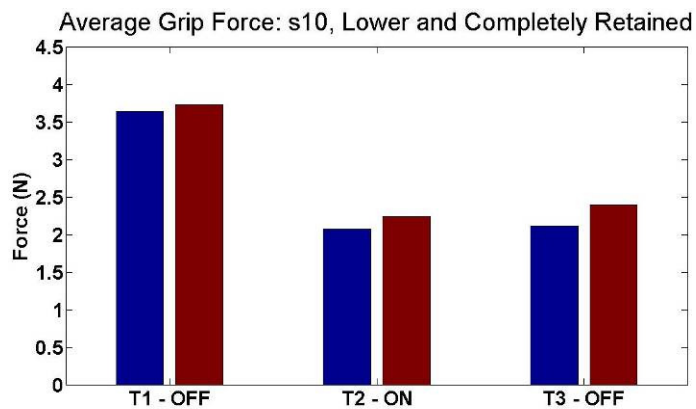


Figure 86. A subject with lower and completely retained forces

Subjects were classified as *Lower and Not Retained* in the following two cases:

(1)  $H(T1/T2) = 1$ ,  $H(T2/T3) = 1$ ,  $H(T1/T3) = 0$ . T1 is indistinguishable from T3 and T2 is lower than both..

(2)  $H(T1/T2) = 1$ ,  $H(T2/T3) = 1$ ,  $H(T1/T3) = 1$ , and  $T3 > T1$ . The force increases in T3, but is higher than the force in T1.

This case implied that a subject did not learn throughout the course of the experiment, and that the improvements were solely due to the tactile feedback in the second trial. An example of a subject's data that was *Lower and Not Retained* is shown in Figure 87.

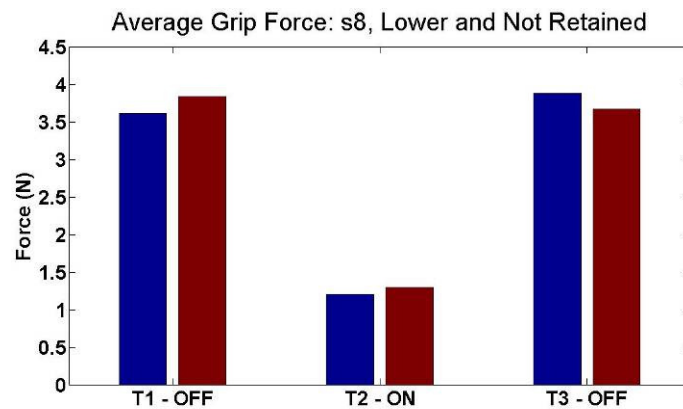


Figure 87. An example of subject with force results that were Lower and Not Retained.

Subjects were classified as *Lower and Partially Retained* in the remaining two cases:

(1)  $H(T1/T2) = 1$ ,  $H(T2/T3) = 1$ ,  $H(T1/T3) = 1$ , and  $T1 > T2 > T3$ . T1, T2, and T3 are all different. T3 is greater than T2, but smaller than T1.

(2)  $H(T1/T2) = 1$ ,  $H(T2/T3) = 0$ ,  $H(T1/T3) = 0$ . T2 is less than T1. T3 was highly varying and indistinguishable from both T2 and T1.

This implied that there was some impact due to learning, but that the effects due to tactile feedback were more appreciable. An example of a subject's data that was *Lower and Partially Retained* is shown in Figure 88.

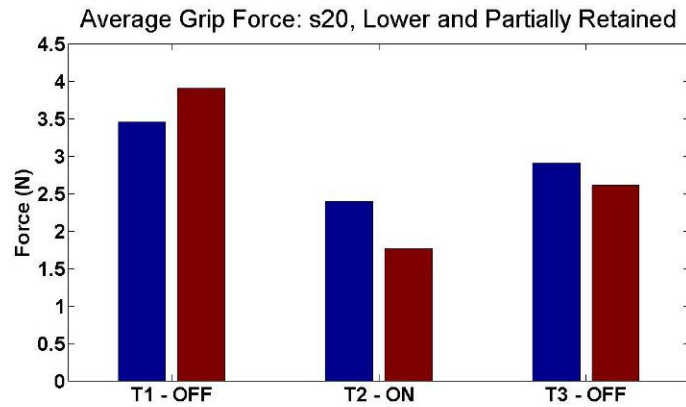


Figure 88. An example of subject with force results that were Lower and Partially Retained.

Once the classification criteria was established, each subject-hand was placed into these categories according to the p-values from the pair-wise comparisons. The following pie charts (Figure 89 – Figure 92) show the percent of subjects who fell into each category for all subjects, when grouped by experience level, and for dominant/non-dominant hand.

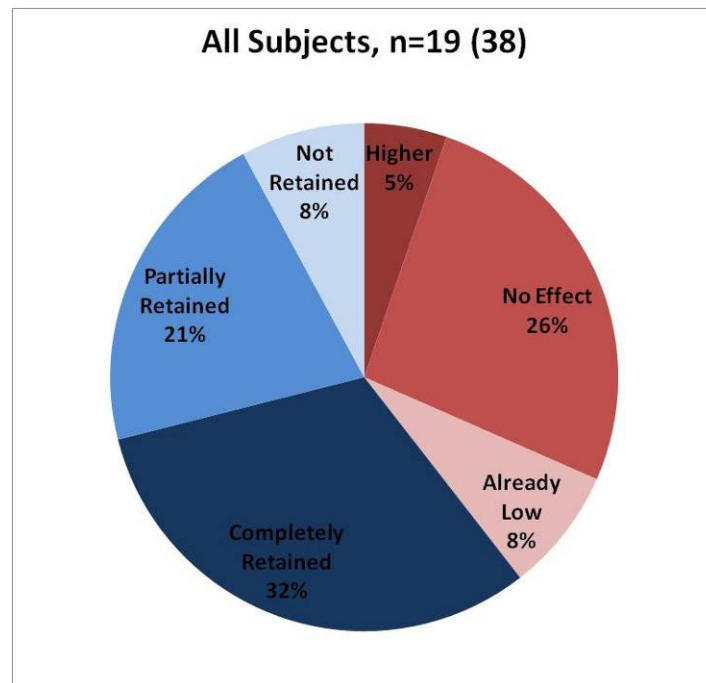


Figure 89. Subject-by-Subject Analysis: Classification of all subjects, both hands.

Approximately 8% of subjects (all experts) used forces lower than 2.5 N. Approximately 61% of subjects showed decreased forces from the first condition (T1) to the second condition

(T2). Approximately half of the subjects that improved grip force completely retained the lower forces, whereas the other half only partially retained this information, if at all. The remaining 30% of subjects (all novices) had no effect due to tactile feedback or learning.

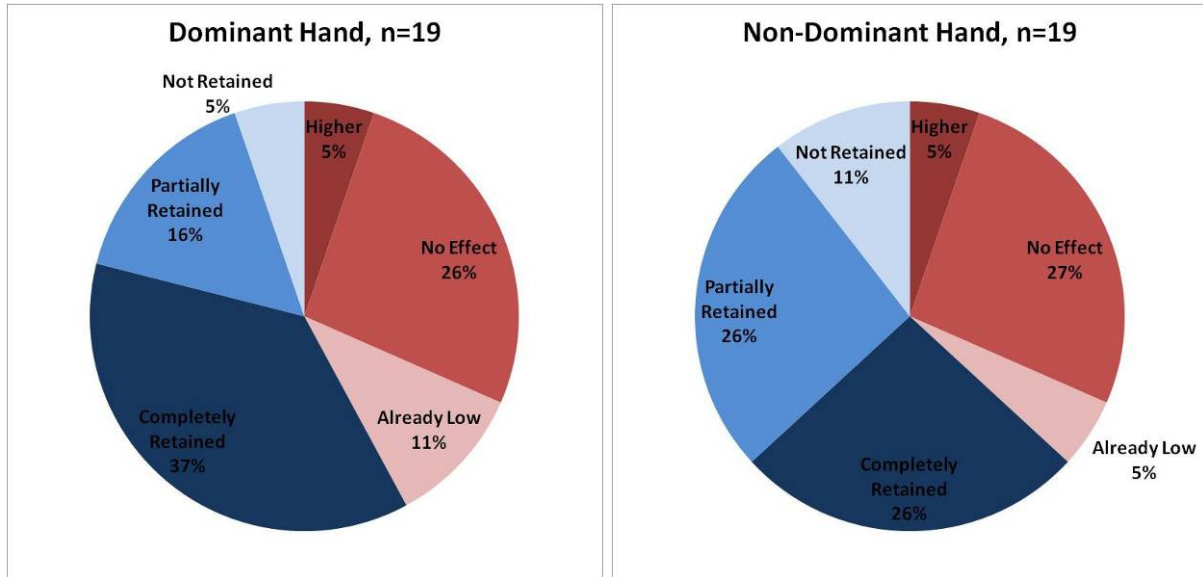


Figure 90. Subject-by-Subject Analysis: Classification of all subjects, (Left) only dominant hand (Right) Non-dominant hand.

A comparison of dominant and non-dominant hand showed that the dominant hand had a higher incidence of initially low forces, and when improvement was observed, a higher incidence of complete retention.



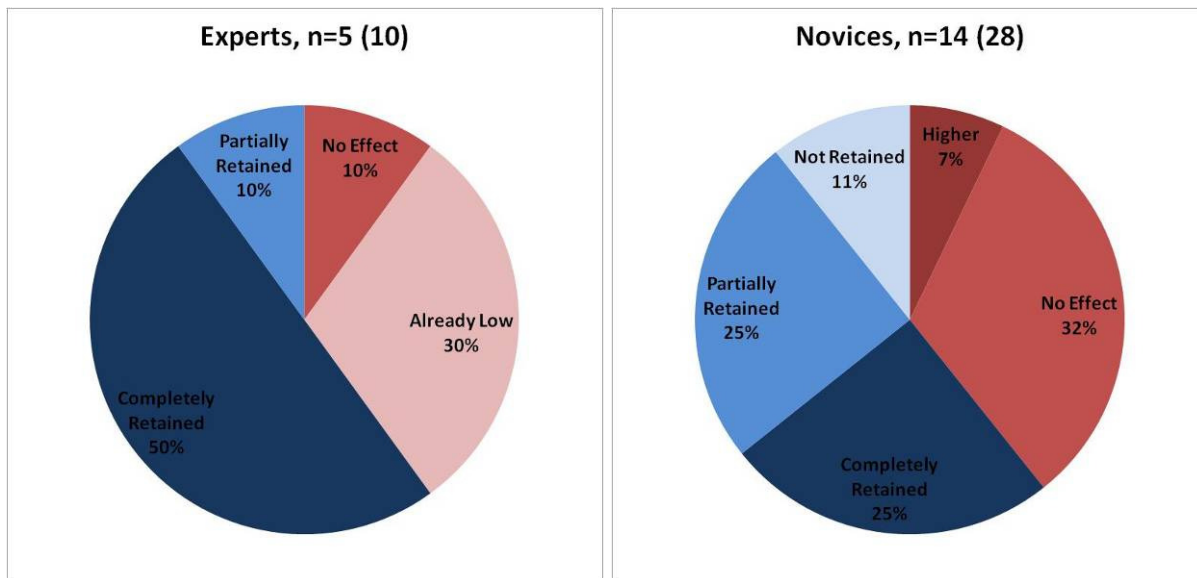


Figure 91. Subject-by-Subject Analysis: (Left) Classification of the five expert subjects (six or more robotic surgery cases). (Right) and the Novice subjects

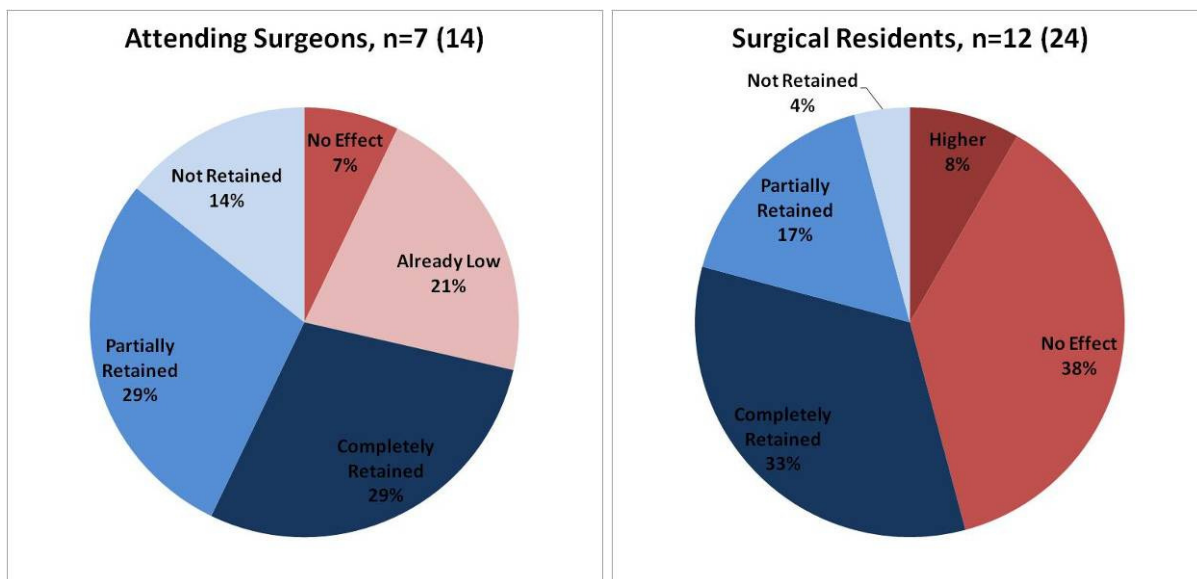


Figure 92. Subject-by-Subject Analysis: Classification of (Left) attending surgeons and (Right) surgical residents.

A majority of expert subjects (80%) had low forces in the third condition (T3), due to either already low forces (30%), or complete retention of benefit (50%). One expert subject had no improvement due to tactile feedback. This subject showed forces at around 2.8 N, which was slightly higher than the category's threshold.

For novice subjects, 61% of subjects showed significant decreases in grip force from T1 to T2. A majority of these did not completely retain the low forces in the third condition, indicating that while there may have been some learning, the impact due to tactile feedback was more appreciable. Thirty-nine percent (39%) of novice subjects saw no improvements across the experiment and all of these showed forces higher than 2.5 N.

At the end of the experiment, subjects filled out a questionnaire. This was analyzed to help determine possible reasons or way to improve the system.

### ***Survey Analysis:***

Following the experiment, subjects were asked to fill out a survey. It contained questions concerning the subject's level of experience – both in the medical profession and with regard to robotic surgery – as well as questions concerning the experiment.

The survey scored subjects' level agreement with nine statements:

- (1) Tactile Feedback helped me perform the task.
- (2) Tactile feedback had no effect on my performance.
- (3) With tactile feedback, I grasped tissue with less force.
- (4) The balloon inflations were easy to feel.
- (5) I found myself ignoring the balloon inflations.
- (6) The balloon inflations were intuitive.
- (7) The inflations became more difficult to feel over time.
- (8) Avoiding drops was my highest priority.
- (9) Delicate grasping was my highest priority.

For each statement, subjects indicated their level of agreement with one of five answers, which were scored on the following scale: Strongly Disagree: 1, Disagree: 2, Neither Agree nor Disagree: 3, Agree: 4, Strongly Agree: 5.

For each group of subjects (All Subjects, Experts, Novices, Attendings, Residents), mean scores were calculated. Three additional groups were analyzed based on results of the force data analysis:

(1) *No Effect*: subjects that showed no significant decreases in grip force for both hands

(2) *One Hand*: subjects that showed a significant decrease in grip force for one hand.

(3) *Both Hands*: subjects that showed a significant decrease in grip force across both hands.

The results for the survey answers is shown in Figure 93 – Figure 95.

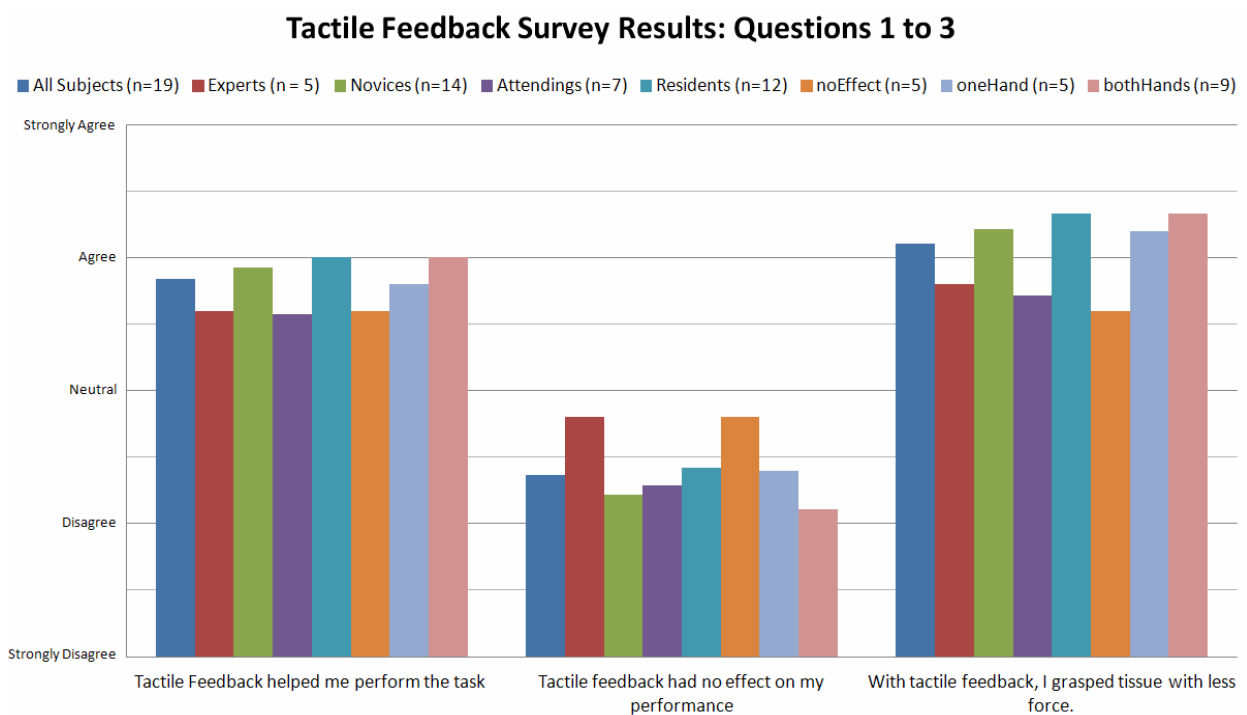


Figure 93. Live Tissue Study Survey Results, Questions 1 to 3

### Tactile Feedback Survey Results: Questions 4 to 6

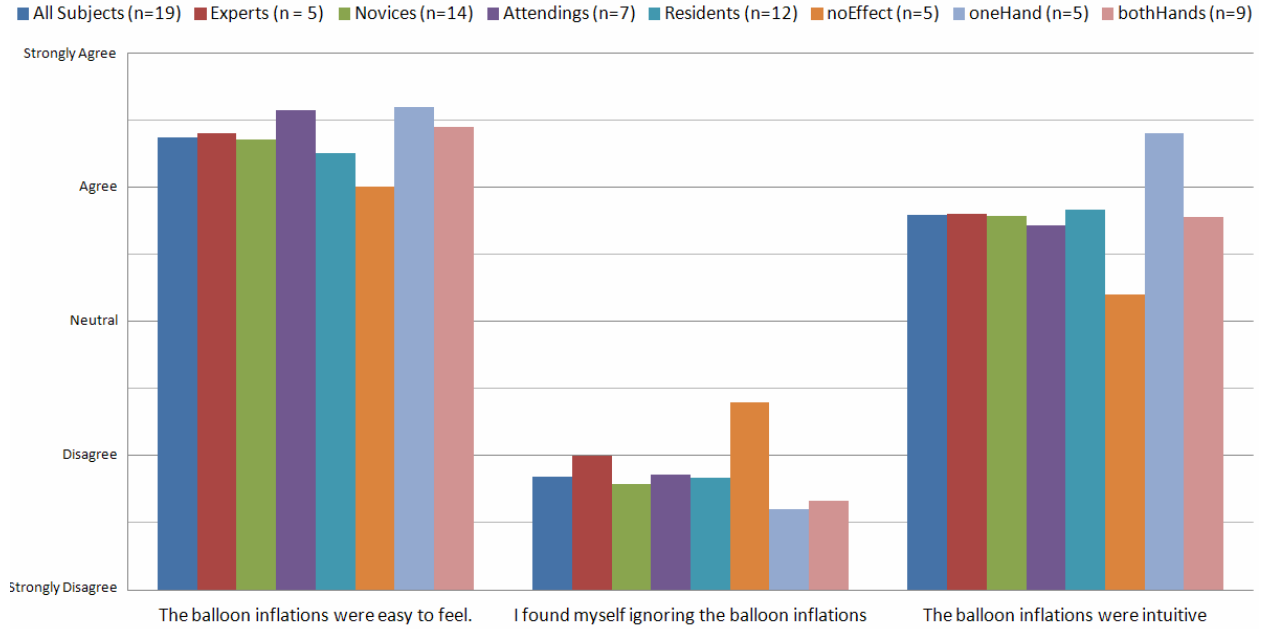


Figure 94. Live Tissue Study Survey Results, Questions 4 to 6

### Tactile Feedback Survey Results: Questions 7 to 9

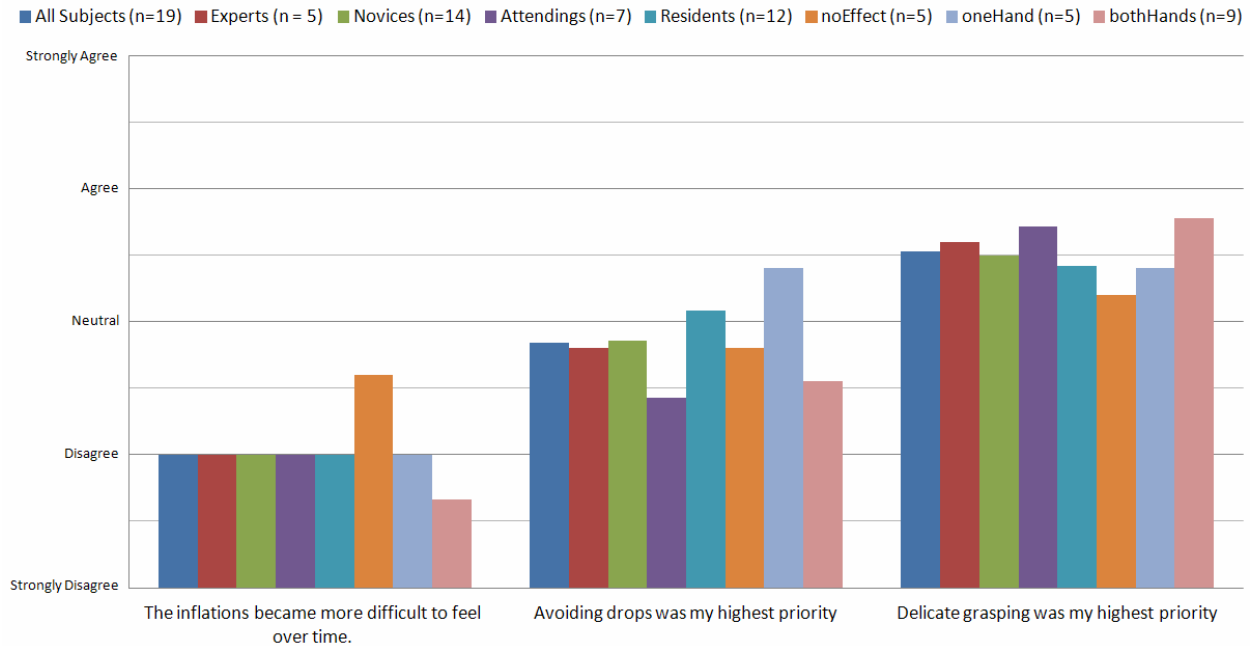


Figure 95. Live Tissue Study Survey Results, Questions 7 to 9

In general, the subject groups tended to give similar answers to the survey questions. Subjects noted that tactile feedback helped performance and decreased grasping force. Responses indicated that the balloon inflations were perceptible and not ignored, and that efforts were directed more towards delicate grasping, although residents paid additional attention to avoiding drops.

There were also several notable differences. Expert subjects tended towards neutral in the first three questions. Additionally, the group that did not benefit from tactile feedback (“No Effect”) agreed more with the statements: *Tactile feedback did not effect performance, I found myself ignoring balloon inflations, and the inflations became more difficult to feel over time.* This group disagreed more with the statements: *With tactile feedback, I grasped tissue with less force, the balloon inflations were easily to feel, the balloon inflations were intuitive, and Delicate grasping was my highest priority.*

This indicated some potential reasons for novice subjects showing no improvement. It was found that one novice subject had difficulty perceiving the balloons, and this became even more difficult farther into the trial, possibly due to acclimation. The three remaining novice subjects with no effect indicated challenges with interpretation of the balloons, which suggested a need for additional training in the use of the system. The final no effect subject was an expert with already low forces.

### **6.2.3 Discussion**

The population analysis showed that both grasping force and the number of sites of damage decreased ( $P < 0.0125$ ) between the baseline condition where tactile feedback was deactivated to when tactile feedback was activated. For both grasping forces and number of sites of damage, there were no distinguishable differences between the second condition with tactile

feedback, to when the system was deactivated in the third condition. These results suggest that the improvements could be due to the presence of tactile feedback, increased familiarity with the task, or some combination of the two. It is inconclusive whether the improvements due to learning would have occurred without the presence of feedback, and therefore a follow-up study is proposed (Section 9, Future Work).

A linear regression showed a significant correlation between high grasping forces and incidence of damage. While other factors – such as location of grasp (i.e., proximity to delicate vessels), the duration of the hold, and the effect of tugging on the bowel – may also contribute to tissue damage, this observed correlation lends evidence to the claim that using high grip forces may lead to increased incidence of damage, and that reductions in grip force may have measurable benefits clinical outcomes.

The wide distribution of grasping force and tissue damage scores for both T2 and T3 indicate that the potential improvements were dependent on the particular subject being tested. The results from the subject-by-subject analysis lend further evidence to this claim.

This subject-by-subject analysis showed that approximately 60% of subjects had a significant decrease in grip force in the second condition (T2), and that 40% showed no differences across trials. For experts, this “No Effect” group was largely due to baseline forces within 2.5 N. For novices, the survey showed that one subject had difficulty perceiving the balloon inflations, and the remaining three were unsure how to interpret them. This suggests that the system could be improved for more intuitive use, or should be paired with an additional period of training.

For 36% of novice subjects, there was a decrease in force from T1 to T2, and a subsequent increase in force in T3. These results match the original robotic surgery training

study performed prior to this research [153], and suggests that a tactile feedback system permanently incorporated with a surgical robotic system would result in decreased forces and damage while grasping.

For approximately 32% of the total subject pool, there was a decrease in force from T1 to T2 and this low force was completely retained in T3. This matched the results from the population analysis. For these subjects, the benefits could be purely due to increased familiarity with the task. Further investigation is proposed in a follow-up study. The number of expert subjects with already low grip forces, and high incidence of retention, indicate that tactile feedback possibly served as a trigger for existing learned kinesthetic memory for fine control of grip when using the robotic surgery system, or attunement to feedback present in the visual display. Together, this may suggest benefit from the use of tactile feedback during robotic surgery training, with the idea that novices may see more retention of low forces over the long term.

#### **6.2.4 Conclusion**

This study has demonstrated the first successful and extended operation of a complete tactile feedback system in an *in-vivo* environment. Nineteen subjects, including five robotic surgery experts and fourteen novices used the da Vinci surgical system integrated with the improved tactile feedback system to pass porcine bowel. The results from this experiment showed a wide variability between subjects, and decreased levels of force and damage when tactile feedback was active that were retained when the system was subsequently deactivated.

The retention of low forces in expert users suggests the potential of tactile feedback as a training device, with novices possibly acquiring expert-level force levels with practice over the longer term. Future studies should be completed to isolate the effects of tactile feedback on

training from improvements purely due to familiarization with the robotic controller, and to quantify the impact of the tactile feedback system on training of novices over the long term.

The correlation between high levels of force and high incidence of damage shows that reducing grasping forces may have realizable clinical benefit.



## 7 Expansion of Tactile Feedback to Remote Surgical Systems

In remote surgical systems, the disconnect between patient and subject is more pronounced than in robotic surgery due to potentially critical latencies in the visual feed. The purpose of this task was to expand the improved tactile feedback to remote surgical applications. This was completed by developing a remote tactile feedback system, integrating it with a remote surgical system, and conducting a preliminary investigation that evaluated the impact of tactile feedback on grasping force when performed over a network.

### 7.1 Remote Tactile Feedback System

#### 7.1.1 System Development

The updated tactile feedback system was converted into a remote tactile feedback system by adding Ethernet-connected computers to the loop and developing software (National Instruments LabVIEW®) for encoding and transmitting tactile information over the Internet (Figure 96) [158].

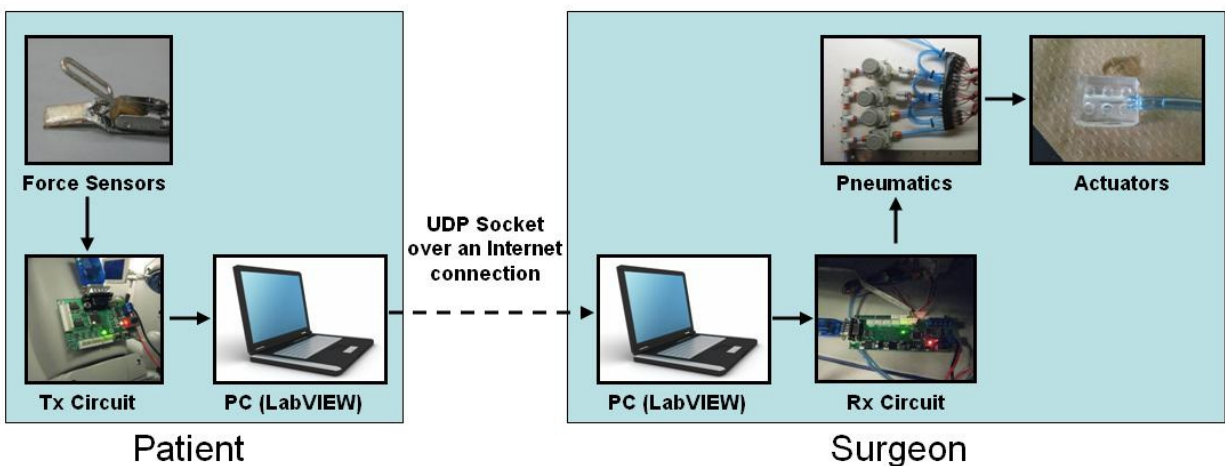


Figure 96. Remote Surgery Tactile Feedback System Architecture

The PC communication software (LabVIEW) was divided into two parts: a *HapticSender.vi* that ran on the Patient Side, and a *HapticReceiver.vi* that ran on the Surgeon side.

*HapticSender.vi* received serial packets from the Tx Circuit through the Keyspan Serial Converter in RS-232, and forwarded them over a UDP socket. It also logged the force data for future statistical analysis.

*HapticReceiver.vi* received packets on the UDP socket and then forwarded them to the Rx Circuit through a second Keyspan Converter. The Tx and Rx Circuits were designed to transmit or receive tactile information independent of the source or destination, and therefore these circuits functioned without any change to their software.

Successful operation of the remote tactile feedback system was validated by setting the sensor and actuator subsystems in separate locations, manually triggering the force sensors, and observing actuator response.

Latency is a critical issue in remote medical systems and so the next step was to determine a quantifiable estimate the system’s transcontinental time delay.

### 7.1.2 Estimating Transcontinental Latency

Latency of the remote tactile feedback system was broken down into three components: processing time, transmission time, and pneumatic filling time (Figure 97).

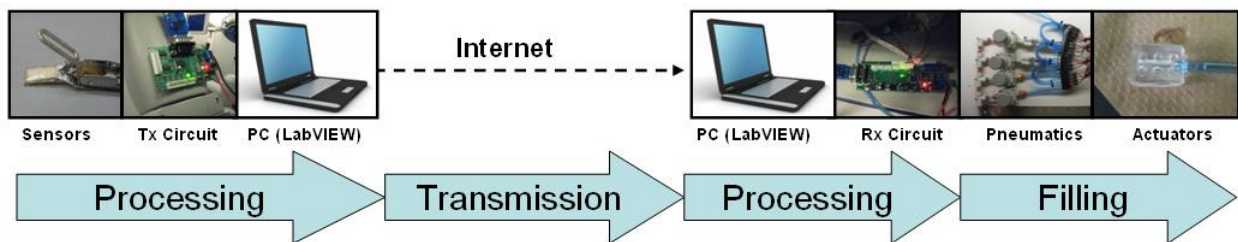


Figure 97. Total latency of the remote tactile feedback system

Experiments were conducted to estimate the latency of each of these three components. Total latency was quantified by summing the results from the individual experiments and reporting the mean, standard deviation, and worst case scenarios.

To capture processing latency, the tactile feedback system was run over a local area network (<1 ms round trip time), effectively setting the transmission delay to zero. Processing latency was then quantified by capturing operation of the system with a high speed (300 fps) camera, and counting frames between sensor triggering and pneumatic system activation (Figure 98). This experiment was performed over ten trials. Processing latency had a range of 40 – 59 ms, including error due to the 3 ms frame time.

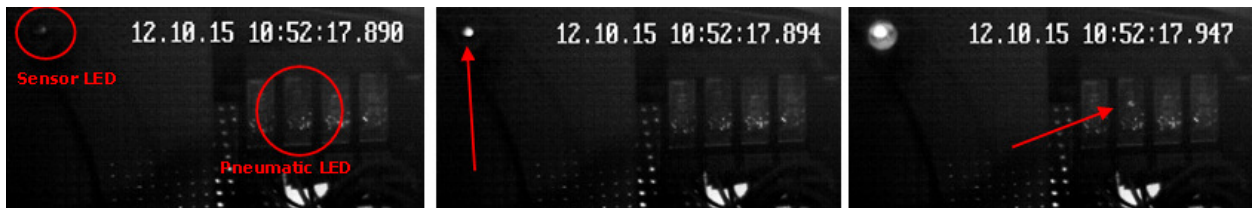


Figure 98. (Left) Neither sensor nor pneumatic system is activated at 17.890 s. (Center) Sensor contact at 17.894 s. A voltage divider circuit causes an LED to turn on. (Right) Pneumatic system LED turns on at 17.947 s. Processing latency for this trial was 53 ms.

Transmission latency was estimated by sending 1000 packets sized to a tactile feedback data message (19 characters) over a standard internet connection from UCLA (CA) to a representative east coast location (Johns Hopkins, in this case) and halving the measured round trip time (Figure 99). Internet congestion can vary with time of day and day of the week. This experiment was performed at 2 PM, PST, on a weekday.

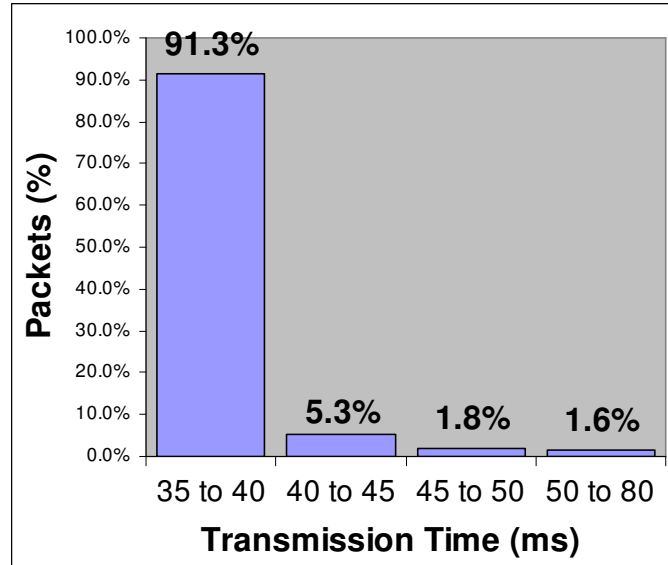


Figure 99. Histogram of the one-way transcontinental internet latency.

Pneumatic filling latency was measured using the high speed camera and counting frames between signaling the pneumatic system (LED on) and full deflection of actuator membrane (Figure 100). Together these latency components provided an estimate of overall delay (Table 9).



Figure 100. (Left) Pneumatic system LED off, and no balloon inflation at 50.142 s (Center) Pneumatic system activated (LED on) at 50.146 s. (Right) Balloon inflation at 50.182 s. Filling time for this trial was 36 ms

Table 9. Summary of latency estimates for remote tactile feedback system

	Range (ms)	Worst Case(ms)	Mean (ms)	Std. Dev. (ms)
Processing	40 – 59	59	51.1	4.9
Transmission	38.1 – 79.0	79 (50*)	39.2	2.8
Pneumatic Filling	30 – 39	39	35.0	1.7
Total Latency	108 – 177	177 (148*)	125.3	5.9

\*98.4 % of packets arrived within 50 ms

The results showed a mean total latency of 125.3 ms with a standard deviation of 5.9 ms. The transcontinental surgery reported an overall latency of 155 ms, which was faster than the limits of human perception [46]. For over 98% of packets, the transmission latency from UCLA to Johns Hopkins was less than 50 ms. For these packets, the worst case latency was 148 ms, which considers the slowest processing time and filling times, as well as the experimental error of the camera capture measurement method ( $\pm 3$  ms). For the remaining 2% of packets, the worst case latency measured in the experiment was as high as 177 ms. This can be theoretically higher, although the probability of this occurring decreases exponentially.

Improvements can be made to future versions of the system to shorten this delay, such as using an MCU with a faster processor, or eliminating the MCU's from the loop and using data acquisition systems to read and process data directly in the Client/Server computers.

## ***7.2 Initial Integration with Remote Surgery Systems***

Two remote surgery systems were accessible during the time of this research: the University of Washington RAVEN-II [51] and the UCLA LapaRobot Tele-mentoring System [52]. The next sections describe early integration efforts with each of these two systems, some of the associated challenges, and the eventual solution: a combination system that utilizes the best aspects of each.

### **7.2.1 University of Washington RAVEN II**

The RAVEN and RAVEN-II surgical systems were developed as a collaboration between engineers at the University of Washington BioRobotics Laboratory and clinicians from the Center for Video Endoscopic Surgery. It consists of a pair of cable-actuated, seven degree-of-

freedom (DOF) robotic manipulators (Figure 101). Kinematics optimizations were performed to select the best link angles for the surgical workspace [51].



Figure 101. The RAVEN-II Surgical Robot

Control software for the robotic manipulators was written in C and C++, runs on a Real-Time Application Interface (RTAI) Ubuntu Linux platform, and integrated aspects of the Robotic Operating System (ROS) initially developed by the Stanford Artificial Intelligence Laboratory [159]. A programmable logic controller (PLC) acted as the interface between the control software and the motors.

The robotic manipulators were operated remotely by two PHANToM Omni controllers (Sensable®) (Figure 102), and a USB foot pedal for engaging and disengaging the brakes. These controllers were chosen by the University of Washington as a cost-effective way of testing the robotic manipulators and for facilitating quick collaboration between multiple sites.



Figure 102. Commercially available force feedback controllers (Phantom Omni) used for RAVEN-II control.

Software for the Omni controllers was written in Windows Visual C++ and ran on 64-bit Windows 7. It used the OpenHaptics SDK to interface with the omni controllers, and the Qt library for forming the GUI. Two main programs were needed to operate the RAVEN-II controllers: *GUI\_Server* and *Omni\_Client*. These two programs communicated over a TCP/IP socket, despite running on the same machine.

Several experiments were performed by the University of Washington (UW) BioRobotics Laboratory using the RAVEN, including a Mobile Robotic Telesurgery in a remote environment (2006), remote training tasks between UW and Imperial College, London (2006), a locally performed suture tying experiment in live tissue (2007), and the NASA Extreme Environment Missions (NEEMO) at the underwater Aquarius Undersea Habitat (2007) [51].

In 2011, a research grant was written by the University of Washington and six other collaborating institutions (UC Santa Cruz, Harvard, Johns Hopkins, University of Nebraska, UC Berkley, and UCLA). This grant was awarded by the National Science Foundation (NSF), Major Research Instrumentation (MRI) group, and resulted in the construction of seven RAVEN-II systems that were sent to the contributing organizations [160]. In 2012, one of these RAVEN-II

systems was received and assembled at the CASIT research center at UCLA and used in this research.

Tactile feedback was integrated with the RAVEN-II system by mounting sensors onto end-effectors of the RAVEN-II graspers and balloon actuators onto the PHANToM Omni controllers. Tactile feedback control software ran on two separate computers using the previously described system architecture (Section 7.1.1).

This integrated system was tested by using the PHANToM Omnis and the RAVEN-II to pick up rubber pieces and observing balloon inflation. During this experiment, it was discovered that the Omni controllers proved to be an awkward, non-intuitive method of control due to the frequent use of a foot pedal to clutch, and the need to push and hold buttons to open and close the graspers. Additionally, a mechanical weakness in the grasper tips and cable coupling caused the RAVEN-II to slightly open the grasper as objects were lifted. This eliminated contact with the force sensors and immediately caused the objects to drop.

While the cable coupling challenge was solved through changes to RAVEN-II software, the non-intuitive control scheme prevented the use of the RAVEN-II / Phantom Omni system for a remote surgery grip force study.

### **7.2.2 UCLA LapaRobot Tele-Mentoring System**

The initial version of the UCLA LapaRobot (Figure 103) was developed by the UCLA Graphics and Vision Laboratory in the Department of Computer Science. It functioned as a human-in-the-loop tele-operated robot and was composed of a control station and a surgical robot [52]. Magnetic position sensors tracked the motion of laparoscopic instruments manipulated by a surgeon at the control station. These motions were encoded and transmitted



over a standard Internet connection to the surgical robot. The robot received these commands and actuated the laparoscopic instruments.



Figure 103. (Left) The LapaRobot Control Station allows the surgeon to tele-operate using standard laparoscopic instruments in a conventional arrangement. (Right) The surgical robot is operated to perform the training task.

Integration of remote tactile feedback with this first version of the LapaRobot was completed using a Shuttle PC and Measurement Computing analog input board (Figure 104) on the sensor side, and a PC laptop on the actuator side. Rather than the LabVIEW described earlier, this software was written in C, and used COMEDI analog drivers and transmission over a UDP socket.



Figure 104. Initial version of Remote Tactile feedback system with Data Acquisition Board and Shuttle PC connected to Internet.

Later, a second version of the LapaRobot was developed by the Mechatronics and Controls Laboratory in the UCLA Department of Mechanical and Aerospace Engineering. (Figure 105). By using an arc-based motion scheme, this system made significant improvements

to range of motion, degrees of freedom, and dexterity. Additionally, the master and slave robots offered bilateral control, and the scope of the project directed towards tele-mentoring rather than purely remote manipulation. Control software for the second version of the LapaRobot was composed using National Instruments LabVIEW® and ran on the NI Real-Time Operating System (RTOS).

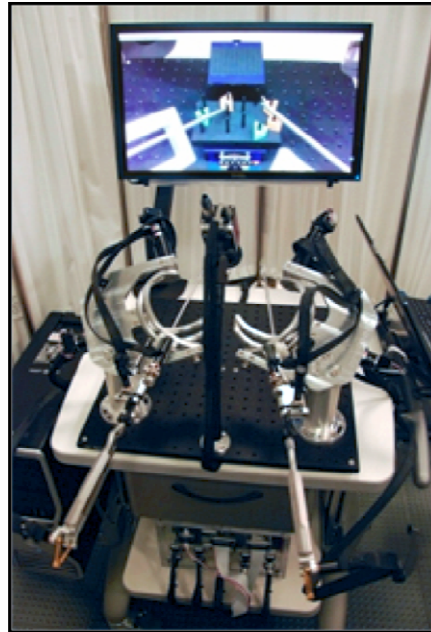


Figure 105. Second Version of LapaRobot Telementoring System

A second version of the remote tactile feedback software was written using National Instruments LabVIEW® to be compatible with the software of the second version of the LapaRobot. This was done by modifying the existing DAQ User Interface (Section 4.5) and leveraging the existing communication protocol.

This software was integrated into the existing LapaRobot computers and merged with the LapaRobot control software. The combined systems were validated by enabling simultaneous operation of the LapaRobot and remote tactile feedback system observing successful performance.

Unfortunately, the second version of the LapaRobot suffered from occasional power and heating challenges when actuating the heavy laparoscopic instruments. These challenges made the system too unreliable to use in a remote surgery grip force study.

### **7.3 The LapaRaven: A Combination Remote Surgery System with Integrated Tactile Feedback**

The primary difficulty in using the LapaRobot was the occurrence of power and heating issues when actuating the instruments. The primary challenge associated with the RAVEN-II was the awkward non-intuitive use of Phantom Omni controllers, which necessitated frequent use of a foot pedal and buttons to open and close the robotic graspers.

A new remote surgical system, *The LapaRaven*, was designed by integrating the two systems and leveraging the most effective components of each (Figure 106) [161].

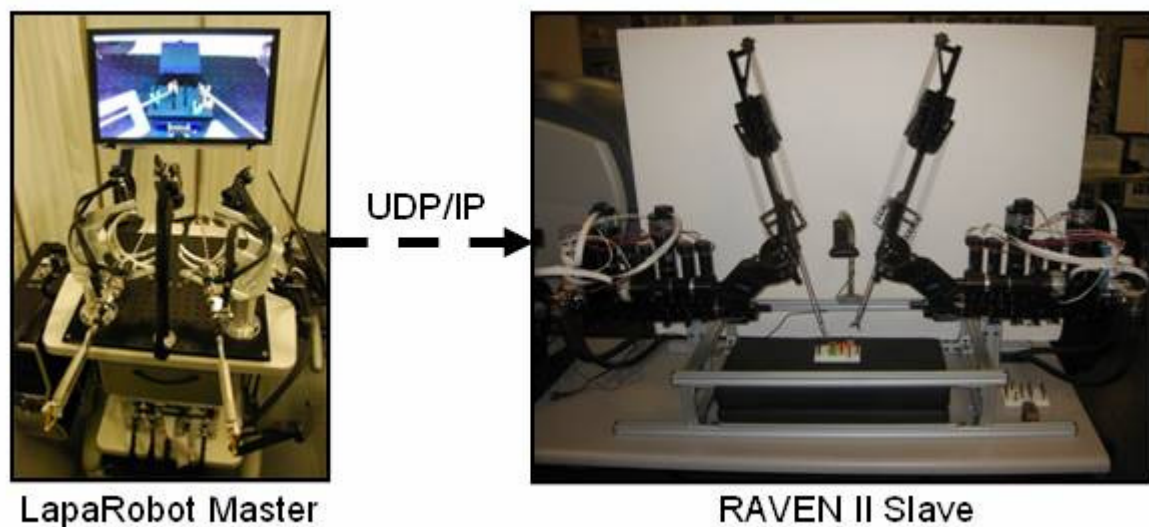


Figure 106. Overview of LapaRaven Concept

In this combined system, the LapaRobot replaced the Phantom Omnis and acted as a more intuitive surgeon-operated control scheme. It communicated over a standard internet connection (UDP/IP) with the RAVEN-II system. The RAVEN-II interpreted the LapaRobot

messages and moved through the surgical environment. A visual feed was accomplished by using a webcam on the RAVEN-II side and communicating through Skype.

There were several drawbacks of using this system, including the loss of RAVEN-II wrist actuation (pitch and yaw), difficulty in precise control of push-pull and grasping with the LapaRobot Controller, and the lack of depth perception provided by the webcam.

Despite these drawbacks, the LapaRaven improved functionality over the Omni-controlled RAVEN-II and LapaRobot systems alone.

The following sections describe the hardware, software, and tactile feedback integration that was needed to make the LapaRaven usable for a preliminary investigation into tactile feedback in remote surgery.

### 7.3.1 LapaRaven Hardware

A block diagram of the combined system hardware is shown in Figure 107. No changes were made to the hardware on either the LapaRobot or RAVEN-II.

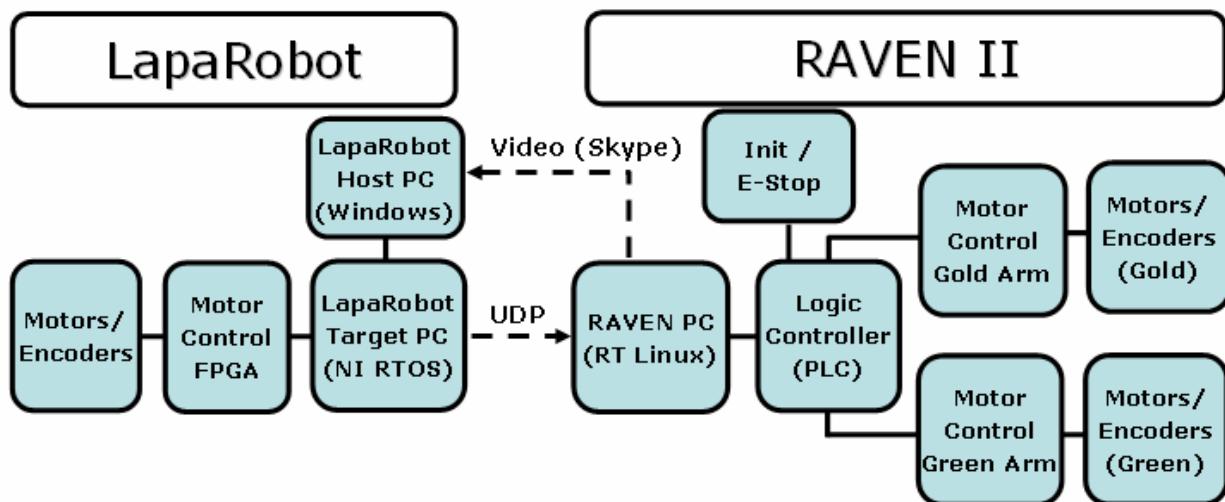


Figure 107. LapaRaven Hardware

The LapaRobot utilized two computers: a host PC running Windows that supported the LabVIEW development environment and the Skype connection, and a Target PC with the National Instruments Real-Time Operating System (RTOS) that ran the actual LapaRobot software. The target PC communicated to the ten motors and encoders (five for each arm) through a custom Motor Control FPGA and amplifier control box. In the LapaRaven, only the grasping motor was actuated, which was done to provide a spring back that was similar to non-robotic graspers. All other motors were used only to provide encoder values for position sensing.

RAVEN-II software ran on a computer using Ubuntu Linux with real-time scheduling capability. This computer communicated over USB to a Programmable Logic Controller (PLC). The PLC in turn communicated to the seven motors and encoders on each arm through separate motor controller circuit boards. The E-Stop and Initialize buttons communicated directly with the PLC.

Software development was performed on the Linux PC on the RAVEN-II side and the host/target PCs for the LapaRobot. Embedded software on the RAVEN-II's PLC and the LapaRobot's FPGA remained unchanged.

### **7.3.2 LapaRaven Software**

The overall strategy with LapaRaven development was to write a new standalone software program, while leveraging as much of the existing code base as possible. This was done by systematically re-testing and re-enabling the needed modules of RAVEN-II software. These modules were copied to new files and modified as needed.

For the LapaRobot, there was an existing LabVIEW VI written by the Mechatronics and Controls Laboratory. (“*Master Server no clutch vfinal.VI*”) that was used for displaying and logging encoder values. This program was copied to *LapaRaven\_Master.VI* and then modified to

eliminate data logging, and to add functionality for bundling encoder values into a single data message, and transmitting this data message over a UDP/IP socket to the Raven's IP address at a specified port (Figure 108).

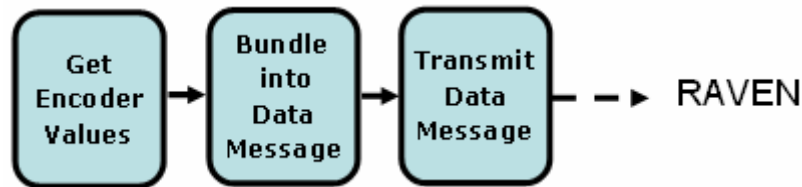


Figure 108. Software Block Diagram for LapaRaven Controller (LapaRobot)

Software on the RAVEN-II performed the following functions:

- Initialize the PLC
- Listen to the network port for information from the LapaRobot
- Receive user input from the keyboard, (to initialize and change control types)
- Calculate the desired RAVEN position based on these inputs.
- Retrieve the RAVEN's current position from the PLC
- Write commands to the PLC to control and move the motors.
- Display useful information to the console

Software to provide this functionality was written using ANSI C, but with occasional C++ containers, such as vectors and arrays, and compiled using g++.

The main source code file was *laparaven\_slave.cpp*, and it used many additional header (\*.h) and source code (\*.cpp) files within the directory *~/Chris/laparaven/* on the RAVEN-II's Ubuntu Linux computer. A wrapper script, *run\_laparaven*, was written to execute the software.

To improve performance, the system utilized multi-threading, achieved through POSIX pthreads in a similar way as the original RAVEN-II software. Three threads were used: one for networking, one for raven control, and one for the user interface (Figure 109).

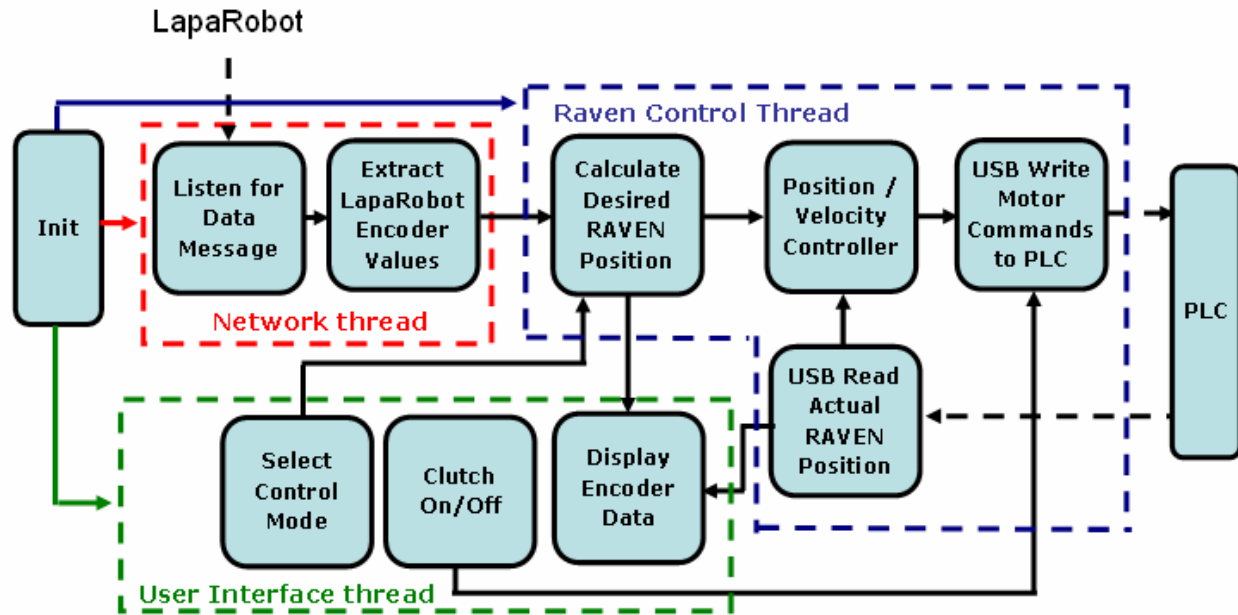


Figure 109. LapaRaven Software Block Diagram

The network thread managed the UDP socket and handled all communication from the LapaRobot.

The control thread calculated the desired RAVEN-II position based on inputs from the console and LapaRobot, read the RAVEN-II's current state from the PLC, and wrote motor commands. This thread operated over a defined 1 ms time slice and was scheduled with a real-time priority.

The user interface thread displayed information to the console, received user inputs, and passed flags to the control thread. Non-blocking user input and a customizable console display was achieved through using the *ncurses* software library [162]. Passing data between threads was protected through POSIX mutex locks. Shared flags were declared volatile so that the compiler would prevent data corruption.

The LapaRaven console is shown in Figure 110.

```

File Edit View Terminal Help
F2 to Quit, F3 to Wait, F4 to Go:
268335 LapaRobot Packets Received
267464 RAVEN USB Packets Received
267464 RAVEN USB Packets Transmitted
      SASR   BASR   PSR   TSR   GSR
right:  0     0     0    -1  -8493
left:   3    14     0   6923  8980
RAVEN Encoders: GOLD ARM
  enc_val:  -510  -105  -60   8   -2727  -23   1097   1109
enc_val_a:  -510  -105  -60   8   -2706  -2   1118   1130
enc_val_d:    9    46    0    8   -3230  0    620   620
curr_cmd:    0     0     0    0     0     0     0     0
RAVEN Encoders: GREEN ARM
  enc_val:    0     1     0     0     1     0     1     1
enc_val_a:    0     1     0     0     1     0     1     1
enc_val_d:    0     0     0     0     0     0     885   885
curr_cmd:    0     0     0     0     0     0     0     0
Run Level is: WAIT
Choose Control: F7-Hold F8-Home F9-LapaRobot
Control Mode is: LAPA CONTROL █

usb_io: Found board files:: brl_usb39 brl_usb30
Starting in Wait Mode
usb_io: Gold Arm on board #39.
usb_io: Done clearing buffer, moving on.
usb_io: Green Arm on board #30.
usb_io: Done clearing buffer, moving on.
Using realtime, priority: 96

```

Figure 110. LapaRaven Console Output

At the top of the console are outputs indicating the number of packets received from the LapaRobot Master, followed by the number of packets transmitted to and received from the RAVEN-II PC to the Programmable Logic Controller (PLC) that interfaced with the motors.

For the LapaRobot, the console displays the five encoder values for the right and left hand (Small Arc, Big Arc, Poke, Twist, Grasp). Beneath this are four values for each RAVEN joint: the actual encoder value (`enc_val`), the actual encoder value adjusted for cable coupling (`enc_val_a`), the desired encoder value (`enc_val_d`), and the current motor command (`curr_cmd`).

The *run level* indicates the current state of the RAVEN. Possible states are shown in Table 10.



Table 10. LapaRaven Run Levels

<b>Run Level</b>	<b>PLC State</b>	<b>Description</b>
STOP	0	Initial state, follows start up or red e-stop. RAVEN cannot move.
INIT	1	RAVEN is initializing. Enter this state from STOP by hitting the silver start button. When done, RAVEN will automatically enter WAIT. In the LapaRaven, initialization occurs rapidly, so that it appears to go directly from STOP to WAIT.
WAIT	2	Pedal up state. RAVEN is initialized, but brakes are engaged. Desired encoder positions can change, but the RAVEN will not move.
GO	3	Pedal down state. RAVEN is initialized and will proceed to the desired encoder position. Desired encoder positions will change as controller is moved.

Following this is the *control mode*. Control modes are shown in Table 11.

Table 11. LapaRaven Control Modes

<b>Control Mode</b>	<b>Description</b>
LAPACONTROL	LapaRobot control.  Desired RAVEN position is calculated from LapaRobot encoder values.
HOME	Return to home position. Home position is the position that the RAVEN was in when the <i>run_laparaven</i> program was run. It is expected that the RAVEN will first be homed using UW's original RAVEN-II program.  Desired RAVEN position is set to zero for all joints.
HOLD	Safe mode. Do not engage the motors in any way. This does not actually keep the RAVEN in its position. Gravity or manually moving the joints will still have an effect.  Desired RAVEN position is continually set to the actual RAVEN position.

These encoder values and other parameters that describe robotic arm data were stored in a *robot\_device* structure (Figure 111). The *robot\_device* describes the RAVEN II (or LapaRobot) as a whole. The *mechanism* substructure describes each robotic arm independently. Each *mechanism* has seven *joint* structures, one for each of the seven degrees of freedom.

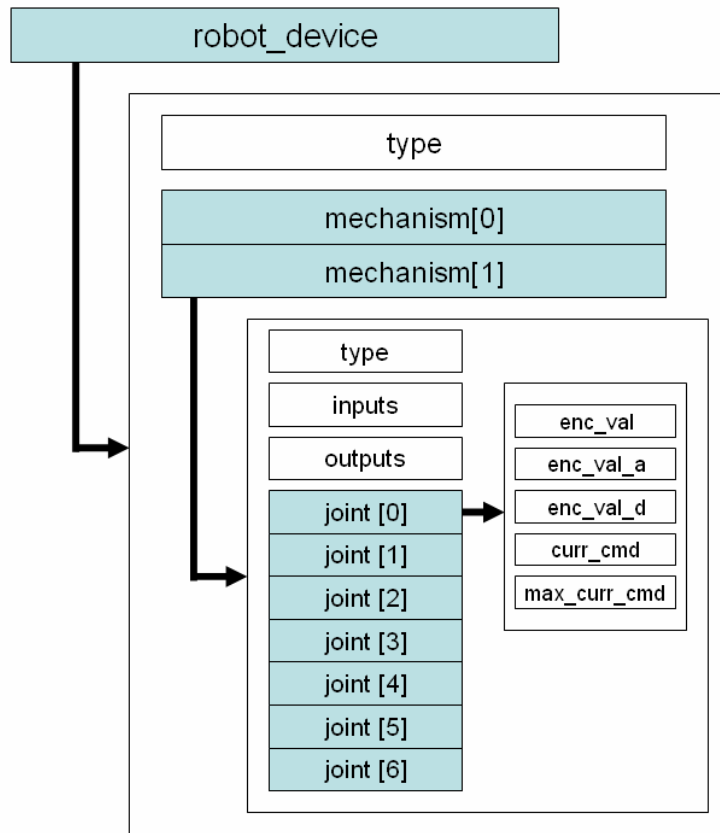


Figure 111. Robot Device Data Structure

The *param\_pass* data structure (Figure 112) described other useful information about the state of the system as a whole.

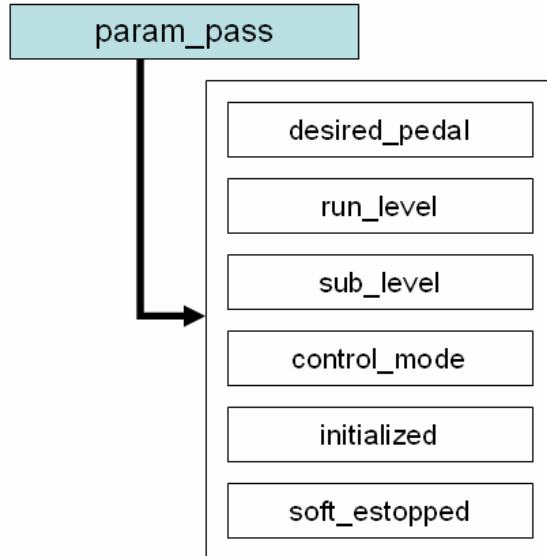


Figure 112. Param\_pass data structure

Equations were needed for converting the LapaRobot Master’s set of encoder values to desired encoder positions for the RAVEN motors. These were determined by measuring the desired working space and ranges of the encoders on each of the machines in each degree of freedom. Both systems utilized arc-based approaches to position their robotic mechanisms in space, and so a one-to-one mapping scheme was used.

An additional challenge with using the RAVEN-II was that cable lengths for roll, yaw, and grasper closure were coupled with the absolute position of the push-pull platform, and therefore, the reported encoder values from the RAVEN-II’s PLC did not directly correspond to the position in these degrees of freedom. To account for this, adjusted encoder positions (enc\_val\_a) were calculated from both the joint’s reported encoder position and the platform’s encoder position.

The LapaRaven system was validated by enabling each of the joints, operating the LapaRobot Master, and observing similar motions from the RAVEN-II.

### 7.3.3 Tactile Feedback Integration

The remote tactile feedback system and LapaRaven systems ran separate programs on separate computers, so there was no need for software integration. The LapaRobot host computer was additionally utilized as the Tactile Feedback Client. The overall block diagram for the LapaRaven with integrated tactile feedback is shown in Figure 113.

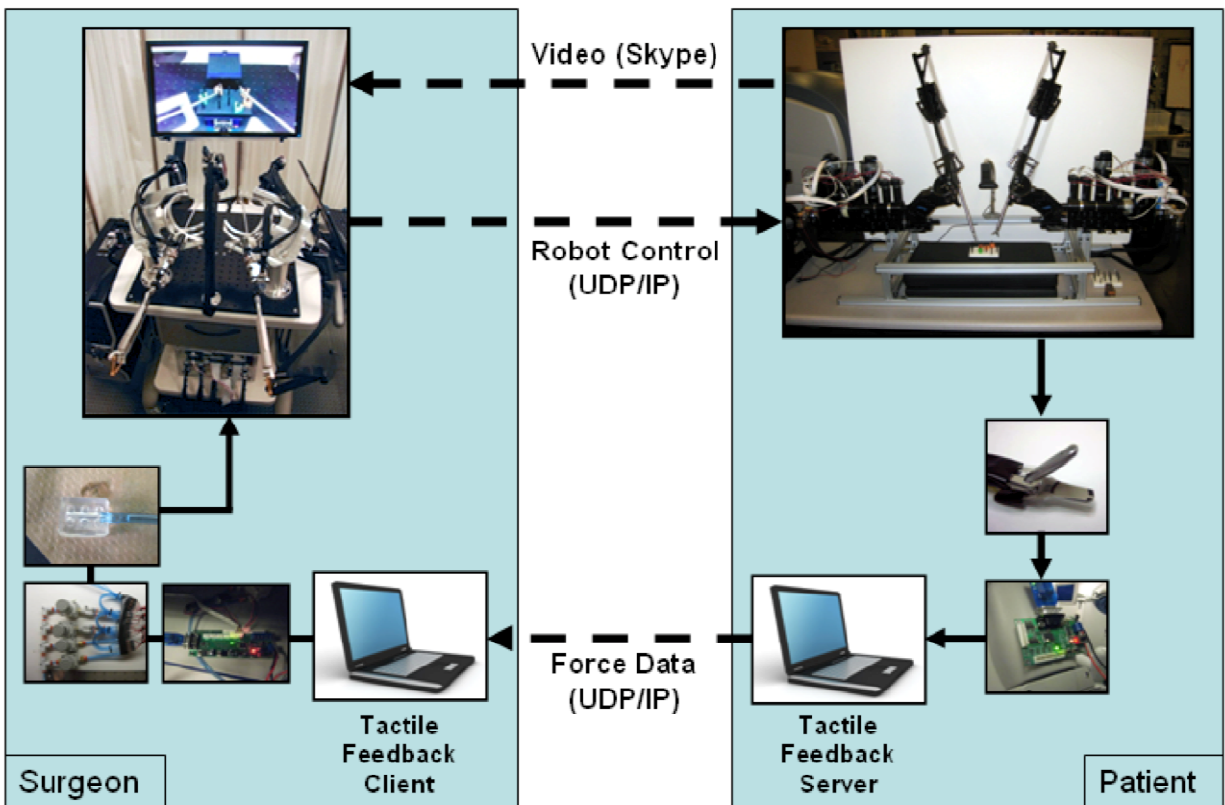


Figure 113. LapaRaven with Tactile Feedback, System Overview

Sensors were mounted on RAVEN-II grasper tips (Figure 114). The grasper tips for the RAVEN II had a slightly different geometry than da Vinci and Storz grasper tips. Sensors were trimmed to match the size of the new instruments. Wires were connected using silver epoxy because the previously used crimps interfered with the RAVEN-II operation and caused an electrical short through contact with the instrument. These silver epoxy connections were

delicate and broke easily. This issue can be solved by using da Vinci instruments and da Vinci tool adaptors.



Figure 114. (Left) Raven grasper tip (Right) Flexiforce sensor mounted

The LapaRobot was incompatible with the custom handles used in the non-robotic laparoscopic grasper, so standard Storz handles were used. Initially, actuators were mounted on LapaRobot handles (Figure 115). Because of challenges with using the LapaRobot instruments and forces required to overcome motor friction and weight of the instrument, it was often more comfortable to wear the balloon actuator around the user's finger, rather than mounting it directly on the instruments.

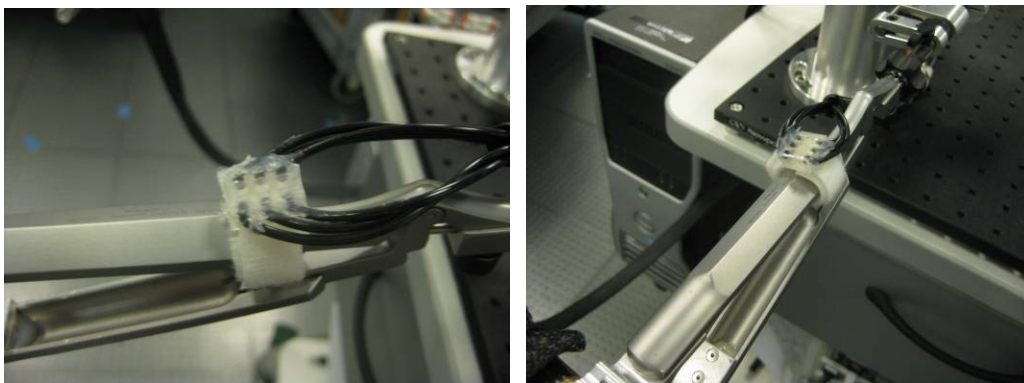


Figure 115. Pneumatic actuator mounted on LapaRobot instrument handle

The complete LapaRaven with integrated tactile feedback was tested by using the system to pick up objects and observing balloon inflation.

While still improving over the Omni / RAVEN-II and LapaRobot systems, the LapaRaven was still a challenging system to control. These challenges derived mainly from motor stiffness in the push-pull and grasping joints on the LapaRobot Master and the monoscopic nature of the web camera that provided the visual feed.

## **7.4 Remote Surgery Grip Force Study**

A preliminary investigation was performed to evaluate the impact of tactile feedback on grasping force while using the LapaRaven remote surgery system over a simulated network. Similar studies had been performed for local robotic surgery [153], and with a non-robotic laparoscopic grasper [157]. The purpose of this investigation was to determine whether there were similar effects with an unfamiliar control scheme and effect of time delays over a network.

Additional objectives of this evaluation were to determine technical shortcomings in using of the system, and impacts due to latency.

### **7.4.1 Methods**

Five novice subjects used the LapaRaven to retrieve six vertically mounted dimes (Figure 116) using their dominant hand in each of three conditions: (1) tactile feedback off, (2) tactile feedback on, and (3) tactile feedback off, in a similar method as previous studies. In initial observations, it was found that dimes were grasped more easily and in a more consistent, repeatable manner than the rubber blocks used in the traditional Fundamental of Laparoscopic Surgery (FLS) exams. They were preferred in the study because subjects were novices and because of additional difficulties in with the monoscopic camera and control scheme.

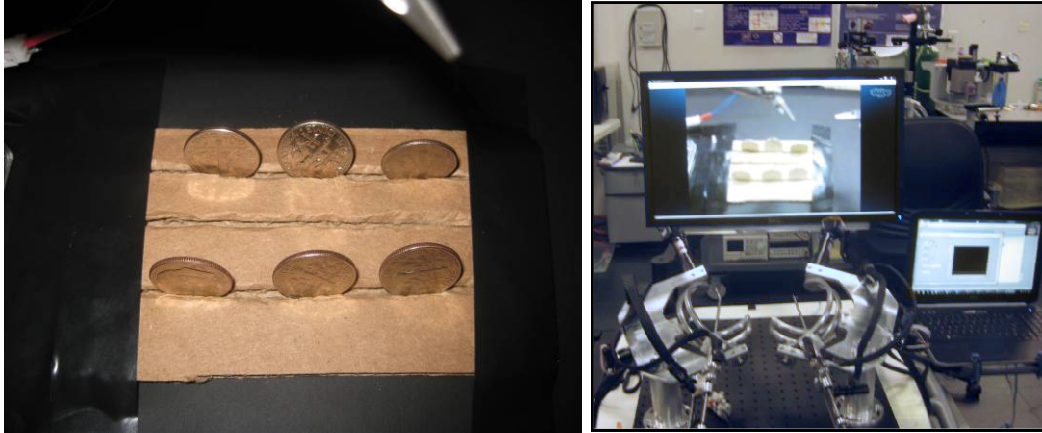


Figure 116. (Left) Subjects used the LapaRaven to retrieve six vertically mounted dimes. (Right) Perspective from the LapaRobot Master.

In the initial set of trials, the LapaRaven was set to run on a simulated network with a specified time delay of 100 ms. For comparison, each subject complete the study a second time with the time delay removed. In an effort to control short-term learning effects, this second study was performed at least twenty-four hours later.

Prior to the experiment, subjects were instructed in the task and given a few minutes to practice operating the robots. Subjects were additionally instructed on challenges with the system: specifically the stiffness with manipulating the LapaRobot Master's push-pull, and the lack of depth perception. Because of challenges with depth perception, subjects were verbally guided through push-pull (i.e. instructed to move the instrument higher or lower) until the dime was in the grasping field. Prior to the second condition, subjects were familiarized with the tactile feedback system by opening and closing the graspers and acknowledging perception of balloon inflation.

During each grasping event, average grip force was measured through the sensors mounted on the RAVEN-II graspers and logged using the data acquisition aspect of the user interface (National Instruments LabVIEW®). Grasping events were manually tagged during the course of the experiment and verified in post-processing and data analysis.

## 7.4.2 Statistical Analysis and Results

Saturation of force sensors resulted in a non-Gaussian distribution of data, and so statistical analysis was performed using non-parametric statistical methods. A box and whisker plot shows the mean forces for both the 100 ms delay conditions and the 1 ms delay conditions (Figure 117). A bar graph is shown alongside for comparison.

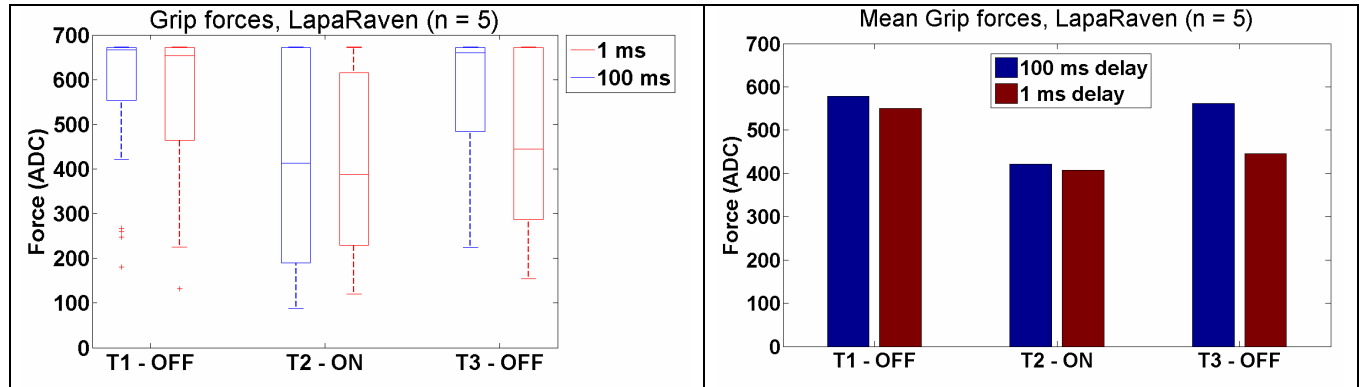


Figure 117. Mean grip forces for remote surgery grip force study, all five subjects.

The pool of subjects was compared using Friedman's Test with six repetitions per subject in order to test the following nine hypotheses. The first three describe the pair-wise comparisons when the delay was 100 ms, the second three when the delay under 1 ms, and the last three determine comparisons between the two delays.

$H_{1,a}$ : There were significant differences between condition 1 (T1) and condition 2 (T2) with 100 ms delay

$H_{2,a}$ : There were significant differences between condition 2 (T2) and condition 3 (T3) with 100 ms delay

$H_{3,a}$ : There were significant differences between condition 1 (T1) and condition 3 (T3) with 100 ms delay

$H_{4,a}$ : There were significant differences between condition 1 (T1) and condition 2 (T2) with under 1 ms delay.

$H_{5,a}$ : There were significant differences between condition 2 (T2) and condition 3 (T3) with under 1 ms delay.



*H<sub>6,a</sub>: There were significant differences between condition 1 (T1) and condition 3 (T3) with under 1 ms delay.*

*H<sub>7,a</sub>: There were significant differences between 100 ms delay and under 1 ms delay for condition 1 (T1).*

*H<sub>8,a</sub>: There were significant differences between 100 ms delay and under 1 ms delay for condition 2 (T2).*

*H<sub>9,a</sub>: There were significant differences between 100 ms delay and under 1 ms delay for condition 3 (T3).*

A Bonferonni correction was used and ( $P < 0.0167$ ) considered for significance. These results are shown in Table 12.

Table 12. Hypothesis Testing for LapaRaven Grip Force Study

Delay: 100 ms		Delay: 1 ms		Delay: 1 ms vs. 100 ms	
Comparison	P-Value	Comparison	P-Value	Comparison	P-Value
T1/T2	0.0093*	T1/T2	0.0007*	T1	0.2322
T2/T3	0.00085**	T2/T3	0.0787	T2	0.7918
T1/T3	0.8175	T1/T3	0.0451	T3	0.0122*

This analysis reveals that in both delay conditions, there was a significant decrease in grip force between T1 and when tactile feedback was activated in T2. The primary difference between the two delay conditions is that with 100 ms latency, there was limited to no learning effect for all subjects. In the situation with 1 ms latency, there was a wider distribution of grip forces in T3, indicating a higher variability between subjects.

Figure 118 shows the mean grips forces for each of the five subjects in all conditions.

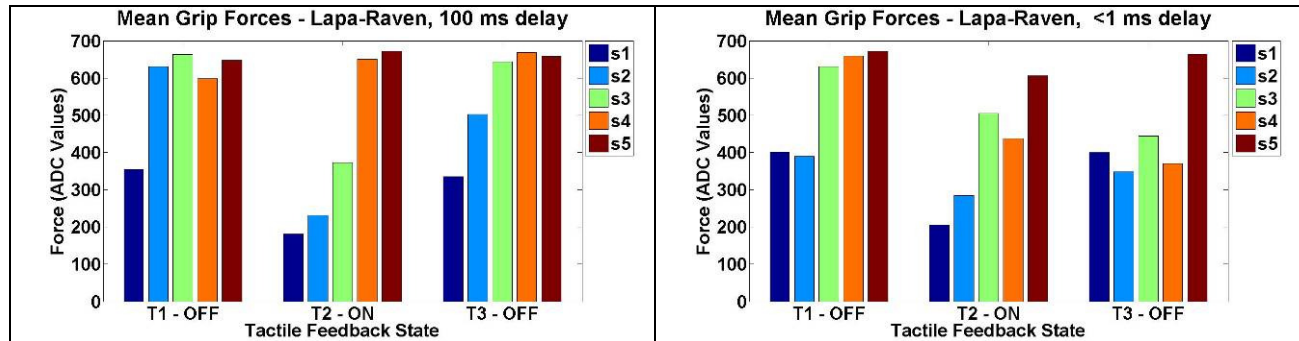


Figure 118. Mean forces for all subjects when using the LapaRaven with (Left) 100 ms delay (Right) 1 ms delay

This data shows that in the 100 ms delay condition, tactile feedback offered benefit for three of the five subjects, and for each of these subjects, the low forces were, at most, partially retained.

In the 1 ms delay condition, there was noticeable benefit for four of the five subjects, and these values were retained in the third condition (T3), indicating a greater impact due to learning.

One subject (s2) showed a decrease in baseline force (T1) when the network delay was removed. This could also be due to a long-term learning effect. One subject (s5) expressed difficulty in exerting precise control when grasping with the LapaRobot controller and showed no significant differences across any of the conditions.

### 7.4.3 Discussion

The population analysis for grasping force with a 100 ms network delay showed that grasping force was significantly lower ( $P < 0.0093$ ) when the tactile feedback system was activated, compared to both the before (T1) and after (T3) states when tactile feedback was inactive.

These results differed from the live tissue study which used a more easily controlled da Vinci robot. These differences may be due to increased challenge with manipulating the

LapaRaven, the difficulty exercising precise control over grasping, and the tendency for subjects to proceed more slowly when awaiting balloon inflation.

When the network delay was removed, there was a significant decrease in grasping force ( $P = 0.0007$ ) and observable benefit for four of the five subjects. With no network delay, there was a wider distribution in the third condition and more often the low forces were retained when the system was subsequently deactivated. The results for the low delay study are similar to those observed in the live tissue study. Together these results seem to indicate that learning is more often present in a system that is easier to use.

There were no significant changes to baseline force (T1) when comparing the two network conditions. This could be due to the sensitivity of the system and the saturation point of the sensors. When looking at each subject individually, one of the five showed a significant decrease in baseline force when the network delay was removed.

The LapaRaven demonstrated the first remote surgery system with integrated tactile feedback. While it is difficult to determine conclusive results with only five subjects, these preliminary findings suggest that the benefits due to tactile feedback may be more significant in systems that are harder to use, such as those with latency in the visual feed, and that tactile feedback could become a critical component of future telesurgical systems.

It is suggested that future work be performed with additional subjects using a more robust control scheme and better camera, both on local networks with induced latencies, and at remote locations.

## 8 Conclusion

The aims of this research were to improve tactile feedback technology, expand the technology to other minimally invasive surgical applications, and perform studies to evaluate the impact of this feedback.

To improve the tactile feedback technology, many of the components of the previous feedback system were re-designed. The pneumatic system saw two rounds of improvement that removed unintentional vibration and provided direct inflation feedback as originally intended. A new two-part, wireless electronic system was designed to interface with this new pneumatic system. New control software was written to support wireless communication, the new hardware, and the new pneumatic system. This software utilized an anti-jitter threshold algorithm, and a layered message protocol to handle wireless communication. The sensor mounting process was improved, and a new process developed for protecting sensors from moisture damage, thus enabling use in live tissue. A second actuator geometry was designed to fit in a custom handle for non-robotic laparoscopic surgery.

This system was expanded and integrated with three minimally invasive surgical applications: non-robotic laparoscopic surgery, robotic surgery in an *in-vivo* environment for pre-clinical application, and remote surgery. A suitable, fully functioning remote surgery system was not available, and so a new one was designed by combining two available systems: The University of Washington RAVEN II and UCLA LapaRobot. This LapaRaven system was the first prototype remote surgery system with integrated tactile feedback.

For each of these three applications, studies were performed to evaluate the impacts of tactile feedback. In all three cases, it was found that tactile feedback helped some, but not all

subjects. In laparoscopic surgery it was found that tactile feedback helped novice subjects, but had no impact on experts.

The *in-vivo* robotic surgery study showed that there was a high variability between subjects. Together, the pool of subjects showed significantly lower forces and fewer sites of damage when tactile feedback was activated, and that these low values were retained when the system was turned off. A significant correlation was found between higher average forces and incidence of damage.

The preliminary investigation of remote surgery showed significantly decreased grasping forces for most subjects. With a 100 ms time delay, there was little to no retention of grasping forces, whereas when this delay was removed, subjects tended to learn and continue to use low forces after the feedback system was deactivated.

Together these results suggest that reductions to grasping force may have a positive impact on damage to tissue and clinical outcomes. This lends support for continued improvement of the tactile feedback technology towards clinical viability, and the eventual use of integrated tactile feedback with surgical robotic and minimally invasive training systems.

## 9 Future Work

The results from this research suggest several possible directions both in continuing to advance the tactile feedback technology, and further evaluations of its benefit. It is my hope that this section will serve as a starting point for those who wish to continue this research.

### ***9.1 Robotic Surgery Training Study***

The live tissue study (Section 6.2) concluded that for the subject pool as a whole – and for approximately 30% of participants when analyzed individually – forces were significantly lower when the tactile feedback system was activated and that these low values were completely retained when the system was deactivated for the third trial. These lower forces could have been caused by increased familiarity with the task (i.e., learning effect) or due to the presence of tactile feedback.

The purpose of a robotic surgery training study is to separate the learning effect due to task familiarization from the effect due to tactile feedback. This experiment would have two to three matched groups of subjects performing a training task over several iterations until proficient (usually six iterations for peg transfer). One group will have no tactile feedback throughout the course of the experiment. The remaining groups will have a tactile feedback intervention at some specified iteration in the middle. In a task with six iterations, this intervention could occur after the second iteration for one group and after the fourth for another.

## ***9.2 Evaluating Tactile Feedback on Additional Performance Metrics***

During the course of this research, grasping force was used as the primary metric in evaluating tactile feedback in minimally invasive surgery. Additional studies can be performed that evaluate tactile feedback against other performance metrics.

A collaboration has been formed with researchers in the UCLA Graphics and Vision Lab (MAGiX) who have been developing a machine vision system for automatically assessing (Auto-Assess) a person's performance during Fundamentals of Laparoscopic Surgery (FLS) tasks [163]. Rather than just use time-to-completion to evaluate performance, the goal of this Auto-Assess system is to track other factors, such as the path of the surgical instrument, jerk, and control effort.

After the Auto-Assess system is refined, it may be used as a mechanism for evaluating the impact of tactile feedback on a person's control of robotic, non-robotic, and remote surgical instruments.

## ***9.3 Custom Micro-scale Force Sensing Array***

Future tactile feedback systems will require a sensing array that is both small enough to fit on a surgical instrument and has sufficient signal to noise ratio to detect forces on the range of 1 – 5 N. These sensors must not interfere with operation of the robotic system, and be sufficiently robust and sterilizable for continued live tissue work and eventual clinical application.

Ideally, such a sensor could be integrated directly into a custom surgical instrument, although this may preclude the use of proprietary robotic systems (i.e. the da Vinci). Several

expert robotic users have also suggested the importance of measuring shear force as an aid for tensioning sutures and to prevent excessively tugging on delicate tissues.

During the course of this research, several designs had been analyzed and a MEMS capacitive sensor determined as having the best precision within the size constraints, while still being practically-suited towards sterilization environments.

Through a collaboration with Professor Robert Candler’s MEMS Research group, this force sensor was designed, modeled analytically and with a simulation (COMSOL), and then fabricated in the UCLA Nanoelectronics Research Facility (Figure 119 – Figure 120) [164].

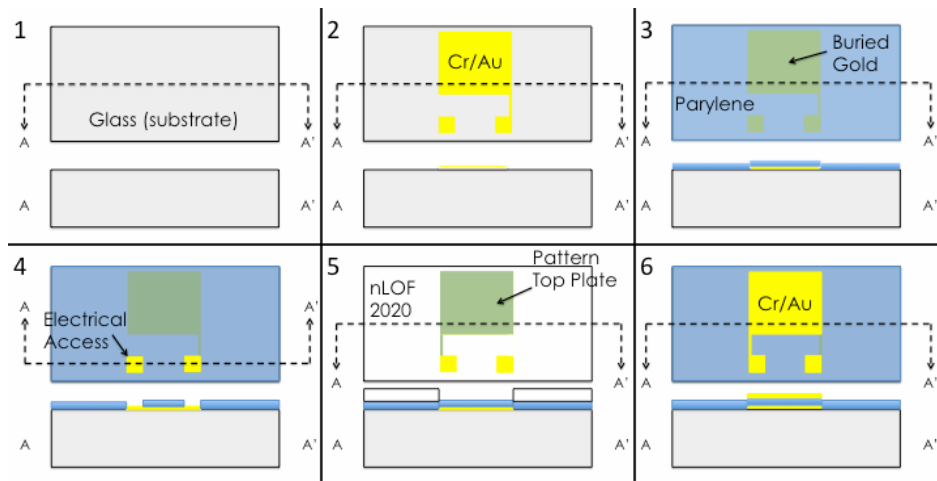


Figure 119. Process flow of the capacitive sensor design.

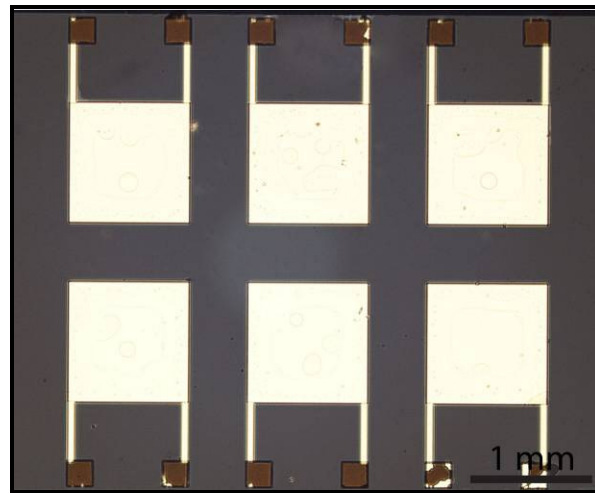


Figure 120. Capacitive sensor fabricated at UCLA Nanoelectronics facility



Capacitive sensors are limited by potential cross-element interference and parasitic capacitance present in cabling. Therefore, any signal conditioning electronics should be near the sensor at the tip of the surgical instrument.

It was separately theorized that a tooth-shaped geometry could possibly improve signal resolution, although design of this sensor was constrained by unreasonable fabrication complexity and remains untested [165].

Further research and references concerning force sensing systems can be found in Section 2.4.3.

## ***9.4 Improvements to the Tactile Feedback System***

While the improved tactile feedback system was sufficient for experiments in live tissue, there are still potential improvements to ease-of-use, ergonomics, and scalability.

### **9.4.1 Scalable Continuous Pneumatic System**

Three iterations of the pneumatic system are described earlier in this work (Section 4.3). While the third iteration (and the one used in this research) improved upon the unintentional vibrations of previous systems, the use of solenoid valves does not effectively scale with increases in independent actuator elements. With this pneumatic design, a four actuator system utilizes sixteen valves. For a system with four separate six-element actuator arrays, there would be twenty-four (24) independent actuator elements, which would require ninety-six (96) valves. This adds significant cost (approximately \$3000 for just valves), size, plumbing complexity, and severe challenges with maintenance in the event of a leak.

After some experience with the pneumatic system, one could notice that output pressures can be adjusted by manually rotating the knob of the high precision regulators. This can be

automated by using a stepper motor with a mechanical link to the regulator knob and eliminating the valves entirely. This would maintain the performance of the current system (i.e., no vibration noise), be a continuous spectrum of inflation (rather than quantizing into levels), and have better scalability (one motor per output element). Cost and size comparisons will depend on the specifics of the design and precision of the motors.



Figure 121. Design concept for motorized pneumatic regulator

Much experimentation was performed using the initial version electro-pneumatic regulators (ITV-0010). It is strongly suggested that these not be used in any future designs.

#### **9.4.2 On-board Wireless Integration**

Having separate circuit boards for the sensors (Tx) and actuators (Rx) facilitated use of the system in space-constrained surgery suites and research laboratories. Currently, a Roving Networks Bluetooth dongle converts RS-232 from the dsPIC's UART to a paired Bluetooth signal. This system is easy to use, but can be made smaller by integrating the Bluetooth (or other wireless) units directly onto a new PCB design. This is a sub-project that could be recommended for an enterprising undergraduate researcher.

### **9.5 Continued RAVEN-II Collaborations**

While the LapaRaven system was sufficient in the short term for evaluating tactile feedback in remote surgery, difficulties in control and vision limit its longer term use.

Instead, it is recommended that a more robust and intuitive control scheme be used for the RAVEN-II in future studies. Specifically, a collaboration should be formed with Mimic, the company that designed the dV Trainer [34].



Figure 122. The Mimic dV Trainer

Mounting Flexiforce sensors onto the RAVEN tools proved to be a delicate operation due to the use of silver epoxy. It is suggested that collaborations continue with the University of Washington BioRobotics Laboratory and the collaborating company, Advanced Dexterity, in pursuing da Vinci tool adaptors. The use of da Vinci instruments with Flexiforce sensors has proven to be robust enough to survive extended live tissue experiments and can be used with the RAVEN-II.

For continued use of the RAVEN-II, it is suggested that there be an investment into a robust 3D Vision system, similar to the one used by the University of Washington BioRobotics Laboratory.

With a robust dV Trainer control mechanism, a 3D vision system, and da Vinci tool adaptors, the RAVEN-II can possibly be used for more advanced studies, although the current software should be carefully evaluated specifically with variable grasping in mind (i.e. the ability

to control one's grasping force). The RAVEN-II currently uses position-position control and often has trouble maintaining force on a grasped object with the current release of software.

## **9.6 Trans-continental Remote Surgery Tactile Feedback Studies**

A preliminary investigation into tactile feedback for remote surgery showed that for some subjects tactile feedback significantly decreased grip force when operated over a simulated network. With an improved remote surgery system such as a Mimic-controlled RAVEN-II, more extensive studies can be performed both over a simulated network and over an actual network.

A collaboration can be initiated with an interested research group at the Yale Department of Urology with CASIT Alumni, Richard Fan, who is familiar with this tactile feedback research. Other potential sources of collaboration can be found with any of the other RAVEN-II sites, including University of Washington BioRobotics, Johns Hopkins, Harvard BioRobotics, University of Nebraska, UC Berkley, and UC, Santa Cruz [160].

## **References**

- 
- 1 Jacobs, J. K., Goldstein, R. E., & Geer, R. J. (1997). Laparoscopic adrenalectomy. A new standard of care. *Annals of surgery*, 225(5), 495.
  - 2 Flowers, J. L., Jacobs, S., Cho, E., Morton, A., Rosenberger, W. F., Evans, D., ... & Bartlett, S. T. (1997). Comparison of open and laparoscopic live donor nephrectomy. *Annals of surgery*, 226(4), 483.
  - 3 Grace, P. A., Quereshi, A., Coleman, J., Keane, R., McEntee, G., Broe, P., ... & Bouchier Hayes, D. (1991). Reduced postoperative hospitalization after laparoscopic cholecystectomy. *British journal of surgery*, 78(2), 160-162.
  - 4 Culjat, M. O., King, C. H., Franco, M. L., Lewis, C. E., Bisley, J. W., Dutson, E. P., & Grundfest, W. S. (2008, August). A tactile feedback system for robotic surgery. In *Engineering in Medicine and Biology Society, 2008. EMBS 2008. 30th Annual International Conference of the IEEE* (pp. 1930-1934). IEEE.
  - 5 King, C. H. (2008) *Design, Fabrication, Optimization and Evaluation of a Multinodal Tactile Feedback System for Teleoperated Robot-Assisted Minimally Invasive Surgery*. (Doctoral dissertation, University of California, Los Angeles).
  - 6 Lanfranco, A. R., Castellanos, A. E., Desai, J. P., & Meyers, W. C. (2004). Robotic surgery: a current perspective. *Annals of Surgery*, 239(1), 14.

- 
- 7 Oehler, M. K. (2009). Robot assisted surgery in gynaecology. *Australian and New Zealand Journal of Obstetrics and Gynaecology*, 49(2), 124-129.
- 8 Kontarinis, D. A., Son, J. S., Peine, W., & Howe, R. D. (1995, May). A tactile shape sensing and display system for teleoperated manipulation. In *Robotics and Automation, 1995. Proceedings., 1995 IEEE International Conference on* (Vol. 1, pp. 641-646). IEEE.
- 9 Sakpal, S. V., Bindra, S. S., & Chamberlain, R. S. (2010). Laparoscopic cholecystectomy conversion rates two decades later. *JSLS: Journal of the Society of Laparoendoscopic Surgeons*, 14(4), 476.
- 10 Gould, J. C., Kent, K. C., Wan, Y., Rajamanickam, V., Levenson, G., & Campos, G. M. (2011). Perioperative safety and volume: outcomes relationships in bariatric surgery: a study of 32,000 patients. *Journal of the American College of Surgeons*, 213(6), 771-777.
- 11 Niebisch, S., & Peters, J. H. (2012). Update on Fundoplication for the Treatment of GERD. *Current gastroenterology reports*, 14(3), 189-196.
- 12 Jacoby, V. L., Autry, A., Jacobson, G., Domush, R., Nakagawa, S., & Jacoby, A. (2009). Nationwide use of laparoscopic hysterectomy compared with abdominal and vaginal approaches. *Obstetrics & Gynecology*, 114(5), 1041-1048.
- 13 Mamidanna, R., Burns, E. M., Bottle, A., Aylin, P., Stonell, C., Hanna, G. B., & Faiz, O. (2012). Reduced risk of medical morbidity and mortality in patients selected for laparoscopic colorectal resection in England: a population-based study. *Archives of surgery*, 147(3), 219.
- 14 Strong, V. E., Devaud, N., Allen, P. J., Brennan, M. F., & Coit, D. (2009). Laparoscopic versus open subtotal gastrectomy for adenocarcinoma: a case-control study. *Annals of surgical oncology*, 16(6), 1507-1513.
- 15 Dageforde, L. A., Moore, D. R., Landman, M. P., Feurer, I. D., Pinson, C. W., Poulouse, B., ... & Moore, D. E. (2012). Comparison of open live donor nephrectomy, laparoscopic live donor nephrectomy, and hand-assisted live donor nephrectomy: A cost-minimization analysis. *Journal of Surgical Research*, 176(2), e89-e94.
- 16 Gelmini, R., Franzoni, C., Spaziani, A., Patriti, A., Casciola, L., & Saviano, M. (2011). Laparoscopic splenectomy: conventional versus robotic approach—a comparative study. *Journal of laparoendoscopic & advanced surgical techniques*, 21(5), 393-398.
- 17 Shah, J., Buckley, D., Frisby, J., & Darzi, A. (2003). Depth cue reliance in surgeons and medical students. *Surgical Endoscopy and Other Interventional Techniques*, 17(9), 1472-1474.
- 18 Cartmill, J. A., Shakeshaft, A. J., Walsh, W. R., & Martin, C. J. (1999). High pressures are generated at the tip of laparoscopic graspers. *Australian and New Zealand journal of surgery*, 69(2), 127-130.
- 19 Heijnsdijk, E. A. M., van der Voort, M., de Visser, H., Dankelman, J., & Gouma, D. J. (2003). Inter-and intraindividual variabilities of perforation forces of human and pig bowel tissue. *Surgical Endoscopy and other interventional Techniques*, 17(12), 1923-1926.
- 20 De, S., Rosen, J., Dagan, A., Hannaford, B., Swanson, P., & Sinanan, M. (2007). Assessment of tissue damage due to mechanical stresses. *The International Journal of Robotics Research*, 26(11-12), 1159-1171.
- 21 Anup, R., & Balasubramanian, K. A. (2000). Surgical stress and the gastrointestinal tract. *Journal of Surgical Research*, 92(2), 291-300.
- 22 Marucci, D. D., Shakeshaft, A. J., Cartmill, J. A., Cox, M. R., Adams, S. G., & Martin, C. J. (2000). Grasper trauma during laparoscopic cholecystectomy. *Australian and New Zealand Journal of Surgery*, 70(8), 578-581.
- 23 Heijnsdijk, E. A. M., Dankelman, J., & Gouma, D. J. (2002). Effectiveness of grasping and duration of clamping using laparoscopic graspers. *Surgical Endoscopy and other interventional Techniques*, 16(9), 1329-1331.
- 24 Satava, R. M. (2002). Surgical robotics: the early chronicles: a personal historical perspective. *Surgical Laparoscopy Endoscopy & Percutaneous Techniques*, 12(1), 6-16.
- 25 Schurr, M. O., Buess, G., Neisius, B., & Voges, U. (2000). Robotics and telemanipulation technologies for endoscopic surgery. *Surgical endoscopy*, 14(4), 375-381.

- 
- 26 Berkelman, P. J., Whitcomb, L. L., Taylor, R. H., & Jensen, P. (2000, January). A miniature instrument tip force sensor for robot/human cooperative microsurgical manipulation with enhanced force feedback. In *Medical Image Computing and Computer-Assisted Intervention—MICCAI 2000* (pp. 897-906). Springer Berlin Heidelberg.
- 27 Louw, D. F., Fielding, T., McBeth, P. B., Gregoris, D., Newhook, P., & Sutherland, G. R. (2004). Surgical robotics: a review and neurosurgical prototype development. *Neurosurgery*, *54*(3), 525-537.
- 28 Jacob, B. P., & Gagner, M. (2003). Robotics and general surgery. *Surgical Clinics of North America*, *83*(6), 1405-1419.
- 29 Moorthy, K., Munz, Y., Dosis, A., Hernandez, J., Martin, S., Bello, F., ... & Darzi, A. (2004). Dexterity enhancement with robotic surgery. *Surgical Endoscopy And Other Interventional Techniques*, *18*(5), 790-795.
- 30 Munz, Y., Moorthy, K., Dosis, A., Hernandez, J. D., Bann, S., Bello, F., ... & Rockall, T. (2004). The benefits of stereoscopic vision in robotic-assisted performance on bench models. *Surgical Endoscopy And Other Interventional Techniques*, *18*(4), 611-616.
- 31 Dakin, G. F., & Gagner, M. (2003). Comparison of laparoscopic skills performance between standard instruments and two surgical robotic systems. *Surgical Endoscopy And Other Interventional Techniques*, *17*(4), 574-579.
- 32 Sung, G. T., & Gill, I. S. (2001). Robotic laparoscopic surgery: a comparison of the da Vinci and Zeus systems. *Urology*, *58*(6), 893-898.
- 33 <http://www.intuitivesurgical.com/company/history/system.html> (Accessed April 16, 2012)
- 34 <http://www.mimicsimulation.com/> (Accessed August 15, 2013)
- 35 Lowrance, W. T., Eastham, J. A., Savage, C., Maschino, A. C., Laudone, V. P., Dechet, C. B., ... & Sandhu, J. S. (2012). Contemporary open and robotic radical prostatectomy practice patterns among urologists in the United States. *The Journal of urology*, *187*(6), 2087-2093.
- 36 Fagotti, A., Gagliardi, M. L., Fanfani, F., Salerno, M. G., Ercoli, A., D'Asta, M., ... & Scambia, G. (2012). Perioperative outcomes of total laparoendoscopic single-site hysterectomy versus total robotic hysterectomy in endometrial cancer patients: A multicentre study. *Gynecologic Oncology*, *125*(3), 552-555.
- 37 Markar, S. R., Karthikesalingam, A. P., Venkat Ramen, V., Kinross, J., & Ziprin, P. (2011). Robotic vs. laparoscopic Roux-en-Y gastric bypass in morbidly obese patients: systematic review and pooled analysis. *The International Journal of Medical Robotics and Computer Assisted Surgery*, *7*(4), 393-400.
- 38 Tieu, K., Allison, N., Snyder, B., Wilson, T., Toder, M., & Wilson, E. (2012). Robotic-assisted Roux-en-Y gastric bypass: update from 2 high-volume centers. *Surgery for Obesity and Related Diseases*.
- 39 Breitenstein, S., Nocito, A., Puhan, M., Held, U., Weber, M., & Clavien, P. A. (2008). Robotic-assisted versus laparoscopic cholecystectomy: outcome and cost analyses of a case-matched control study. *Annals of surgery*, *247*(6), 987-993.
- 40 Karabulut, K., Agcaoglu, O., Aliyev, S., Siperstein, A., & Berber, E. (2012). Comparison of intraoperative time use and perioperative outcomes for robotic versus laparoscopic adrenalectomy. *Surgery*, *151*(4), 537-542.
- 41 Suri, R. M., Antiel, R. M., Burkhart, H. M., Huebner, M., Li, Z., Eton, D. T., ... & Schaff, H. V. (2012). Quality of life after early mitral valve repair using conventional and robotic approaches. *The Annals of thoracic surgery*, *93*(3), 761-769.
- 42 Schmitto, J. D., Mokashi, S. A., & Cohn, L. H. (2011). Past, present, and future of minimally invasive mitral valve surgery. *Journal of Heart Valve Disease*, *20*(5), 493.
- 43 Turner Jr, W. F., & Sloan, J. H. (2006). Robotic-assisted coronary artery bypass on a beating heart: initial experience and implications for the future. *The Annals of thoracic surgery*, *82*(3), 790-794.
- 44 Marescaux, J., Smith, M. K., Fölscher, D., Jamali, F., Malassagne, B., & Leroy, J. (2001). Telerobotic laparoscopic cholecystectomy: initial clinical experience with 25 patients. *Annals of surgery*, *234*(1), 1.

- 
- 45 Marescaux, J., Leroy, J., Rubino, F., Smith, M., Vix, M., Simone, M., & Mutter, D. (2002). Transcontinental robot-assisted remote telesurgery: feasibility and potential applications. *Annals of surgery*, 235(4), 487.
- 46 Marescaux, J., Leroy, J., Gagner, M., Rubino, F., Mutter, D., Vix, M., ... & Smith, M. K. (2001). Transatlantic robot-assisted telesurgery. *Nature*, 413(6854), 379-380.
- 47 Nguan, C., Miller, B., Patel, R., Luke, P. P., & Schlachta, C. M. (2008). Pre-clinical remote telesurgery trial of a da Vinci telesurgery prototype. *The International Journal of Medical Robotics and Computer Assisted Surgery*, 4(4), 304-309.
- 48 Anvari, M., Williams, D., Thirsk, R., Morin, L., McKinley, C., Broderick, T., ... & Dobranowski, J. (2006). Use of a Portable Telesurgical Robot in an Extreme Environment-The NEEMO 7 and 9 Missions. *Surgical Laparoscopy Endoscopy & Percutaneous Techniques*, 16(4), 287.
- 49 Hongo, K., Kobayashi, S., Kakizawa, Y., Koyama, J. I., Goto, T., Okudera, H., ... & Takakura, K. (2002). NeuRobot: telecontrolled micromanipulator system for minimally invasive microneurosurgery-preliminary results. *Neurosurgery*, 51(4), 985-988.
- 50 Park, J. W., Lee, D. H., Kim, Y. W., Lee, B. H., & Jo, Y. H. (2012). Lapabot: A compact telesurgical robot system for minimally invasive surgery: Part II. Telesurgery evaluation. *Minimally Invasive Therapy & Allied Technologies*, 21(3), 195-200.
- 51 Lum, M. J., Friedman, D. C., Sankaranarayanan, G., King, H., Fodero, K., Leuschke, R., ... & Sinanan, M. N. (2009). The RAVEN: Design and validation of a telesurgery system. *The International Journal of Robotics Research*, 28(9), 1183-1197.
- 52 Allen, B. F., Jordan, B., Pannell, W., Lewis, C., Dutson, E., & Faloutsos, P. (2010). Laparoscopic Surgical Robot for Remote In Vivo Training. *Advanced Robotics*, 24(12), 1679-1694.
- 53 Rosen, J., & Hannaford, B. (2006). Doc at a distance. *Spectrum, IEEE*, 43(10), 34-39.
- 54 Hagn, U., Konietschke, R., Tobergte, A., Nickl, M., Jörg, S., Kübler, B., ... & Hirzinger, G. (2010). DLR MiroSurge: a versatile system for research in endoscopic telesurgery. *International journal of computer assisted radiology and surgery*, 5(2), 183-193.
- 55 Kim, K. Y., Song, H. S., Suh, J. W., & Lee, J. J. (2013). A Novel Surgical Manipulator with Workspace-Conversion Ability for Telesurgery.
- 56 Arata, J., Takahashi, H., Yasunaka, S., Onda, K., Tanaka, K., Sugita, N., ... & Hashizume, M. (2008). Impact of network time-delay and force feedback on tele-surgery. *International Journal of Computer Assisted Radiology and Surgery*, 3(3-4), 371-378.
- 57 Tozal, M. E., Wang, Y., Al-Shaer, E., Sarac, K., Thuraisingham, B., & Chu, B. T. (2011). Adaptive Information Coding for Secure and Reliable Wireless Telesurgery Communications. *Mobile Networks and Applications*, 1-15.
- 58 Arata, J., Takahashi, H., Pitakwatchara, P., Warisawa, S. I., Tanoue, K., Konishi, K., ... & Hashizume, M. (2007, April). A remote surgery experiment between Japan and Thailand over Internet using a low latency CODEC system. In *Robotics and Automation, 2007 IEEE International Conference on* (pp. 953-959). IEEE.
- 59 Precup, R. E., Kovács, L., Haidegger, T., Preitl, S., Kovács, A., Benyó, B., ... & Benyó, Z. (2011, May). Time delay compensation by fuzzy control in the case of master-slave telesurgery. In *Applied Computational Intelligence and Informatics (SACI), 2011 6th IEEE International Symposium on* (pp. 305-310). IEEE.
- 60 Islam, S., Liu, P. X., El Saddik, A., & Liu, S. (2011, May). Internet-based teleoperation systems with time varying communication delay. In *Instrumentation and Measurement Technology Conference (I2MTC), 2011 IEEE* (pp. 1-6). IEEE.
- 61 Rayman, R., Primak, S., & Eagleson, R. (2009, May). Effects of network delay on training for telesurgery. In *Wireless Communication, Vehicular Technology, Information Theory and Aerospace & Electronic Systems Technology, 2009. Wireless VITAE 2009. 1st International Conference on* (pp. 63-67). IEEE.

- 
- 62 Rayman, R., Primak, S., Patel, R., Moallem, M., Morady, R., Tavakoli, M., ... & Croome, K. (2005). Effects of latency on telesurgery: an experimental study. In *Medical Image Computing and Computer-Assisted Intervention–MICCAI 2005*(pp. 57-64). Springer Berlin Heidelberg.
- 63 Anvari, M., Broderick, T., Stein, H., Chapman, T., Ghodoussi, M., Birch, D. W., ... & Goldsmith, C. H. (2005). The impact of latency on surgical precision and task completion during robotic-assisted remote telepresence surgery. *Computer Aided Surgery*, *10*(2), 93-99.
- 64 R. Rayman, R., Croome, K., Galbraith, N., McClure, R., Morady, R., Peterson, S., ... & Primak, S. (2006). Long distance robotic telesurgery: a feasibility study for care in remote environments. *The International Journal of Medical Robotics and Computer Assisted Surgery*, *2*(3), 216-224.
- 65 King, H. H., Hannaford, B., Kwok, K. W., Yang, G. Z., Griffiths, P., Okamura, A., ... & Low, T. (2010, May). Plugfest 2009: global interoperability in telerobotics and telemedicine. In *Robotics and Automation (ICRA), 2010 IEEE International Conference on* (pp. 1733-1738). IEEE.
- 66 Satava, R. M. (2009). How the future of surgery is changing: robotics, telesurgery, surgical simulators and other advanced technologies. *J Chirurgie*, *5*, 311-25.
- 67 Wood, D. (2011). No surgeon should operate alone: how telementoring could change operations. *Telemed JE Health*, *17*(3), 150-2.
- 68 Ereso, A. Q., Garcia, P., Tseng, E., Gauger, G., Kim, H., Dua, M. M., ... & Guy, T. S. (2010). Live transference of surgical subspecialty skills using telerobotic proctoring to remote general surgeons. *Journal of the American College of Surgeons*, *211*(3), 400-411.
- 69 SAGES Guidelines for the Surgical Practice of Telemedicine. <http://www.sages.org/publication/id/21/> [Accessed 24 Apr 2012]
- 70 Zambarbieri, D., Schmid, M., & Verni, G. (2001, May). Sensory feedback for lower limb prostheses. In *Intelligent systems and technologies in rehabilitation engineering* (pp. 129-151). CRC Press, Inc..
- 71 Petzold, B., Zaeh, M. F., Faerber, B., Deml, B., Egermeier, H., Schilp, J., & Clarke, S. (2004). A study on visual, auditory, and haptic feedback for assembly tasks. *Presence: teleoperators and virtual environments*, *13*(1), 16-21.
- 72 Shing, C. Y., Fung, C. P., Chuang, T. Y., Penn, I. W., & Doong, J. L. (2003). The study of auditory and haptic signals in a virtual reality-based hand rehabilitation system. *Robotica*, *21*(02), 211-218.
- 73 Gallo, S., Santos-Carreras, L., Rognini, G., Hara, M., Yamamoto, A., & Higuchi, T. (2012, March). Towards multimodal haptics for teleoperation: Design of a tactile thermal display. In *Advanced Motion Control (AMC), 2012 12th IEEE International Workshop on* (pp. 1-5). IEEE.
- 74 Kaczmarek, K. A., Webster, J. G., Bach-y-Rita, P., & Tompkins, W. J. (1991). Electrotactile and vibrotactile displays for sensory substitution systems. *Biomedical Engineering, IEEE Transactions on*, *38*(1), 1-16.
- 75 Grill, W. M., & Mortimer, J. T. (1994). Electrical properties of implant encapsulation tissue. *Annals of biomedical engineering*, *22*(1), 23-33.
- 76 Navarro, X., Krueger, T. B., Lago, N., Micera, S., Stieglitz, T., & Dario, P. (2005). A critical review of interfaces with the peripheral nervous system for the control of neuroprostheses and hybrid bionic systems. *Journal of the Peripheral Nervous System*, *10*(3), 229-258.
- 77 Van der Putten, E. P. W., van den Dobbelsteen, J. J., Goossens, R. H., Jakimowicz, J. J., & Dankelman, J. (2010). The Effect of augmented feedback on grasp force in laparoscopic grasp control. *Haptics, IEEE Transactions on*, *3*(4), 280-291.
- 78 Burdea, G., & Burdea, G. C. (1996). *Force and touch feedback for virtual reality*(pp. 3-4). New York: Wiley.
- 79 Okamura, A. M. (2009). Haptic feedback in robot-assisted minimally invasive surgery. *Current opinion in urology*, *19*(1), 102.
- 80 Guyton, A. C., & Hall, J. E. (2005). *Textbook of Medical Physiology*.
- 81 <http://www.scf-online.com> (Accessed April 25, 2012).



- 
- 82 Johansson, R. S., Häger, C., & Riso, R. (1992). Somatosensory control of precision grip during unpredictable pulling loads. *Experimental Brain Research*, 89(1), 192-203.
- 83 Macefield, V. G., Häger-Ross, C., & Johansson, R. S. (1996). Control of grip force during restraint of an object held between finger and thumb: responses of cutaneous afferents from the digits. *Experimental Brain Research*, 108(1), 155-171.
- 84 Cavusoglu, M. C., Williams, W., Tendick, F., & Sastry, S. S. (2003). Robotics for telesurgery: second generation Berkeley/UCSF laparoscopic telesurgical workstation and looking towards the future applications. *Industrial Robot: An International Journal*, 30(1), 22-29.
- 85 Lee, S., Lee, J., Choi, D. S., Kim, M., & Lee, C. W. (1999). The distributed controller architecture for a master arm and its application to teleoperation with force feedback. In *Robotics and Automation, 1999. Proceedings. 1999 IEEE International Conference on* (Vol. 1, pp. 213-218). IEEE.
- 86 Brooks Jr, F. P., Ouh-Young, M., Batter, J. J., & Jerome Kilpatrick, P. (1990, September). Project GROPE - Haptic displays for scientific visualization. In *ACM SIGGraph computer graphics* (Vol. 24, No. 4, pp. 177-185). ACM.
- 87 Cai, Y., Ishii, M., & Sato, M. (1996, October). A human interface device for cave: size virtual workspace. In *Systems, Man, and Cybernetics, 1996., IEEE International Conference on* (Vol. 3, pp. 2084-2089). IEEE.
- 88 Baumann, R., & Clavel, R. (1998, May). Haptic interface for virtual reality based minimally invasive surgery simulation. In *Robotics and Automation, 1998. Proceedings. 1998 IEEE International Conference on* (Vol. 1, pp. 381-386). IEEE.
- 89 King, C., Higa, A. T., Culjat, M. O., Han, S. H., Bisley, J. W., Carman, G. P., Dutson, E. P. & Grundfest, W. S. (2006). A pneumatic haptic feedback actuator array for robotic surgery or simulation. *Studies in health technology and informatics*, 125, 217.
- 90 Bethea, B. T., Okamura, A. M., Kitagawa, M., Fitton, T. P., Cattaneo, S. M., Gott, V. L., ... & Yuh, D. D. (2004). Application of haptic feedback to robotic surgery. *Journal of Laparoendoscopic & Advanced Surgical Techniques*, 14(3), 191-195.
- 91 Wottawa, C., Fan, R., Bisley, J. W., Dutson, E. P., Culjat, M. O., & Grundfest, W. S. (2011). Applications of tactile feedback in medicine. *Studies in health technology and informatics*, 163, 703.
- 92 Bouzit, M., Popescu, G., Burdea, G., & Boian, R. (2002). The rutgers master II-ND force feedback glove. In *Haptic Interfaces for Virtual Environment and Teleoperator Systems, 2002. HAPTICS 2002. Proceedings. 10th Symposium on* (pp. 145-152). IEEE.
- 93 Nakamura, M., & Jones, L. (2003, March). An actuator for the tactile vest-a torso-based haptic device. In *Haptic Interfaces for Virtual Environment and Teleoperator Systems, 2003. HAPTICS 2003. Proceedings. 11th Symposium on* (pp. 333-339). IEEE.
- 94 Fan, R. E., Culjat, M. O., King, C. H., Franco, M. L., Boryk, R., Bisley, J. W., Dutson, E. P. & Grundfest, W. S. (2008). A haptic feedback system for lower-limb prostheses. *Neural Systems and Rehabilitation Engineering, IEEE Transactions on*, 16(3), 270-277.
- 95 Schiff, W., & Foulke, E. (Eds.). (1982). *Tactual perception: a sourcebook*. Cambridge University Press.
- 96 [http://www.tiresias.org/reports/braille\\_cell.htm](http://www.tiresias.org/reports/braille_cell.htm) (Accessed August, 15 2008)
- 97 Phillips, J. R., Johansson, R. S., & Johnson, K. O. (1990). Representation of braille characters in human nerve fibres. *Experimental Brain Research*, 81(3), 589-592.
- 98 Coles, T. R., Meglan, D., & John, N. W. (2011). The role of haptics in medical training simulators: a survey of the state of the art. *Haptics, IEEE Transactions on*, 4(1), 51-66.
- 99 Shinohara, M., Shimizu, Y., & Mochizuki, A. (1998). Three-dimensional tactile display for the blind. *Rehabilitation Engineering, IEEE Transactions on*, 6(3), 249-256.

- 
- 100 Gleeson, B. T., Horschel, S. K., & Provancher, W. R. (2010). Design of a fingertip-mounted tactile display with tangential skin displacement feedback. *Haptics, IEEE Transactions on*, 3(4), 297-301.
- 101 Summers, I. R., & Chanter, C. M. (2002). A broadband tactile array on the fingertip. *The Journal of the Acoustical Society of America*, 112, 2118.
- 102 Haga, Y., Mizushima, M., Matsunaga, T., & Esashi, M. (2005). Medical and welfare applications of shape memory alloy microcoil actuators. *Smart materials and structures*, 14(5), S266.
- 103 Howe, R. D., Kontarinis, D. A., & Peine, W. J. (1995, December). Shape memory alloy actuator controller design for tactile displays. In *Decision and Control, 1995., Proceedings of the 34th IEEE Conference on* (Vol. 4, pp. 3540-3544). IEEE.
- 104 Taylor, P. M., Hosseini-Sianaki, A., & Varley, C. J. (1996, April). An electrorheological fluid-based tactile array for virtual environments. In *Robotics and Automation, 1996. Proceedings., 1996 IEEE International Conference on* (Vol. 1, pp. 18-23). IEEE.
- 105 Bicchi, A., Scilingo, E. P., Sgambelluri, N., & De Rossi, D. (2002, July). Haptic interfaces based on magnetorheological fluids. In *Proceedings 2th International Conference Eurohaptics 2002* (pp. 6-11).
- 106 Porquis, L. B., Konyo, M., & Tadokoro, S. (2011, September). Enhancement of human force perception by multi-point tactile stimulation. In *Intelligent Robots and Systems (IROS), 2011 IEEE/RSJ International Conference on* (pp. 3488-3493). IEEE.
- 107 Cohn, M. B., Lam, M., & Fearing, R. S. (1993, March). Tactile feedback for teleoperation. In *Applications in Optical Science and Engineering* (pp. 240-254). International Society for Optics and Photonics.
- 108 Asamura, N., Yokoyama, N., & Shinoda, H. (1998). Selectively stimulating skin receptors for tactile display. *Computer Graphics and Applications, IEEE*, 18(6), 32-37.
- 109 Sato, K., Igarashi, E., & Kimura, M. (1991, June). Development of non-constrained master arm with tactile feedback device. In *Advanced Robotics, 1991. Robots in Unstructured Environments', 91 ICAR., Fifth International Conference on* (pp. 334-338). IEEE.
- 110 Moy, G., Wagner, C., & Fearing, R. S. (2000). A compliant tactile display for teletaction. In *Robotics and Automation, 2000. Proceedings. ICRA'00. IEEE International Conference on* (Vol. 4, pp. 3409-3415). IEEE.
- 111 Doh, E., Lee, H., Park, J., & Yun, K. S. (2011, June). Three-axis tactile display using PDMS pneumatic actuator for robot-assisted surgery. In *Solid-State Sensors, Actuators and Microsystems Conference (TRANSDUCERS), 2011 16th International* (pp. 2418-2421). IEEE.
- 112 Caldwell, D. G., Tsagarakis, N., & Giesler, C. (1999). An integrated tactile/shear feedback array for stimulation of finger mechanoreceptor. In *Robotics and Automation, 1999. Proceedings. 1999 IEEE International Conference on* (Vol. 1, pp. 287-292). IEEE.
- 113 Rogers, C. H. (1970). Choice of stimulator frequency for tactile arrays. *Man-Machine Systems, IEEE Transactions on*, 11(1), 5-11.
- 114 Phillips, J. R., & Johnson, K. O. (1985). Neural mechanisms of scanned and stationary touch. *The Journal of the Acoustical Society of America*, 77, 220.
- 115 King, C. H., Franco, M., Culjat, M. O., Higa, A. T., Bisley, J. W., Dutson, E., & Grundfest, W. S. (2008). Fabrication and characterization of a balloon actuator array for haptic feedback in robotic surgery. *Journal of Medical Devices*, 2, 041006.
- 116 Grosjean, C., Lee, G. B., Hong, W., Tai, Y. C., & Ho, C. M. (1998, January). Micro balloon actuators for aerodynamic control. In *Micro Electro Mechanical Systems, 1998. MEMS 98. Proceedings., The Eleventh Annual International Workshop on* (pp. 166-171). IEEE.
- 117 Yuan, G., Wu, X., Yoon, Y. K., & Allen, M. G. (2005). Kinematically-stabilized microbubble actuator arrays. In *Micro Electro Mechanical Systems, 2005. MEMS 2005. 18th IEEE International Conference on* (pp. 411-414). IEEE.

- 
- 118 Buess, G. F., Schurr, M. O., & Fischer, S. C. (2000). Robotics and allied technologies in endoscopic surgery. *Archives of Surgery*, 135(2), 229.
- 119 Brown, J. D., Rosen, J., Chang, L., Sinanan, M. N., & Hannaford, B. (2004). Quantifying surgeon grasping mechanics in laparoscopy using the blue DRAGON system. *Studies in health technology and informatics*, 34-36.
- 120 Nicholls, H. R., & Lee, M. H. (1989). A survey of robot tactile sensing technology. *The International Journal of Robotics Research*, 8(3), 3-30.
- 121 Puangmali, P., Althoefer, K., Seneviratne, L. D., Murphy, D., & Dasgupta, P. (2008). State-of-the-art in force and tactile sensing for minimally invasive surgery. *Sensors Journal, IEEE*, 8(4), 371-381.
- 122 Kattavenos, N., Lawrenson, B., Frank, T. G., Pridham, M. S., Keatch, R. P., & Cuschieri, A. (2004). Force-sensitive tactile sensor for minimal access surgery. *Minimally Invasive Therapy & Allied Technologies*, 13(1), 42-46.
- 123 Mei, T., Li, W. J., Ge, Y., Chen, Y., Ni, L., & Chan, M. H. (2000). An integrated MEMS three-dimensional tactile sensor with large force range. *Sensors and Actuators A: Physical*, 80(2), 155-162.
- 124 Tholey, G., Pillarisetti, A., Green, W., & Desai, J. P. (2004). Direct 3-D force measurement capability in an automated laparoscopic grasper. In *Proc. 4th Int. Conf. EuroHaptics*.
- 125 Patel P. Synthetic Skin Sensitive to the Lightest Touch. Article. *IEEE Spectrum*. September 2010.
- 126 Kalantari, M., Ramezanifard, M., Ahmadi, R., Dargahi, J., & Kovacs, J. (2010, March). Design, fabrication, and testing of a piezoresistive hardness sensor in minimally invasive surgery. In *Haptics Symposium, 2010 IEEE* (pp. 431-437). IEEE.
- 127 <http://www.tekscan.com/> (Accessed Sept. 23, 2009.)
- 128 Dargahi, J., Parameswaran, M., & Payandeh, S. (2000). A micromachined piezoelectric tactile sensor for an endoscopic grasper-theory, fabrication and experiments. *Microelectromechanical Systems, Journal of*, 9(3), 329-335.
- 129 Mirbagheri, A., Dargahi, J., Najarian, S., & Ghomshe, F. T. (2007). Design, Fabrication, and Testing of a Membrane Piezoelectric Tactile Sensor with Four Sensing Elements. *American Journal of Applied Sciences*, 4(9), 645.
- 130 Najarian, S., Dargahi, J., & Mehrizi, A. A. (2009). *Artificial tactile sensing in biomedical engineering* (pp. 105-22). New York: McGraw-Hill.
- 131 Gray, B. L., & Fearing, R. S. (1996, April). A surface micromachined microtactile sensor array. In *Robotics and Automation, 1996. Proceedings., 1996 IEEE International Conference on* (Vol. 1, pp. 1-6). IEEE.
- 132 <http://www.pressureprofile.com/> (Accessed Sept. 23 2009)
- 133 Leineweber, M., Pelz, G., Schmidt, M., Kappert, H., & Zimmer, G. (2000). New tactile sensor chip with silicone rubber cover. *Sensors and Actuators A: Physical*, 84(3), 236-245.
- 134 Palasagaram, J. N., & Ramadoss, R. (2006). MEMS-capacitive pressure sensor fabricated using printed-circuit-processing techniques. *Sensors Journal, IEEE*, 6(6), 1374-1375.
- 135 Schostek, S., Ho, C. N., Kalanovic, D., & Schurr, M. O. (2006). Artificial tactile sensing in minimally invasive surgery-a new technical approach. *Minimally Invasive Therapy & Allied Technologies*, 15(5), 296-304.
- 136 Wettels, N., Santos, V. J., Johansson, R. S., & Loeb, G. E. (2008). Biomimetic tactile sensor array. *Advanced Robotics*, 22(8), 829-849.
- 137 Ohmura, Y., Kuniyoshi, Y., & Nagakubo, A. (2006, May). Conformable and scalable tactile sensor skin for curved surfaces. In *Robotics and Automation, 2006. ICRA 2006. Proceedings 2006 IEEE International Conference on* (pp. 1348-1353). IEEE.
- 138 Hirose, S., & Yoneda, K. (1990, May). Development of optical six-axial force sensor and its signal calibration considering nonlinear interference. In *Robotics and Automation, 1990. Proceedings., 1990 IEEE International Conference on* (pp. 46-53). IEEE.

- 
- 139 Wen, Z., Wu, Y., Zhang, Z., Xu, S., Huang, S., & Li, Y. (2003). Development of an integrated vacuum microelectronic tactile sensor array. *Sensors and Actuators A: Physical*, 103(3), 301-306.
- 140 Moy, G. (2002). *Bidigital teletaction system design and performance* (Doctoral dissertation, University of California).
- 141 Ottermo, M. V., Stavdahl, Ø., & Johansen, T. A. (2009). A remote palpation instrument for laparoscopic surgery: design and performance. *Minimally Invasive Therapy & Allied Technologies*, 18(5), 259-272.
- 142 Kianzad, S., Amini, A., & Karkouti, S. O. (2011, February). Force control of laparoscopy grasper using antagonistic shape memory alloy. In *Biomedical Engineering (MECBME), 2011 1st Middle East Conference on* (pp. 335-338). IEEE.
- 143 Harsha, A. M., Abeykoon, S., & Ohnishi, K. (2008, March). Tactile sensation improvement of a bilateral forceps robot with a switching virtual model. In *Advanced Motion Control, 2008. AMC'08. 10th IEEE International Workshop on* (pp. 526-531). IEEE.
- 144 Schoonmaker, R. E., & Cao, C. G. (2006, October). Vibrotactile force feedback system for minimally invasive surgical procedures. In *Systems, Man and Cybernetics, 2006. SMC'06. IEEE International Conference on* (Vol. 3, pp. 2464-2469). IEEE.
- 145 Rizun, P., & Sutherland, G. (2005, March). Tactile feedback laser system with applications to robotic surgery. In *Eurohaptics Conference, 2005 and Symposium on Haptic Interfaces for Virtual Environment and Teleoperator Systems, 2005. World Haptics 2005. First Joint* (pp. 426-431). IEEE.
- 146 Sarmah, A., & Gulhane, U. D. (2010, December). Surgical robot teleoperated laparoscopic grasper with haptics feedback system. In *Emerging Trends in Robotics and Communication Technologies (INTERACT), 2010 International Conference on* (pp. 288-291). IEEE.
- 147 Zbyszewski, D., Bhaumik, A., Althoefer, K., & Seneviratne, L. D. (2008, September). Tactile sensing using a novel air cushion sensor: A feasibility study. In *Intelligent Robots and Systems, 2008. IROS 2008. IEEE/RSJ International Conference on* (pp. 41-46). IEEE.
- 148 Zbyszewski, D., Polygerinos, P., Seneviratne, L. D., & Althoefer, K. (2009, October). A novel MRI compatible air-cushion tactile sensor for minimally invasive surgery. In *Intelligent Robots and Systems, 2009. IROS 2009. IEEE/RSJ International Conference on* (pp. 2647-2652). IEEE.
- 149 Liu, H., Elhage, O., Dasgupta, P., Challacombe, B., Murphy, D., Seneviratne, L., & Althoefer, K. (2009, June). A haptic probe for soft tissue abnormality identification during minimally invasive surgery. In *Reconfigurable Mechanisms and Robots, 2009. ReMAR 2009. ASME/IFTOMM International Conference on* (pp. 417-422). IEEE.
- 150 Ahn, B., Kim, Y., & Kim, J. (2011, September). New approach for abnormal tissue localization with robotic palpation and mechanical property characterization. In *Intelligent Robots and Systems (IROS), 2011 IEEE/RSJ International Conference on* (pp. 4516-4521). IEEE.
- 151 King, C. H., Culjat, M. O., Franco, M. L., Bisley, J. W., Dutson, E., & Grundfest, W. S. (2008). Optimization of a pneumatic balloon tactile display for robot-assisted surgery based on human perception. *Biomedical Engineering, IEEE Transactions on*, 55(11), 2593-2600.
- 152 Franco, M. L., King, C. H., Culjat, M. O., Lewis, C. E., Bisley, J. W., Holmes, E. C., ... & Dutson, E. P. (2009). An integrated pneumatic tactile feedback actuator array for robotic surgery. *The International Journal of Medical Robotics and Computer Assisted Surgery*, 5(1), 13-19.
- 153 King, C. H., Culjat, M. O., Franco, M. L., Lewis, C. E., Dutson, E. P., Grundfest, W. S., & Bisley, J. W. (2009). Tactile feedback induces reduced grasping force in robot-assisted surgery. *Haptics, IEEE Transactions on*, 2(2), 103-110.
- 154 King, C. H., Culjat, M. O., Franco, M. L., Bisley, J. W., Carman, G. P., Dutson, E. P., & Grundfest, W. S. (2009). A multielement tactile feedback system for robot-assisted minimally invasive surgery. *Haptics, IEEE Transactions on*, 2(1), 52-56.

- 
- 155 Fan R. E. (2011) *Design and Testing of a Sensory Feedback System for Persons with Lower-limb Amputation*. (Doctoral dissertation, University of California, Los Angeles).
- 156 Wottawa, C., Fan, R. E., Lewis, C. E., Jordan, B., Culjat, M. O., Grundfest, W. S., & Dutson, E. P. (2009, April). Laparoscopic grasper with an integrated tactile feedback system. In *Complex Medical Engineering, 2009. CME. ICME International Conference on* (pp. 1-5). IEEE.
- 157 Wottawa, C. R., Cohen, J. R., Fan, R. E., Bisley, J. W., Culjat, M. O., Grundfest, W. S., & Dutson, E. P. (2012). The role of tactile feedback in grip force during laparoscopic training tasks. *Surgical endoscopy*, 1-8.
- 158 Wottawa C. R., Lim, C., Fan, R. E., Culjat, M. O., Dutson, E. P., Tsao, T. C., Grundfest, W. S. A Remote Tactile Feedback System for Telesurgery and Telementoring. *2012 Biomedical Engineering Society (BMES) Annual Meeting: Atlanta, 24-27 October 2012*
- 159 Quigley, M., Conley, K., Gerkey, B., Faust, J., Foote, T., Leibs, J., ... & Ng, A. Y. (2009, May). ROS: an open-source Robot Operating System. In *ICRA workshop on open source software* (Vol. 3, No. 3.2).
- 160 Hannaford, B., Rosen, J., Friedman, D., King, H., Roan, P., Cheng, L., ... & White, L. (2013). Raven-II: an open platform for surgical robotics research. *Biomedical Engineering, IEEE Transactions on*. 60(4):954-959
- 161 Wottawa, C. R., Priester, A., Kang, C., Simonelli, J., Tsao, T.C., Dutson, E.P., Grundfest, W.S.. Integration of the University of Washington RAVEN II Surgical Robot, UCLA LapaRobot Tele-mentoring System, and the UCLA Remote Tactile Feedback System. *14th UC System-wide Bioengineering Symposium*. 19-21 June 2013.
- 162 [www.tldp.org/HOWTO/NCURSES-Programming-HOWTO/](http://www.tldp.org/HOWTO/NCURSES-Programming-HOWTO/) (Accessed June 3, 2013)
- 163 Allen, B., Nistor, V., Dutson, E., Carman, G., Lewis, C., & Faloutsos, P. (2010). Support vector machines improve the accuracy of evaluation for the performance of laparoscopic training tasks. *Surgical endoscopy*, 24(1), 170-178.
- 164 Paydar, O. H., Wottawa, C. R., Fan, R. E., Dutson, E. P., Grundfest, W. S., Culjat, M. O., & Candler, R. N. (2012, August). Fabrication of a thin-film capacitive force sensor array for tactile feedback in robotic surgery. In *Engineering in Medicine and Biology Society (EMBC), 2012 Annual International Conference of the IEEE* (pp. 2355-2358). IEEE.
- 165 Wottawa, C. R. Capacitive tooth force sensor and its application to haptic feedback in robotic surgery. (March 2010 NSF Proposal CCSS, unpublished)